



Universitetet
i Stavanger

FACULTY OF SCIENCE AND TECHNOLOGY

MASTER'S THESIS

Study program/specialization: Petroleum Engineering - Master of Science Degree Programme	Spring semester, 2009 Open / Confidential
Author: Knut Undheim Stanghelle (signature author)
Instructor: Rune W. Time, University of Stavanger Supervisor: Trygve Hjelmaas, Talisman Energy Norge AS	
Title of Master's Thesis: Evaluation of artificial lift methods on the Gyda field	
ECTS: 30	
Subject headings: Well performance, multiphase flow, artificial lift, selection of artificial lift, gas lift, ESP, PROSPER, production modeling.	Pages: 97 + attachments/other: 0 + CD with report in PDF format Stavanger, 11.06.2009

Abstract

Since a production peak in 1995 the oil production on the Gyda field has decreased. Water cut is increasing and reservoir pressure is decreasing. This thesis is a study of the artificial lift methods being evaluated to increase the production in the late life of the field.

A thorough investigation of gas lift and Electrical Submersible Pump (ESP) theory, design, and production output is carried out. The theory of artificial lift selection is also presented.

Based on reservoir inputs and completion design, production has been simulated in PROSPER for different scenarios and methods.

The main conclusions and recommendations are as follows:

- Gas lifting is a simple, well tried method where little can go wrong, while ESPs are a complex solution which will require a large amount of planning and administrative resources.
- ESPs have a limited lifetime which increases cost later in a project. The expected lifetime of an ESP well on Gyda is two years. The initial cost for a gas lift well and ESP well will not be so different, because a lot of the wells need a full workover before they can be used for gas lifting.
- Production through gas lifting is not only dependent on injection rate, but can be optimized through the completion design. Setting the valves deeper gives an increased production.
- A new gas compressor is needed if a gas lifting campaign is to be initiated.
- Baker Hughes Centrilift's ESP design was verified for the start up (May 2010) conditions. But production can fall beneath minimum design rate after some years, and a new evaluation of design must be done when the pumps are changed at failure.
- The production simulation of the pilot wells A-19 and A-26 shows that the ESP solution is superior to the gas lift. A secondary effect from the ESP pressure drawdown can also increase production and recovery factor for the field.
- Even though ESPs seem to be the superior choice, an economical evaluation of the projects entire lifetime is needed. A Net Present Value analysis will give the different projects a comparable value, which includes the costs and production from start to finish.

Preface

This study is the finishing thesis for my master degree in petroleum technology at the University of Stavanger. The work of this thesis is 30 study points, and it is written during spring 2009.

Artificial lifting of wells is something that will become more and more important in the years to come. A large part of the fields in the world are going into their late life production. Talisman Energy Norge AS is a company which has its focus on producing mature fields in the North Sea. Through collaboration we came up with the topic of evaluating the artificial lift methods on the Gyda field.

I would like to thank the people in Talisman Energy Norge AS for excellent guidance and help. Both the drilling and wells department and subsurface department have provided me with valuable input data. A special thanks to Trygve Hjelmaas who has been my supervisor during this study, and Rune W. Time, who has been my instructor from the University of Stavanger.

Stavanger, 03.06.2009

Knut Undheim Stanghelle

Contents

1. Introduction	8
2. The Gyda field	9
2.1. Facts	10
2.2. Field description	11
3. Well performance	14
3.1. Drive mechanisms	14
3.2. Inflow performance	15
3.3. Outflow performance	18
3.3.1. Other effects	19
3.4. Operating point	20
4. Multiphase flow	21
5. Artificial lift	25
5.1. Artificial lift on Gyda	26
5.2. Artificial lift selection	27
5.2.1. Selection by Consideration of Depth/Rate System	27
5.2.2. Selection by Advantages and Disadvantages	27
5.2.3. Selection by Net Present Value Comparison	30
6. Electrical Submersible Pumps (ESPs)	32
6.1. Centrifugal pump	34
6.2. Seal chamber section	38
6.3. The motor	38
6.4. The power cable	39
6.5. ESP run life	40
6.5.1. Case studies	44
6.6. ESP design for Gyda	46
6.7. ESP secondary effect	48
7. Gas lift	49
7.1. The unloading process	51
7.2. Gas lift performance curve	52
7.3. Gas lift valves	53
7.4. Gas lift completion procedure	57

8. PROSPER	59
8.1. Basic theory of PROSPER.....	61
8.2. Building a base model for A-19 and A-26.....	62
8.2.1. PVT.....	63
8.2.2. IPR.....	64
8.2.3. Equipment.....	66
8.2.4. Results.....	70
9. Gas lift design	72
9.1. Modelling A-19 and A-26 with gas lift.....	73
9.2. Positioning of valves.....	76
9.3. Results.....	78
9.4. Sensitivity of injection depth.....	79
10. ESP design	81
10.1. Modelling A-19 and A-26 with ESP.....	82
10.2. Results.....	84
11. Production forecast	86
11.1. Well A-19.....	87
11.2. Well A-26.....	89
12. Economical evaluation	91
13. Conclusions	93
References	95
Abbreviations	97

List of figures

2.1	Southern North Sea	9
2.2	The Gyda platform	10
2.3	Gyda reservoir	12
2.4	Production history of the Gyda field	13
3.1	IPR curve	16
3.2	VLP curve	20
3.3	Operating point	20
4.1	Flow regimes in horizontal flow	21
4.2	Flow regimes in vertical flow	22
4.3	Flow regime map for vertical flow	22
5.1	Run life of ESP systems	30
6.1	Basic ESP	32
6.2	ESP surface system	33
6.3	The inside of a centrifugal pump	34
6.4	Shaft with the rotating impellers attached	35
6.5	ESP operating range	36
6.6	Standard pump curves	37
6.7	Seal	38
6.8	Round design	39
6.9	Flat design	39
6.10	Factors acting on ESP run life	40
6.11	ESP run life on Beatrice	44
6.12	Dual ESP system design for Gyda	46
6.13	ADV	47
6.14	ESP secondary effect	48
7.1	Gas lift	49
7.2	The unloading process	51
7.3	Gas lift performance curve	52
7.4	Conventional unloading valve	53
7.5	IPO gas lift valve operating principle	55
7.6	Cross section of square edge orifice and venturi valve	56
7.7	Gas passage characteristics comparison	56
7.8	Valve installation with KOT	57
8.1	PROSPER front display	59
8.2	System summary	62
8.3	PVT correlations	63
8.4	Survey data for A-19	66
8.5	Survey data for A-26	67
8.6	Completion schematic of A-19	68
8.7	Completion schematic of A-26	69
8.8	Production point of A-19 in May 2010	70
8.9	Production point of A-26 in May 2010	71
8.10	A-26 with no intersection between IPR and VLP	71
9.1	Gas lift design menu	73
9.2	Gas lift performance curve for A-19	74
9.3	Gas lift performance curve for A-26	75
9.4	Valve spacing for A-19	76
9.5	Valve spacing for A-26	77
9.6	Injection depth analysis on A-19	79
9.7	Injection depth analysis on A-26	80
10.1	Centrilift 562 P110	81

10.2	Pump curves for the Centrilift 562 P110.....	82
10.3	ESP input in PROSPER.....	83
10.4	A-19 ESP system.....	84
11.1	Production forecast for A-19.....	88
11.2	Production forecast for A-26.....	90

List of tables

5.1	Advantages and disadvantages of ESP and gas lift.....	28
5.2	Design considerations and overall Comparisons.....	29
6.1	Wytch Farm ESP run life.....	45
8.1	General PVT input for A-19 and A-26.....	64
8.2	IPR input for A-19.....	65
8.3	IPR input for A-26.....	65
8.4	Temperature profile.....	70
9.1	Lift gas data.....	73
9.2	Results from gas lift design.....	78
9.3	Injection depth analysis on A-19 and A-26.....	79
10.1	ESP system data.....	81
10.2	Results from ESP simulation.....	84
11.1	A-19 "base case".....	87
11.2	A-19 "ESP case".....	87
11.3	A-19 "gas lift case".....	87
11.4	A-26 "ESP case".....	89
11.5	A-26 "gas lift case".....	89
12.1	Capital cost of projects.....	91

1. Introduction

The Talisman Energy Norge operated Gyda field is in its late life production. The water production is increasing and the reservoir pressure is decreasing. To increase production and extend the lifetime of the field, the operator has decided start an artificial lift project. Because of conditions and desired rates gas lifting and Electrical Submersible Pumps (ESPs) has been evaluated to be the only two alternatives.

The operator is looking at either a full field (10 wells) gas lift campaign or ESPs. If the ESP solution would be found to be the best method, it has been decided that a pilot project is necessary to see how the field responds to the pumps. For this well A-19 and A-26 has been chosen because of their production potential.

The objective of this study is to make a decision supporting document, evaluating each of the scenarios in detail. Simulations based on the field data will give an indication of what rates the different solutions will give.

The first part of the thesis describes the basic theory of well performance and physics. Second, a detailed description of gas lift and ESP methodology and design is given. Theory on decision making within artificial lift is also presented.

The third part of the study is a practical simulation. PROSPER is chosen as the tool to simulate production in the pilot wells A-19 and A-26. Three models are built for each well presenting a “base case”, “ESP case” and “gas lift case”.

For gas lift design the simulation tool is used, but the ESP design is provided by Baker Hughes Centrilift. Based on reservoir simulations a production forecast is made until 2019 for each scenario.

The last section gives a short economical evaluation of the projects, which is an important part of a final decision on artificial lift method.

2. The Gyda field

The Gyda field is located southwest in the North sea, 270 km from Stavanger and 43 km northwest of Ekofisk (Fig. 2.1).

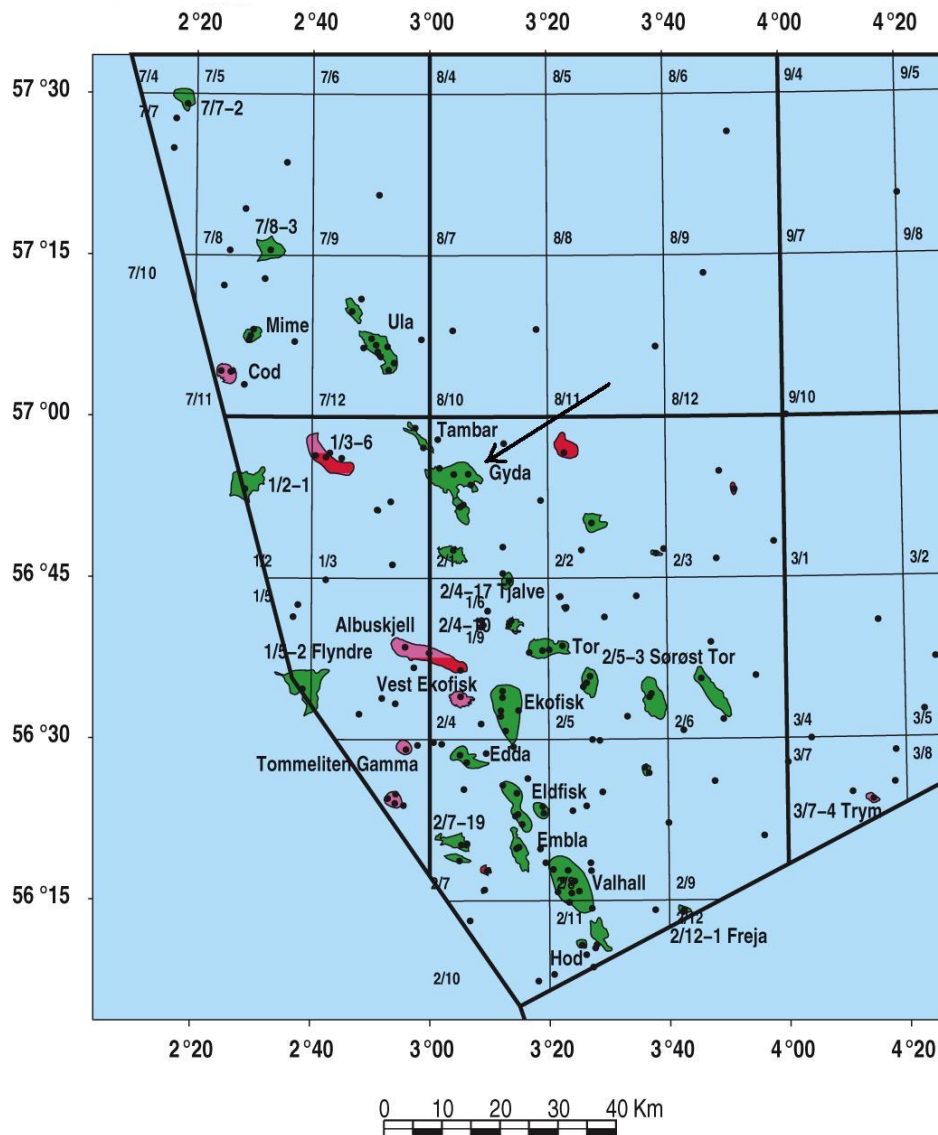


Figure 2.1, Southern North Sea.

It has been developed with a combined drilling, accommodation and processing facility with a steel jacket. The sea depth in the area is 66 metres. The oil is transported to Ekofisk via the oil pipeline from Ula and in Norpipe to Teeside. The gas is transported in a dedicated pipeline to Ekofisk for onward transport in Norpipe to Emden [23].



Figure 2.2, The Gyda platform.

2.1. Facts [23]

Found: The field was discovered by exploration well 2/1-3 in 1980

Production start: 21.06.1990

Operator: Talisman Energy Norge AS (Since 2003)

Owners: DONG E&P Norge AS 34, 00 %
Norske AEDC A/S 5, 00 %
Talisman Energy Norge AS 61, 00 %

Recoverable reserves:

38,8 million Sm³ oil
6,2 billion Sm³ gas
1,9 million ton NGL

Remaining reserves 31.12.2008:

4,1 million Sm³ oil
0,3 billion Sm³ gas
0,0 million ton NGL

2.2. Field description

The Gyda reservoir consists of Upper Jurassic shallow marine sandstone. The trap combines both structural and stratigraphic elements. The field is broadly a westward dipping and westward thickening wedge. The reservoir lies between 3680 and 4170 m TVDSS. The overlying Kimmeridgian aged Mandal formation provides both the seal and the hydrocarbon source for the Gyda Field.

The sands are divided into 3 main units A-, B- and C-sand. The A-sand is in the bottom with a high permeability zone at the top. The permeability in the top of the A-sand is up to 1 D while the base can be 1 mD and below. The B-sand is the middle sand, and in general has poor reservoir quality. The best parts of the sand have permeabilities around 30 mD, while most of it is around 1 mD. The C-sand on the top pinches out towards the crest of the field, and varies in reservoir quality. The C-sand is interbedded with calcite stringers and the eastern parts have poor reservoir quality, equivalent to the B-sand. The western parts of the C-sand have very good reservoir quality, up to 800 mD in places.

The reservoir is cut by numerous Late Jurassic faults with variable throws. Several studies suggest that faults and fractures are at least initially sealing. This creates the opportunity for compartmentalization within the reservoir.

The field is divided into three main segments: Main, South West and South. These segments are confirmed by differences in reservoir fluids, original oil water contacts (OWC) and dynamic pressure data.

Of the 32 wells on Gyda, 17 are currently active. 11 are producing and 6 are injecting. The rest is either temporarily closed or plugged and abandoned.

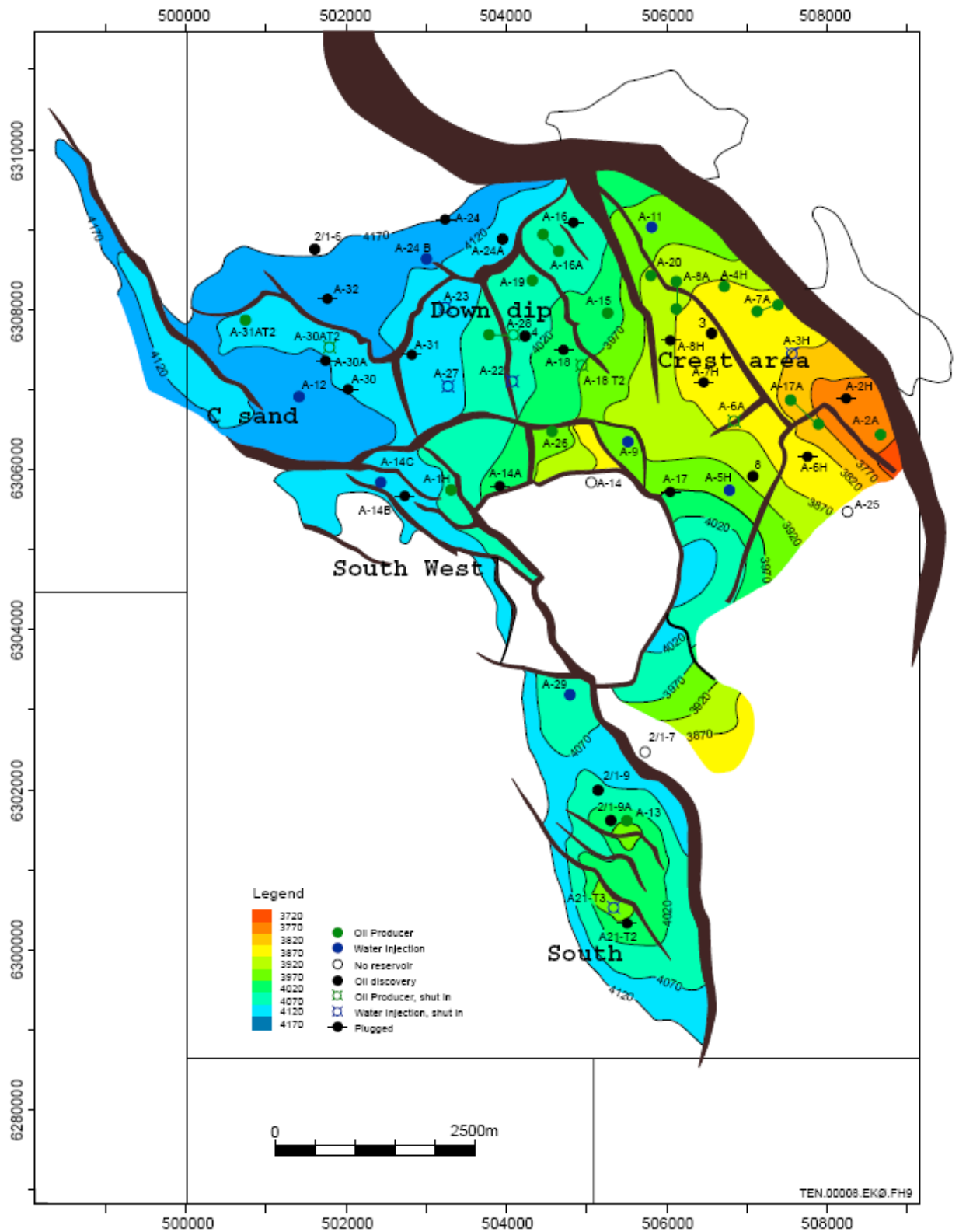


Figure 2.3, Gyda reservoir.

Today Gyda is in its tail phase and experiences increasing water production (Fig. 2.4) and challenges in maintaining the oil production. The production licence period was recently extended to 2028. Several new wells are being drilled on the field. A compressor was installed in 2007 for a gas lift pilot. This has resulted in improved production from the wells. It is also considered to tie-in other deposits in the area to Gyda.

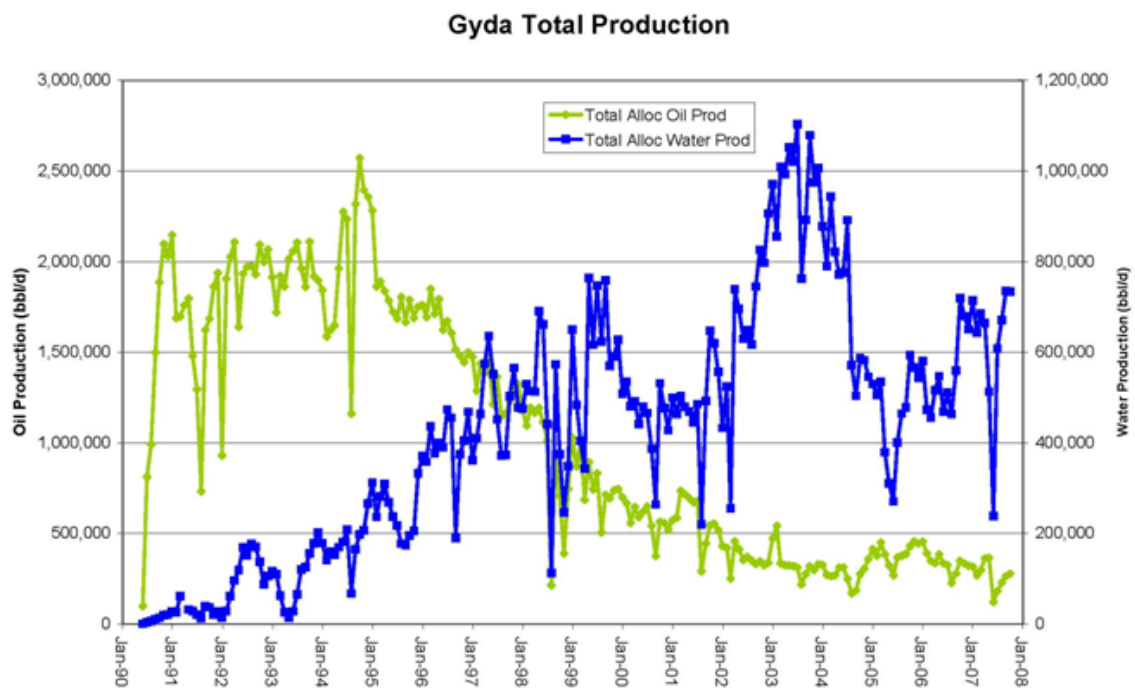


Figure 2.4, Production history of the Gyda field.

3. Well performance

Well performance is dependent on a large number of variables like pressures, formation properties and fluid properties. And these are again dependent on each other.

Different models for the well inflow performance and the vertical lift performance will be described in this chapter, but first a short explanation of the different drive mechanisms from the reservoir will be given.

3.1. Drive mechanisms

According to Dake [3] oil production is due to the following drive mechanisms:

- Natural water drive
- Solution gas drive
- Gas-cap drive
- Compaction drive

Natural water drive

A drop in the reservoir pressure, due to the production of fluids, causes the aquifer water to expand and flow into the reservoir. 50% of oil recovery can be caused by natural water drive.

Solution gas drive

When the reservoir pressure drops below the bubble point pressure solution gas dissolved in oil appears as a free phase. When pressure drops further the highly compressible gas expands expelling the oil from porous media.

Gas-cap drive

High gas compressibility and the extended gas cap size ensure a long lasting and efficient field performance. Up to 35% of the original oil in place can be recovered under a gas-cap drive.

Compaction drive

This drive mechanism might occur during depletion when rock grains are subjected to stress beyond elasticity limit. It leads to a re-compaction of partially deformed or even destroyed rock grains that might result in gradual or abrupt reduction of the reservoir pore volume.

In order to achieve better field performance, secondary and tertiary oil recovery methods are often implemented. Gas lift and downhole pumps are examples of advanced recovery techniques (Enhanced Oil Recovery, EOR).

3.2. Inflow performance [1], [2]

The Inflow Performance Relationship (IPR) describes pressure drawdown as a function of production rate, where drawdown is defined as the difference between static and flowing bottom hole pressure (FBHP).

The simplest approach to describe the inflow performance of oil wells is the use of the productivity index (PI) concept. It was developed using the following assumptions:

- Flow is radial around the well
- A single-phase liquid is flowing
- Permeability distribution in the formation is homogeneous
- The formation is fully saturated with the given liquid.

The flow through a porous media is given by the Darcy equation:

$$\frac{q}{A} = \frac{k}{\mu} \frac{dp}{dl} \quad (\text{Eq. 3.1})$$

Using the assumptions above it can be written as

$$q = \frac{0,00708kh}{\mu B \ln\left(\frac{r_e}{r_w}\right)} (p_R - p_{wf}) \quad (\text{Eq. 3.2})$$

Where:

- q = liquid rate, STB/d
- k = effective permeability, mD
- h = pay thickness, ft
- μ = liquid viscosity, cP
- B = liquid volume factor, bbl/STB
- r_e = drainage radius of well, ft
- r_w = radius of wellbore, ft
- p_R = average reservoir pressure
- p_{wf} = flowing bottomhole pressure

Most parameters on the right hand side are constant, which permits collecting them into a single coefficient called PI:

$$q = PI(p_R - p_{wf}) \quad (\text{Eq. 3.3})$$

This gives us:

$$PI = \frac{q}{(p_R - p_{wf})} \quad (\text{Eq. 3.4})$$

This equation states that liquid inflow into a well is directly proportional to the pressure drawdown. It will plot as a straight line on a pressure vs. rate diagram.

The use of the PI concept is quite straightforward. If the average reservoir pressure and the PI are known, use of equation 3.3 gives the flow rate for any FBHP. The well's PI can either be calculated from reservoir parameters, or measured by taking flow rates at various FBHPs.

This works well for a single phase flow, but when producing a multiphase reservoir the curve will not plot as a straight line.

As the oil approaches the well bore and the pressure drops below bubble point, gas comes out of solution. Thus, the free gas saturation in the vicinity of the oil steadily increases, which implies that the relative permeability to gas steadily increases at the expense of the relative permeability of oil. The greater the drawdown, the bigger this effect would be. Since the PI depends on the effective oil permeability, it is expected that it will decrease (Eq. 3.2). Figure 3.1 shows the IPR curve for this condition.

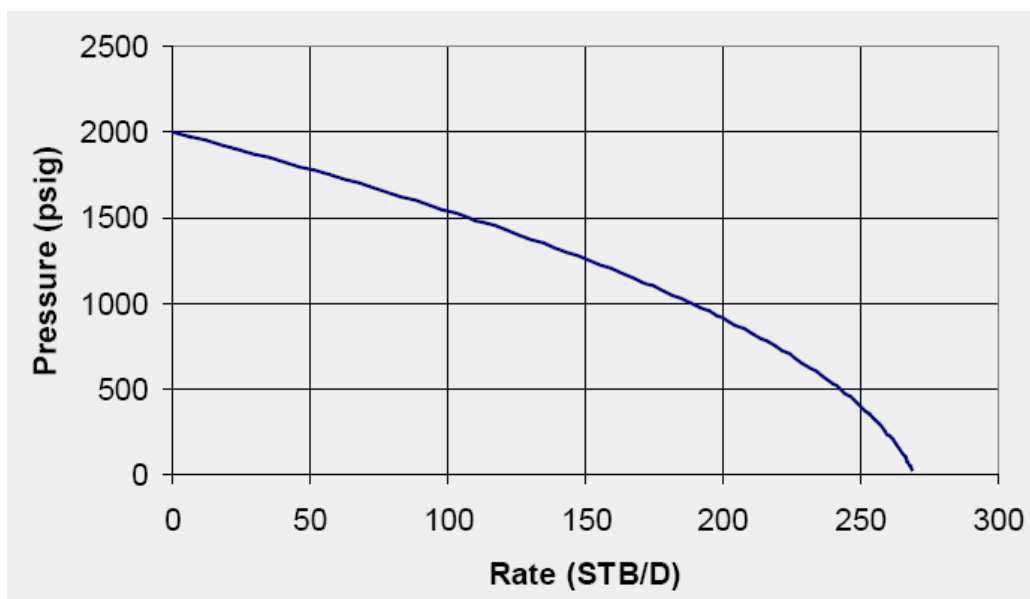


Figure 3.1, IPR curve.

Vogel [9] used a numerical reservoir simulator to study the inflow of wells depleting solution gas drive reservoirs. He considered cases below bubble point and varied parameters like draw downs, fluid and rock properties. Vogel found that the calculated IPR curves exhibited the same general shape, which is given by the dimensionless equation:

$$\frac{q}{q_{\max}} = 1 - 0,2 \frac{P_{wf}}{2} - 0,8 \left(\frac{P_{wf}}{P_R} \right)^2 \quad (\text{Eq. 3.5})$$

The equation is generally accepted for other drive mechanisms as well, and is found to give reliable results for almost any well with a bottom hole pressure below bubble point of the oil.

There are a number of other models designed for special cases e.g. horizontal wells, transient flow, fractured wells, non-Darcy pressure loss, high rates etc.

3.3. Outflow performance

The well's outflow performance, or Vertical Lift Performance (VLP), describes the bottomhole pressure as a function of flow rates. According to Golan and Whitson [1] the outflow performance is dependent on different factors; liquid rate, fluid type (gas-to-liquid ratio, water cut), fluid properties and tubing size.

Gabor [2] divides the total pressure drop in a well into a hydrostatic component, friction component and an acceleration component:

Hydrostatic component represents the change in potential energy due to gravitational force acting on the mixture:

$$\left(\frac{dp}{dl}\right)_h = \rho g \sin \beta \quad (\text{Eq. 3.6})$$

Where: ρ = density of fluid
 β = pipe inclination angle, measured from horizontal
 g = gravity constant

Friction component stands for the irreversible pressure losses occurring in the pipe due to fluid friction on the pipe inner wall:

$$\left(\frac{dp}{dl}\right)_f = \frac{1}{d} f \frac{1}{2} \rho v^2 \quad (\text{Eq. 3.7})$$

Where: f = friction factor
 d = pipe inside diameter
 v = fluid velocity

The type of flow is determined from the Reynolds number:

$$\text{Re} = \frac{\rho v d}{\mu} \quad (\text{Eq. 3.8})$$

Where: μ = fluid viscosity

The boundary between flow regimes are:

$\text{Re} \leq 2000$: Laminar flow
 $2000 < \text{Re} \leq 4000$: Transition between laminar and turbulent flow
 $4000 < \text{Re}$: Turbulent flow

For laminar flow $f = 64/Re$ (Moody friction factor). However, finding the friction factor is more complicated for turbulent flow, and there are several ways to calculate the friction factor.

Acceleration component represents the kinetic energy changes of the flowing mixture and is proportional to the changes in flow velocity. The term is often negligible:

$$\left(\frac{dp}{dl}\right)_a = -\rho v \frac{dv}{dl} \quad (\text{Eq. 3.9})$$

3.3.1. Other Effects

Effect of liquid flow rate on pressure loss

From the friction equation we can see that friction losses increases as liquid rate increases (v increases). Hydrostatic gradient also increases with increased liquid production.

Effect of gas-to-liquid ratio on pressure loss

Increase in gas-to-liquid ratio (GLR) results in reduction of hydrostatic gradient. On the other hand, increased GLR increases friction forces and has a counter effect on the bottomhole pressure. When contribution of the friction becomes higher than that of hydrostatic forces, the actual bottomhole pressure starts to increase. From a gas lift point of view this means that there is a limit of how much gas that beneficially can be injected.

Effect of water cut on pressure loss

Increased water cuts results in increased liquid density, which in turn, increases hydrostatic forces and the bottomhole pressure

Effect of tubing size on pressure loss

From the equation 3.7 we can see that the increased diameter of tubing reduces the pressure gradient due to friction. However, there is a limit to which diameter of tubing can be increased. If the diameter is too big the velocity of the mixture ($v=q/A$, A : pipe cross section) is not enough to lift the liquid and the well starts to load up with liquid, resulting in increase of hydrostatic pressure.

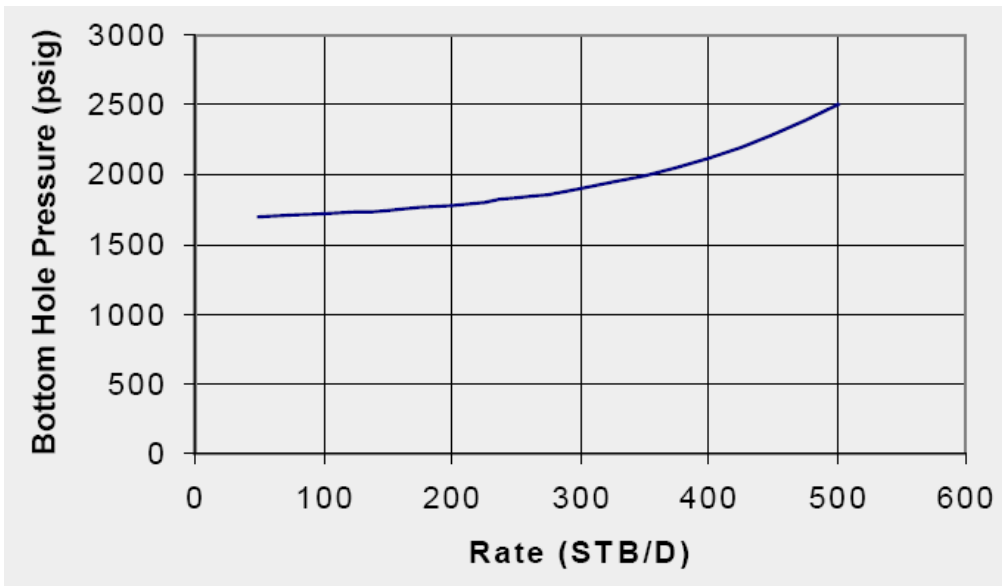


Figure 3.2, VLP curve

3.4. Operating point

To calculate the well production rate, the bottom-hole pressure that simultaneously satisfies both the IPR and VLP relations is required. By plotting the IPR and VLP in the same graph the producing rate can be found. The system can be described by an energy balance expression, simply the principle of conservation of energy over an incremental length element of tubing. The energy entering the system by the flowing fluid must equal the energy leaving the system plus the energy exchanged between the fluid and its surroundings.

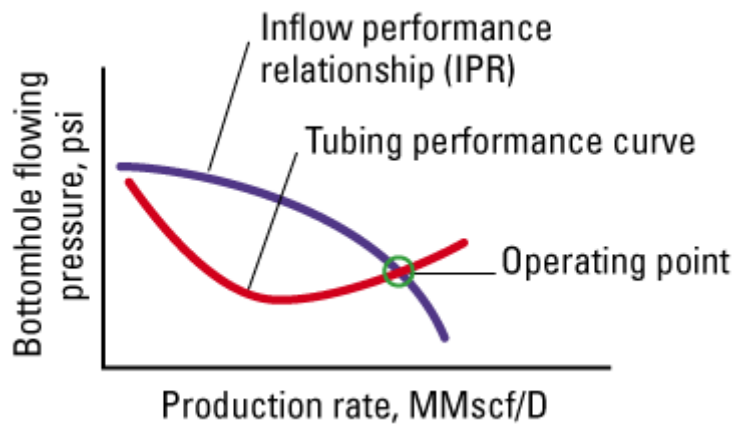


Figure 3.3, Operating point (intersection between IPR and VLP curves).

4. Multiphase flow

Oil wells normally produce a mixture of fluids and gases to the surface while phase conditions usually change along the path. At higher pressures, especially at the well bottom, flow may be single phase. But going up in the well the continuous decrease of pressure causes dissolved gas to gradually escape from the flowing liquid, resulting in multiphase flow. Gas injection into a well is also an example of multiphase flow.

In single phase flow we discriminate between laminar and turbulent flow. In two-phase flow we discriminate in addition between flow regimes that are characteristic for the time and space distribution of gas and liquid flow.

In horizontal flow we discriminate between the flow regimes

- Stratified flow
- Slug flow
- Dispersed bubble flow
- Annular flow

These are shown in figure 4.1. At low velocities the gas and liquid are separated as in stratified flow. At high velocities gas and liquid become mixed. Slug flow is an example of a flow regime in between, representing both separation and mixing. Slug flow is consequently referred to as an intermittent flow regime [5].

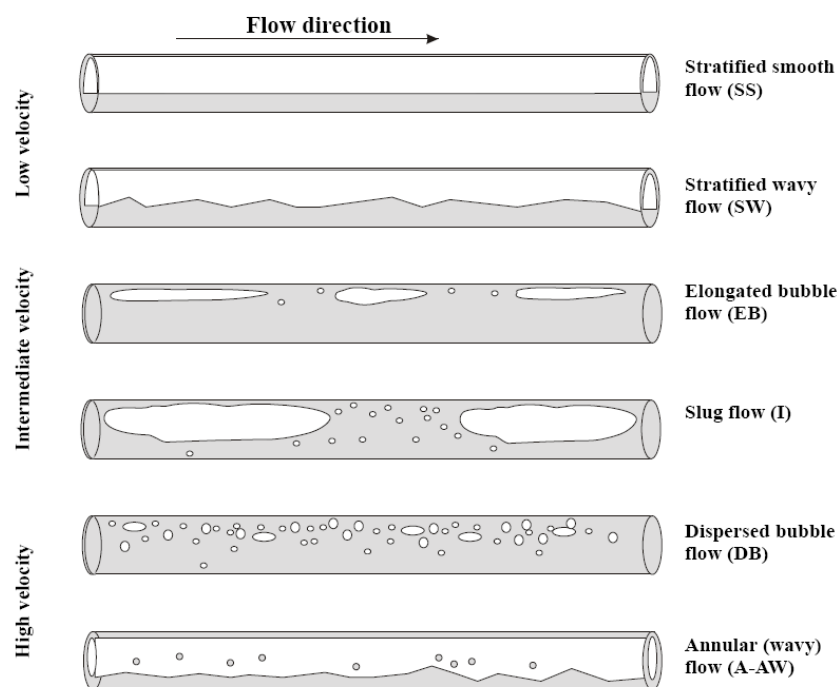


Figure 4.1, Flow regimes in horizontal flow [5].

In vertical flow we discriminate between the flow regimes

- Slug flow
- Churn flow
- Dispersed bubble flow
- Annular flow

Figure 4.2 illustrates the flow regimes in vertical flow. The same comments that apply to horizontal flow are valid in vertical flow. The big difference is that in vertical (concurrent upward) flow it is not possible to obtain stratified flow. The equivalent flow regime at identical flowrates of gas and liquid is slug flow with very slow bullet shaped Taylor bubbles.

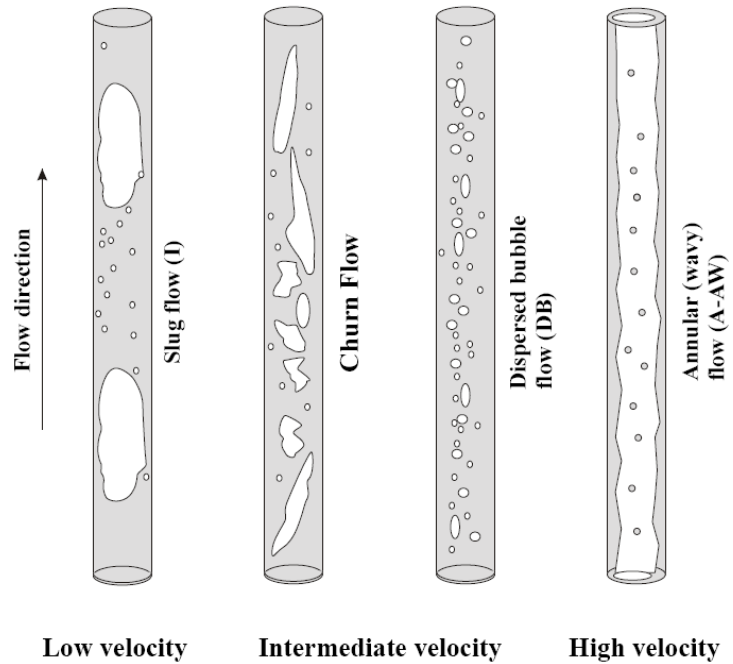


Figure 4.2, Flow regimes in vertical flow [5].

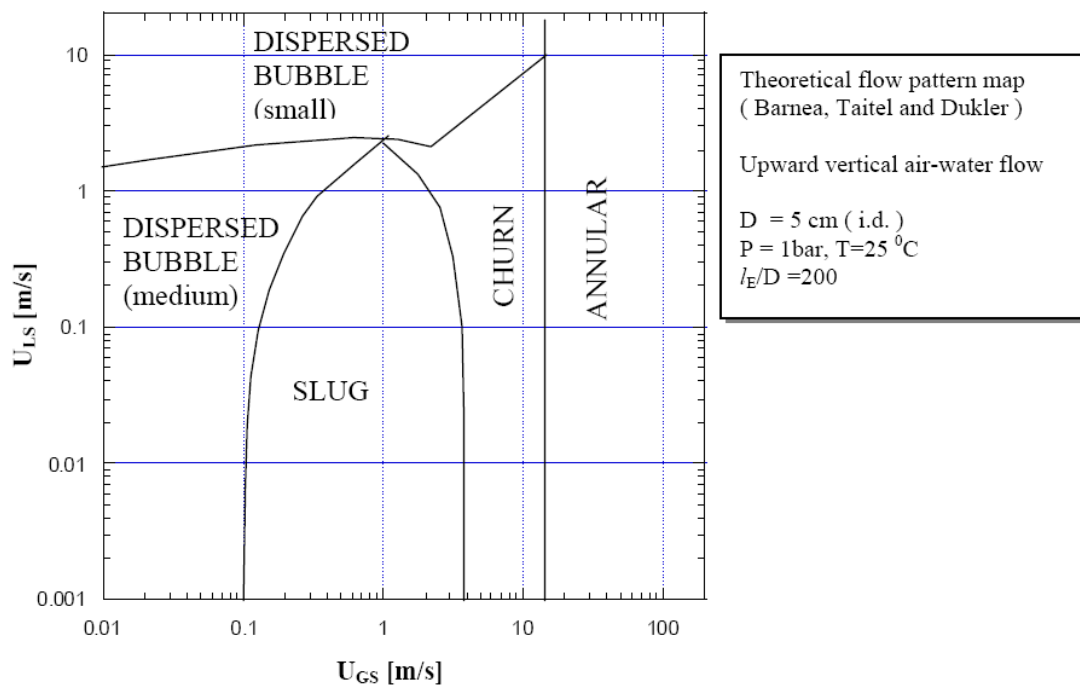


Figure 4.3, Flow regime map for vertical flow [5].

The superficial velocities are defined by:

$$U_{LS} = \frac{q_L}{A} \quad (\text{Eq. 4.1})$$

$$U_{GS} = \frac{q_G}{A} \quad (\text{Eq. 4.2})$$

They are also referred to as apparent velocities or volumetric fluxes. From the definition we see that the volumetric flowrates and the pipe cross section A is known, the superficial velocities follow directly.

The phase velocities are the real velocities of the flowing phases. They may be defined locally (at a certain position in the pipe cross section) or as a cross sectional average for the pipe. They are defined by:

$$u_L = \frac{q_L}{A_L} \quad (\text{Eq. 4.3})$$

$$u_G = \frac{q_G}{A_G} \quad (\text{Eq. 4.4})$$

Gas and liquid in general flow with different phase velocities in pipe flow. The relative phase velocity or the *slip* velocity is defined by:

$$u_S = |u_G - u_L| \quad (\text{Eq. 4.5})$$

The slip velocity thus has the same unit as the phase velocities. In addition the slip ratio is commonly used:

$$S = \frac{u_G}{u_L} \quad (\text{Eq. 4.6})$$

Note that the slip ratio is dimensionless. Slip effect is seen in inclined flow and is caused by the density difference between the gas and liquid, which in turn causes a velocity difference; the gas will rise through the liquid [5].

“Hold up” is a consequence of slip and is defined as the proportion of the pipe that is occupied by liquid.

Multiphase flow correlations are used to predict the liquid holdup and frictional pressure gradient. Correlations in common consider the oil and gas lumped together as one equivalent fluid. They are therefore more correctly termed 2-phase flow

correlations. Depending on the particular correlation, flow regimes are identified and specialised holdup and friction gradient calculations are applied for each flow regime. Some of the correlations most widely accepted for oil wells are:

- Duns and Ros
- Hagedorn and Brown
- Orkiszewski
- Beggs and Brill

5. Artificial lift

Maximizing the use of natural energy in a reservoir is critical to any production installation. In a naturally flowing well there is enough energy stored in the reservoir to flow the produced fluid to the surface. Reservoir pressure and formation gas provide this energy in the flowing well. When reservoir energy is too low for natural flow, or when the desired production rate is greater than the reservoir energy can deliver, it becomes necessary to put the well on some form of artificial lift. As of 2006, 90 % of the world's oil wells are on some form of artificial lift according to Oilfield Review [16].

An oil well usually flows naturally initially, that means the pressure at well bottom is sufficient to overcome the pressure losses in the well and flow line to the separator. When the criteria is no longer met due to decrease in bottom hole pressure, or pressure losses in the well become too great, the natural flow stops and the well dies. The increased pressure losses in the well can come from increased overall density due to decreased gas production, increased water cut or mechanical problems like downhole restrictions (scale etc).

Artificial lift methods fall into two groups, those that use pumps and those that use gas [17].

Pump Types:

- Beam Pump / Sucker Rod Pumps (Rod Lift)
- Progressive Cavity Pumps (Jet /piston lift)
- Subsurface Hydraulic Pumps
- Electric Submersible Pumps (ESP)

Gas Method:

- Gas Lift

5.1. Artificial lift on Gyda

Since a peak in 1995, production on Gyda has decreased (Fig. 2.4). This is due to a decreasing reservoir pressure and increasing water cut which comes from a large amount of water being injected to support the reservoir pressure.

A jet pump was tried on well A-26 in 1995 when BP was operator of the field [12]. The trial was without success due to the plugging of the pump. Scale (calcium sulphate) was found in and above the pump. During this study a second attempt on investigating the use of jet pumps was done. The results showed that the solutions available had too little production potential and the risk of the pumps scaling up again was too high.

In 1997 the use of ESPs was excluded from Gyda because they couldn't withstand the high downhole temperatures of 160 °C. However, the use of ESPs is now up for debate again as pumps are made to run under tougher conditions. Technology developed from steam-assisted gravity drainage (SAGD) operations is planned to be implemented on Gyda. The SAGD equipment can withstand bottom hole temperatures of up to 218 °C [9].

During summer 2007 gas lift was installed on Gyda and has been a big success. The first well to be subject for gas lift (A-17A) increased production rate from 400-500 bbl/d to 1100 bbl/d. This was when all available gas was injected to this single well (56 600 Sm³/day). The second well of interest (A-02A) died due to high water cut and low reservoir pressure. With gas lift Talisman Energy Norge AS (TENAS) succeeded getting this well back on production with initial rate of 1500 bbl/d. Today A-27A is also on gas lift.

As the production rate is decreasing there is no doubt that TENAS should continue improving artificial lift on Gyda. The question is if gas lift or ESP is the best solution.

A-19 and A-26 has been chosen to be a part of a pilot project for artificial lift because of their great potential of higher production. If the pilot project works out good, a full field artificial lift campaign can be realized. Later in this report production is simulated for different scenarios in A-19 and A-26.

5.2. Artificial lift selection

To realize the maximum potential from developing any oil or gas field, the most economical artificial lift method must be selected. This chapter discusses some of the most commonly used methods for selecting an artificial lift system. In most cases, what has worked best or which lift method performs best in similar fields serve as selection criteria. Also, the equipment and services available from vendors can easily determine which lift method will be applied. However, when significant costs for well servicing and high production rates are a part of the scenario, it becomes prudent for the operator to consider most, if not all, of the available evaluation and selection methods.

If the “best” lift method is not selected, such factors as long- term servicing costs, deferred production during workovers, and excessive energy costs (poor efficiency) can drastically reduce the net present value (NPV) of the project.

5.2.1. Selection by Consideration of Depth/Rate System

One simple selection or elimination method is the use of charts that show the range of depth and rate in which particular lift types can function. Charts like this are approximate for initial selection possibilities along with advantage/disadvantage lists (see next section). Particular well conditions, such as high viscosity or sand production, may lead to the selection of a lift method not initially indicated by the charts. Specific designs are recommended for specific well conditions to more accurately determine the rates possible from given depths [4].

5.2.2. Selection by Advantages and Disadvantages

Table 5.1 provides a useful summary of advantages and disadvantages of the two alternative lifting systems on Gyda, while Table 5.2 gives an overall consideration. Much of the selection process can be accomplished with depth rate charts and this extensive set of tables of artificial lift capabilities. But very severe and special conditions can require further study.

Consideration of reservoir characteristics and location are examples of what will fall into this category. If the well may be expected to decline rapidly, it would not be wise to choose a high volume method that will only be required for a short time. Another example would be if there is a lack of electric power or economically supplied electric power; the use of ESPs is not possible [8].

Table 5.1

Advantages and disadvantages of ESP and gas lift [4]			
ESP		Gas lift	
Advantage	Disadvantage	Advantage	Disadvantage
Can lift extremely high volumes.	Only applicable with electric power.	Can handle large volumes of solids with minor problems.	Lift gas is not always available.
Unobtrusive in urban locations	High voltages (1000 V) are necessary.	Handles large volume in high-PI wells.	Not efficient in lifting small fields or one-well leases.
Applicable offshore	Impractical in shallow, low volume wells.	Unobtrusive in urban locations.	Difficult to lift emulsions and viscous crude.
Corrosion and scale treatment easy to perform.	Expensive to change equipment to match declining well capability.	Power source can be remotely located.	Gas freezing and hydrate problems.
Simple to operate.	Cable causes problems in handling tubulars.	Lifting gassy wells is no problem.	Cannot effectively produce deep wells to abandonment.
Easy to install downhole pressure sensor for telemetering pressure to surface by cable.	System is depth limited because of cable cost and inability to install enough power downhole.	Fairly flexible-convertible from continuous to intermittent to plunger lift as well declines.	Some difficulty in analyzing properly without engineering supervision.
Availability of different sizes.	Not easily analyzable unless good engineering know-how.	Easy to obtain downhole pressure and gradients.	Casing must withstand lift pressure.
Lifting costs for high volumes generally very low	Gas and solids production are troublesome.	Sometimes serviceable with wireline unit.	Safety problem with high pressure gas.
Crooked holes present no problem.	Lack of production rate flexibility.	Crooked holes present no problem.	
	More downtime when problems are encountered because of the entire unit being downhole.	Corrosion is not usually as adverse.	
	Casing size limitations.	Applicable offshore.	
	Cannot be set below fluid entry without a shroud to route fluid by the motor. Shroud also allows corrosion inhibitor to protect outside of motor.		

Table 5.2

Design considerations and overall Comparisons [7]		
Consideration/System	ESP	Gas lift
Capital cost details	Relatively low capital cost if electric power available. Costs increase as horsepower increases.	Well gas lift equipment cost low but compression cost may be high. Central compression system reduces overall cost per well.
Downhole Equipment	Requires proper cable in addition to motor, pumps, seals, etc. Good design plus good operating practices essential.	Good valve design and spacing essential. Moderate cost for well equipment (valves and mandrels). Choice of wireline retrievable or conventional valves.
Operating Efficiency	Good for high-rate wells but decreases significantly for <1000 bbl/day. Efficiency can vary from 40% in a low-rate well to 60% in a high-rate.	Fair. Increases for wells that require small injection GLRs. Low for wells requiring high GLRs. Typically 20%, but range from 5 to 30%.
Flexibility of system	Poor for fixed speed. Requires careful design. Variable speed drive provides better flexibility.	Excellent. Gas injection rate varied to change rates. Tubing needs to be sized correctly.
Miscellaneous problems	Requires a highly reliable electric power system. System very sensitive to changes downhole or in fluid properties.	A highly reliable compressor with 95+% run time required. Gas must be properly dehydrated to avoid gas freezing.
Operating costs	Varies. If high horsepower, high energy costs. High pulling costs result from short run life especially in offshore operation. Repair costs often high.	Well costs low. Compression cost varies depending on fuel cost and compressor maintenance.
System reliability	Varies. Excellent for ideal lift cases; poor for problem areas (very sensitive to operating temperatures and electric malfunctions).	Excellent if compression system properly designed and maintained.
Salvage value	Fair. Some trade-in value. Poor open market values.	Fair. Some market for good used compressors and mandrels/valves.
System total	Fairly simple to design but requires good rate data. System not forgiving. Requires excellent operating practices. Each well is an individual producer with a common electric system.	An adequate volume, high pressure, dry, noncorrosive, and clean gas supply source is needed throughout the entire life. System approach needed. Low backpressure beneficial. Good data needed for valve design and spacing.

One of the factors to consider in artificial lift selection is the failure rates for the various systems or the individual components of the systems. Figure 5.1 shows the run-life of ESP systems versus their designed motor Horse Power (HP).

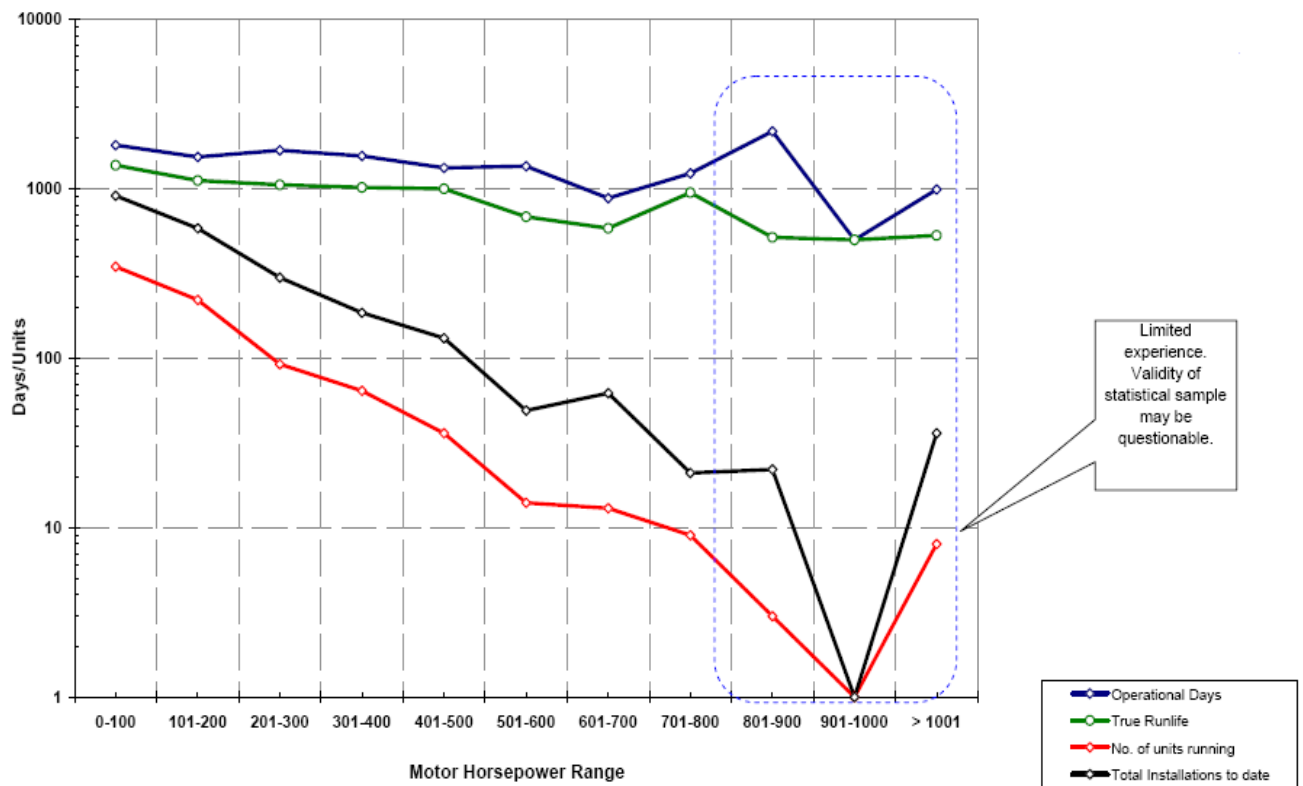


Figure 5.1, Run life of ESP systems. The figure is based on Centrilift data. [13]

It is important to note that data like this, which is based on a manufacturer's experience, may be subject to overestimation.

When planning a new well or field, one must be careful to compare too much with other run life studies. The run life of a system is dependent on local conditions like scale potential, temperature, sand production etc.

5.2.3. Selection by Net Present Value Comparison

A more thorough selection technique depends on the lifetime economics of the available artificial lift methods. The economics, in turn, depend on the failure rates of the system components, fuel costs, maintenance costs, inflation rates, anticipated revenue from produced oil and gas, and other factors that may vary from system to system.

A typical NPV formula can look like this:

$$NPV = \sum_{i=1}^n \frac{WI(Q_{HC} \times P_{HC} - Cost - Tax)_i}{(1+k)^i} \quad (\text{Eq. 5.1})$$

Where:

- WI = Work Interest (Talisman Energy Norge has 61% on Gyda)
- Q = Oil rate
- P = Oil price
- Cost = All costs, operational (Opex) and capital (Capex)
- Tax = Governmental taxes
- k = depreciation rate of the project (percent)

To use the NPV comparison method, the user must have a good idea of the associated costs for each system. This requires that the user evaluate each system carefully for the particular well and be aware of the advantages and disadvantages of each method and any additional equipment that may be required. Because energy costs are part of the NPV analysis, a design for each feasible method must be determined before running the economic analysis to better determine the efficiency of a particular installation [4].

6. Electric Submersible Pumps (ESPs)

Electric Submersible Pump systems incorporate an electric motor and centrifugal pump unit run on a production string and connected back to the surface control mechanism and transformer via an electric power cable.

The downhole components are suspended from the production tubing above the well's perforations. In most cases the motor is located on the bottom of the work string. Above the motor are the seal section, the intake or gas separator, and the pump. The power cable is clamped to the tubing and plugs into the top of the motor.

As the fluid comes into the well it must flow past the motor and into the pump. This fluid flow past the motor, aids in the cooling of the motor. The fluid then enters the intake and is taken into the pump. Each stage (impeller/diffuser combination) adds pressure or head to the fluid at a given rate. The fluid will build up enough pressure, as it reaches the top of the pump, to be lifted to surface and into the separator or flow line.

The basic ESP downhole equipment is:

- The power cable
- The Pump
- The seal chamber section
- The motor
- Monitoring system (optional)

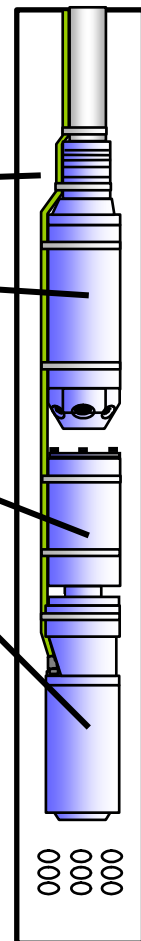


Figure 6.1, Basic ESP

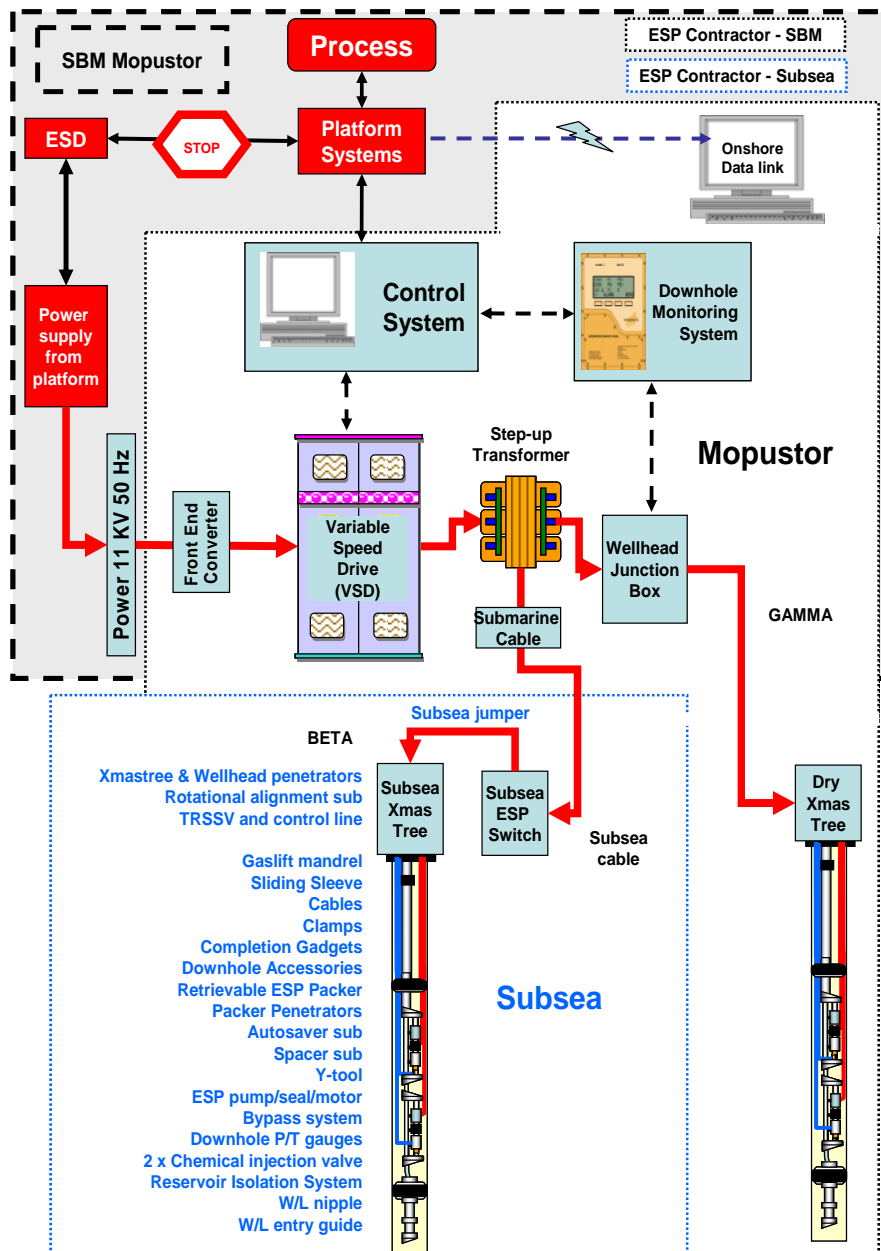


Figure 6.2, ESP surface system.

Figure 6.2 shows an example of a full ESP system. Since this study is more about pump performance and sizing, the surface equipment will not be described in detail. However the importance and complexity of this must not be forgotten in an ESP design. The surface controller provides power to the ESP motor and protects the downhole ESP components. Motor controller designs vary in complexity from the very simple and basic to the very sophisticated, which offers numerous options to enhance the methods of control, protection and monitoring of the operation.

Submersible systems have a wide performance range and are one of the more versatile lift methods. Standard surface electric drives outputs from 150 to 150,000

bbl/d (24 to 24,600 m³/d) and variable speed drives add pump flexibility. High GOR fluids can be handled, but large gas volumes can lock up and destroy pumps. Corrosive fluids are handled by using special materials and coatings. Modified equipment and procedures allow sand and abrasive particles to be pumped without adverse effects. [15]

6.1. Centrifugal pump

The ESP is a multistage centrifugal pump. A cross section of a typical design is shown in figure 6.3.

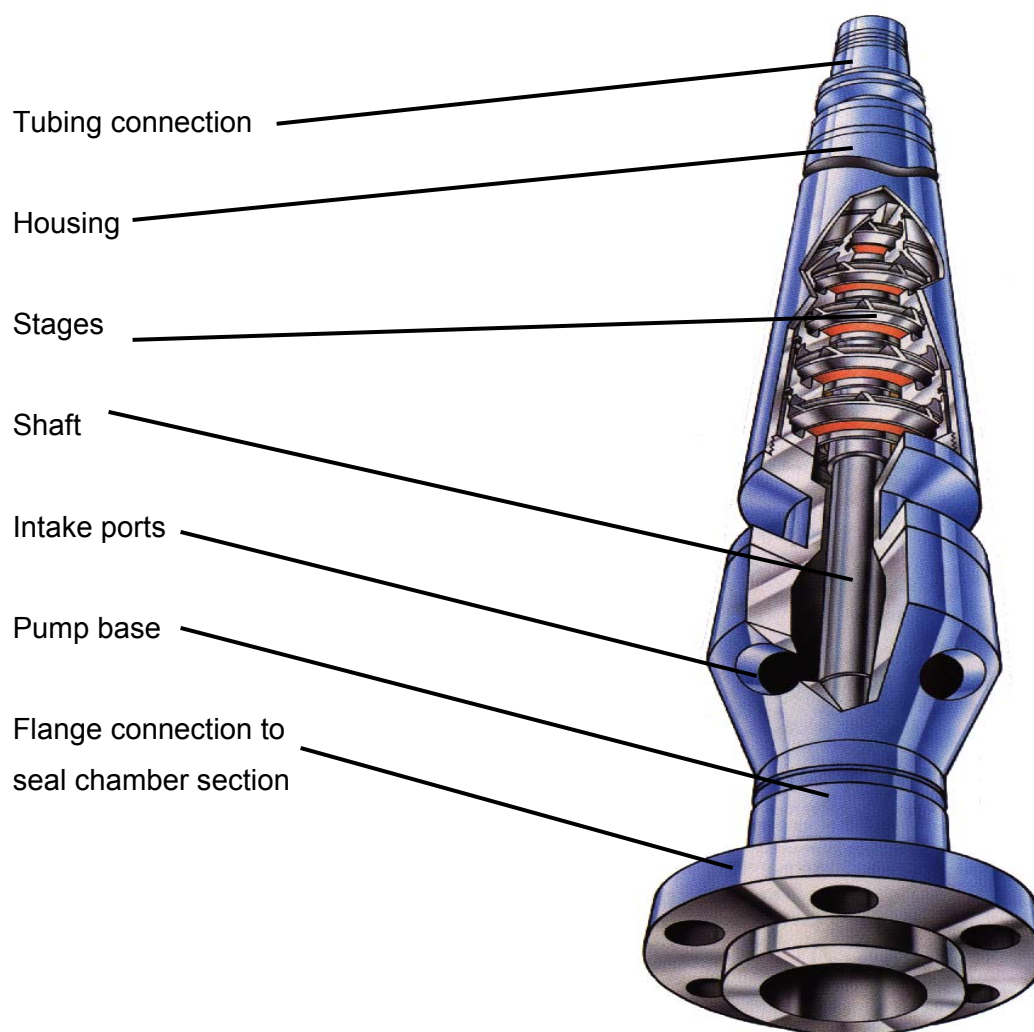


Figure 6.3, the inside of a centrifugal pump.

The *shaft* is connected to the seal-chamber section and motor. It transmits the rotary motion from the motor to the impellers of the pump stage. The shaft and impellers are keyed, and the key transmits the torque load to the impeller.

The *stages* of the pump are the components that impart a pressure rise to the fluid. A stage is made up of a rotating impeller and a stationary diffuser.

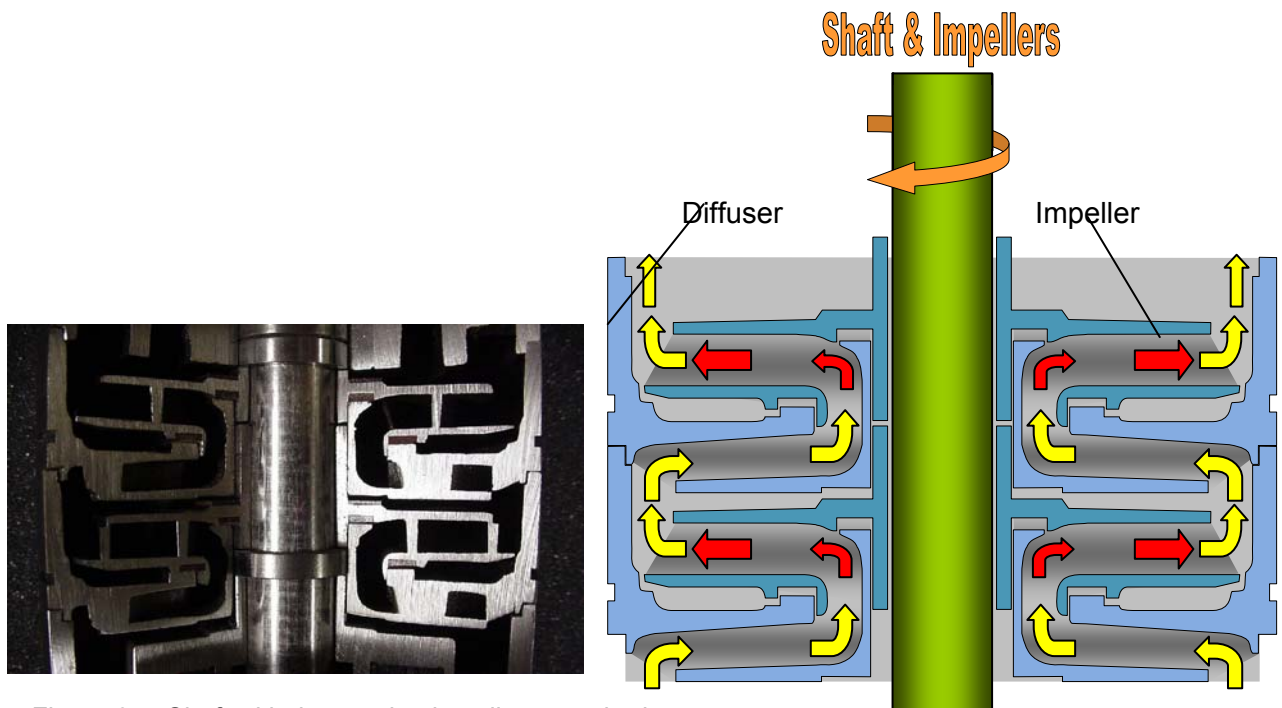


Figure 6.4, Shaft with the rotating impellers attached

The stages are stacked in series to incrementally increase the pressure to that calculated for the desired flow rate. Figure 6.4 shows the flow path. The fluid flows into the impeller eye area and energy, in form of velocity, is imparted to it as it is centrifuged radially outward impeller passageway. Once it exits the impeller, the fluid makes a turn and enters the diffuser passageway. As it passes through this passageway, the fluid is diffused, or the velocity is converted to a pressure. It then repeats the process upon entering the next impeller and diffuser set. This process continues until the fluid passes through all stages, and the design discharge pressure is reached. This pressure increase is often referred to as the total developed head (TDH) of the pump.

There are two styles of stages for the range of flow rates in which ESPs operate. A radial stage has the flow entering the impeller or diffuser parallel to the axis of the shaft and exiting perpendicular to the shaft. This is often referred to as a “pancake” or “mushroom” stage because of its flat shape. The second style is the mixed flow stage which has the flow exiting the impeller at an angle less than 90° to the shaft (see stage in fig 6.5).

The mixed flow design handles larger flow rates than the radial and is not that vulnerable to free gas and particles [4].

A Key feature for both styles of stages is the method by which they carry their produced axial thrust. Usually, the pumps that are under a 6 inch diameter are built as “floater” stages. On these, the impellers are allowed to move axially on the pump shaft between the diffusers. They typically run in a down-thrust position and at high flow rates, they may move into up-thrust.

To maintain the optimum flow path alignment between the impeller and its diffuser, the impeller is designed to maintain a down-thrust position through it’s operating range (figure 6.5).

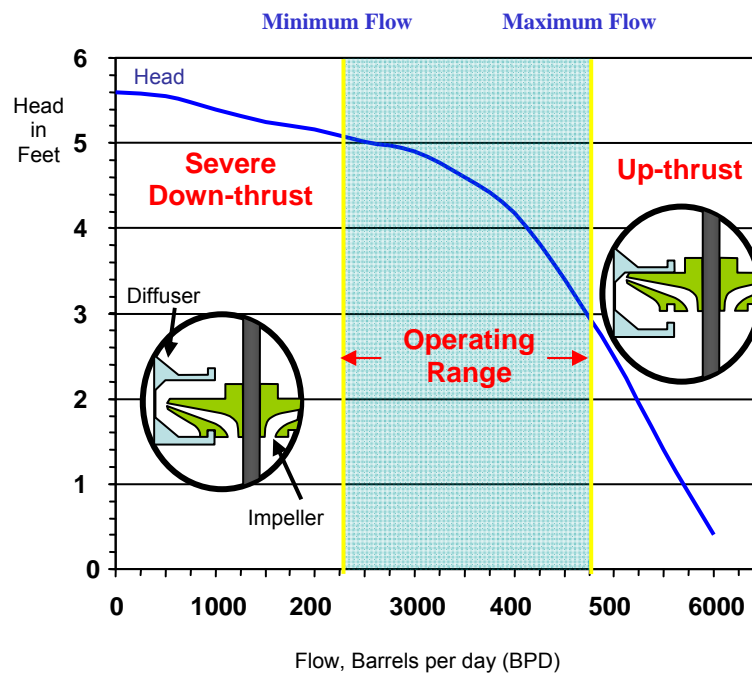


Figure 6.5, ESP operating range

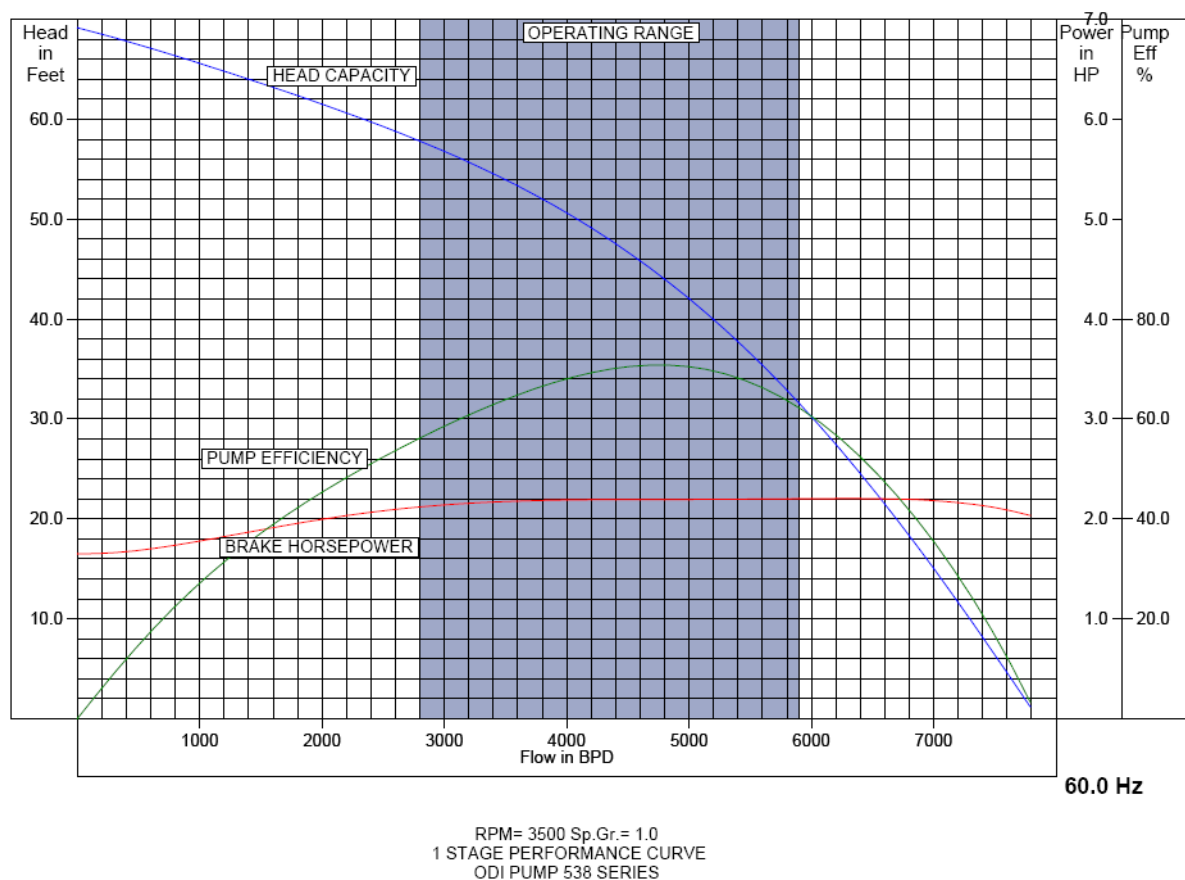
The manufacturers give the pump performance characteristics on the basis of 1 stage, 1,0 SG water at 60- or 50-Hz power. A typical performance graph is shown in figure 6.6. The head, brake horsepower (BHP), and efficiency of the stage are plotted against flow rate on the x-axis. Pump efficiency is given by:

$$\eta_p = \frac{[Q \times TDH \times SG]}{(C \times BHP)}$$

- Where:
- Q = flow rate
 - TDH = Total Head Developed
 - SG = specific gravity
 - BHP = Break horsepower
 - C = constant = 6, 75 (when Q = m³/d and TDH = m)

The head/flow curve shows the head or lift, measured in feet or meters, which can be produced by one stage. Because head is independent of the fluid SG, the pump produces the same head on all fluids, except those that are viscous or have free gas entrained. If the lift is presented in terms of pressure, there will be a specific curve for each fluid, dependent upon its SG.

The highlighted area on the graph is the manufacturer's recommended operating range. It shows the range in which the pump can be reliably operated. The left edge of the area is the minimum operating point, and the right edge is maximum operating point. The best efficiency point (BEP) is between these two points, and it is where the efficiency curve peaks. The shape of the head/flow curve and the thrust characteristics curve of that particular stage determines the minimum and maximum points. The minimum point is usually located where the head curve is still rising, prior to its flattening or dropping of and at an acceptable down-thrust value. The location of the maximum point is based on maintaining the impeller at a performance balance based on consideration of the thrust value, head produced and acceptable efficiency.



Figures 6.6, Standard pump curves for head, efficiency and BHP [19].

6.2. Seal Chamber section

The component located below the lowest pump section and directly above the motor, in a standard ESP configuration, is the seal chamber section. It is basically a set of protection chambers connected in series or in some special cases in parallel. This component has several functions that are critical to the operation and run life of the ESP system, and the motor in particular.

- It protects the motor oil from being contaminated by the wellbore fluid.
- It allows for pressure equalization between the interior of the motor and the wellbore.
- It also absorbs the axial thrust produced by the pump and dissipates the heat that the thrust bearing generates.



Figure 6.7, Seal.

Figure 6.7 shows a mechanical seal which is generally located at the top of each protection chamber and is used to prevent well fluid from migrating down the drive shaft.

6.3. The Motor

The ESP motor is a two-pole, three-phase, squirrel cage, induction design. A two-pole design means that it runs at 3600 rpm at 60 Hz power or roughly 3500 rpm actual operating speed. It operates on three-phase power at voltages as low as 230 and as high as 5000. Generally, the length and diameter determines the motors HP rating. Because the motor does not have a power cable running along its length, it can be manufactured in diameters slightly larger than the pumps and seal chamber sections and still fit in the same casing bores.

6.4. The power cable

The ESP power cable transmits the required surface power to the ESP motor. It is a specially constructed three-phase power cable designed specifically for downhole well environments. The cable design must be small in diameter, protect from mechanical abuse, and impervious to physical and electrical deterioration because of aggressive well environments. They can be manufactured in either round or flat configurations (figure 6.8 and 6.9). The round design is the best conductor, but the flat design is often used beneath the ESP packer and along the pump and seal section because of the small space between ESP and casing.



1=Armour, 2=Jacket, 3=Basic insulation, 4=Physical filler, 5=Conductor

Figure 6.8, round design



1=Armour, 2=Braid, 3=Barrier layer, 4=Jacket, 5=Conductor/insulation gas block, 6=Conductor

Figure 6.9, flat design

6.5. ESP run life

ESP run lives are dependent on numerous variables broadly characterised as; equipment, operation and operating environment. A combination of these factors can produce significant variation in ESP survival times, as presented in Figure 6.10.

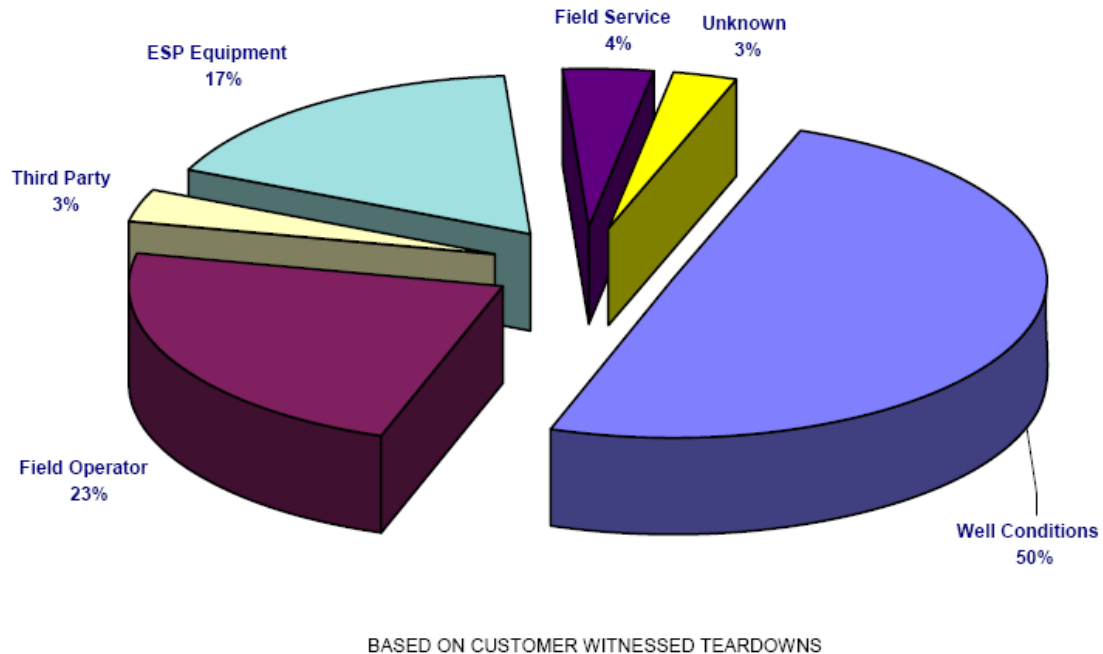


Figure 6.10, Factors acting on ESP run life [13]

The reliability model for ESPs is described as the “bathtub” concept and uses three stages in the life of an ESP:

- Stage one Infant mortality ESP fails to start at installation.
- Stage two In-service failures Operational issues.
- Stage three Wear out Failure due to pump wear out.

The failure rates experienced in each of the three stages are not related and must be analysed separately.

Stage one failures occur within 2 days or less of operation. These are therefore represented as a percentage of installations that are predicted to not start. A typical cause would be damage on installation usually when running in hole (RIH), incorrect electrical connection or foreign objects left in the well damaging the stages of the pump.

Stage two failures are time independent; this is the field operation of the equipment. Electrical failures are common due to insufficient cooling of a unit which occurs at

very low flow rates, through gas locking and dead heading of the pump – all of these are avoidable under careful supervision. A particularly high risk time is at start up when the shaft can snap and undesirable operating ranges may need to be traversed. Pressure cycling can also cause the cabling to the pump to fail.

Stage three failures are analysed less frequently with strip downs as pumps generally are expected to fail at this point or have been replaced as part of a proactive workover plan. Many of the components have a limited life, especially the seals, which will degrade over time [12].

The factors on which the run life is dependent on are listed below:

Design and Sizing

Proper sizing of the ESP unit is the first factor in achieving a long run life. The unit must be sized to operate within the recommended flow range. Well productivity data must be accurate to properly size the equipment. The consequences of improper sizing is that the ESP will be running outside of operating range causing accelerated pump wear, the risk of motor burn out from excessive gas locking or very low flow rates. Inaccurate fluid data can lead to a pump sized for the wrong conditions.

Operating Practice

Poor operating practices are a major cause of failure for ESPs. These can be as a result of lack of knowledge in operating the units or an unexpected change of the operating environment.

Downhole information can be used to provide a better perspective of ESP operation and performance. Only 2% of ESPs in the world have downhole sensors and even those with the data often neglect to use it to control the pumps. Detailed real time information concerning the pump pressures and temperatures the system is experiencing downhole can be used to help protect, control and optimise the operation of the ESP.

BHT Temperature

Bottomhole temperatures greater than 105 °C is considered a high temperature application for ESPs. The motor assembly will need to be checked for clearance at the higher temperatures. The consequence of not taking these measures will be a shorter component life or reduced MTTF (Mean Time To Failure).

Free Gas

As ESPs are designed to pump liquids and not gas, breakout of free gas or alternating slugs of liquid and gas can lead to operational difficulties. As fluid velocity decreases past the motor, cooling will become less efficient, and the danger of the motor over heating and burning out increases. In the extreme, as the proportion of free gas increases, the pump begins to lose head and spin empty of fluid in a condition called gas locking.

Viscosity

High fluid viscosity can cause many problems. As the specific gravity of the fluid increases, so does the pump break horsepower requirement. High viscosity also reduces the pump's ability to lift the fluid and its efficiency, as the viscous fluid produces more frictional pressure loss in the tubing causing the pump to work much harder. The viscosity of produced fluids may change with the application of shear by the pump; this may alter over a range of water cuts. Tight emulsions can be formed under certain conditions.

Corrosion

Corrosion from CO₂ and H₂S can affect the ESP unit by eroding electrical connections, seals and fastenings long before impeller performance is degraded. Appropriate material selection can avoid these issues.

Sand Abrasion

Sand production can be detrimental to ESP performance by reducing pump efficiency through abrasive wear to the stages. More immediate failure is due to increased pump shaft vibration, which in turn leads to mechanical failure of the seals and motor burn out due to the subsequent fluid migration.

The most effective strategy is to eliminate or reduce sand production. Sand production can be managed through controlled start up and an understanding of sand mobilisation rates. The same sand can be produced repeatedly through the pump without making it surface.

Damage to impellers and stages can be reduced by appropriate material selection and an abrasion resistant pump design which provides support and radial shaft stabilisation.

Foreign Material

The production of foreign material can cause damage or failure of an ESP. Although rare, a foreign object can jam the pump resulting in motor burn out, more commonly the material will damage the impellers thus reducing the lift efficiency of the pump.

Deposition

Scale, asphaltenes, paraffin and hydrates can all deposit in ESPs. The result can be blocked or limited pump inflow, reduced efficiency of pump stages or locking of stages, with the consequences being reduced efficiency and the associated danger of motor burn out.

Electrical Failure

Electrical failure can happen at surface or downhole. Problems at surface such as overload of the controller or transformer are easier to rectify than those downhole that interrupt the power source and require a workover intervention to change out ESP.

Old Age

Even if the ESP has been operated within the design envelope and care has been taken operationally, the time will come where certain components reach failure point. The hardware, stages and bearings are usually over designed so the failure is most likely to come from 'consumable' items. Seals will degrade over time, motor oil deteriorates, o-rings and connections all have shelf lives and electrical components within the pump and downhole monitoring package will fail. However, there are many examples of ESPs that have exceeded run life targets of over 5 years in operation.

Reliability Issues Specific to High Horse Power Units

Higher HP units are exposed to greater risk. A higher HP unit contains more motor sections and is therefore physically longer than other units. Installation can lead to the mechanical damage of units which puts them into the infant mortality category of the reliability model. The longer length of the unit, the higher the risk of damage. Dogleg severity and deviation limits will be required to be more stringent than for the shorter models. Increased physical protection can be supplied by running pumps in an enclosed pod to provide defence against mechanical damage whilst RIH. This system is much easier to workover and carries much lower operational risks. High horsepower pumps are made up of several lower horsepower pumps run in series and are therefore dependant on one another. This dependency intrinsically

reduces the reliability of the whole system. Reliability is also reduced by the requirement for higher power and torque to be supplied to one motor which then feeds the others [12].

6.5.1 Case studies

Beatrice (Talisman UK) [10]

The graph below, Figure 6.11, represents the frequency of the run time of pumps installed in the Beatrice Field, where Talisman UK is the Operator. This data shows that 50% of the installed pumps (P50) run for up to 470 days without failure. The available data was for ESPs with a HP range between 165 and 685 HP. Most of the Beatrice ESPs are within two HP intervals (201-300) and (401-500). In order to obtain a more accurate analysis, data represented by these two ranges was used to determine the P50 run life instead.

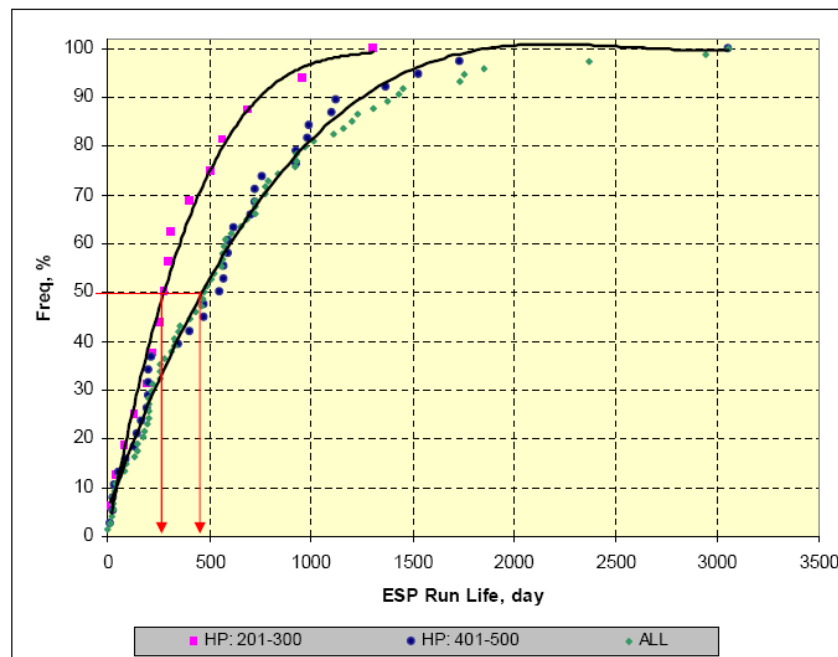


Figure 6.11, ESP run life on Beatrice. The figure shows data from two HP intervals [13].

This Beatrice data analysis covers 54 operating units which is a respectable sample for an individual field. On first inspection, it would seem that the reliability of the ESPs increases with HP, which is contrary to the model that suggests increasing motor complexity is related to a decrease in ESP reliability. However, the range of motor sizes is relatively narrow; most units in the higher HP range are less than 450 HP and the lower range being mainly 250 HP units. Attributing difference in the operating run life over this small range of HPs does not seem reasonable. The run life duration

is being affected by some other factors, namely the operation and operating environment of the pumps.

Wytch Farm

The table below, Table 6.1, represents the frequency of the run time of pumps installed in the Wytch Farm Field, where BP is the operator. This data shows that 50% of the installed pumps (P50) run for up to 1000 days without failure. The available data was for ESPs of a motor size range between 840 HP and 1170 HP. The Wytch Farm data set of 27 units is smaller than the Beatrice data set, but covers a much wider range of motor sizes. The trend here supports the theory that as HP increases, reliability decreases.

Table 6.1, Wytch Farm ESP run life [13]

ESP HP	840	900	1170
P50 Run Life, days	1216	902	859
Average Run Life, days	1073	1108	847

The Wytch Farm run lives are substantially longer than those experienced on the Beatrice field even though much larger horse powered motors are employed.

In order to select which of the two run life results would be more suitable to represent the installation conditions in the Gyda field, a comparison between the properties of both fields against Gyda has to be done. The biggest issue compared to Wytch Farm and Beatrice is the temperature. The two fields have reservoir temperatures of 70 and 80 °C, while Gyda has a reservoir temperature of 160 °C. Scale potential and possible sand production as a result of the high pressure drawdown imposed by the pumps has been identified as two main risks.

Centrilift, which is the ESP supplier, has given an estimated lifetime of approximately two years with a dual ESP solution (described in next section). It must be kept in mind that a manufacturer's estimate may be too optimistic, and it is important that TENAS performs or receive a proper analysis of the ESPs running in Gyda conditions before making a decision.

6.6. ESP design for Gyda

Because of the limited lifetime of ESPs, the suggested design for Gyda is a dual system. This means that two separate systems are installed, one upper and one lower. Only one ESP system operates at the time. The other unit is held as backup until it either fails or is shut down voluntarily.

Dual ESP lift systems enable cost-effective production in applications where rig availability may be at a premium and where the cost of workover impacts the overall profitability of the well.

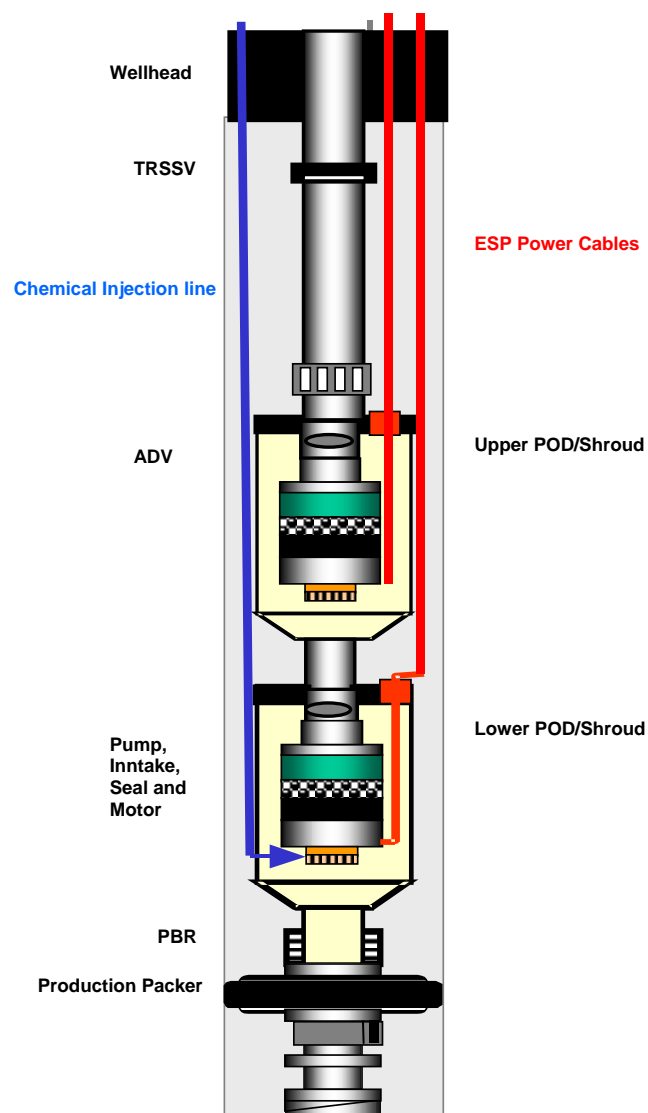


Figure 6.12, Dual ESP system design for Gyda.

The ESPs are planned to be built into shrouds. This is done to seal off the entire system from the casing. The casings in A-19 and A-26 were not originally designed to handle production and interaction with produced fluids. When increased pressure variation from the pumps also was added, it was decided that the sealed system was superior.

To divert the flow between the upper and lower system, Automatic Diverter Valves (ADV) are placed above each pump section. The valves will be in a closed position when there is a pressure build-up from beneath, and will open when there is a pressure build-up from above. This means that when the ESP is operating the valve will stay in a closed position and opens when the pump is turned off. Therefore the production flow can now be directed around or through each ESP depending on which one is operating. The ADV also protects the pump against solids and fluid fall-back when it is turned off, which again increases the run life of the pump. The design allows for bullheading, for killing the well or scale squeezing. A schematic of the ADV operating is shown in figure 6.13 [22].

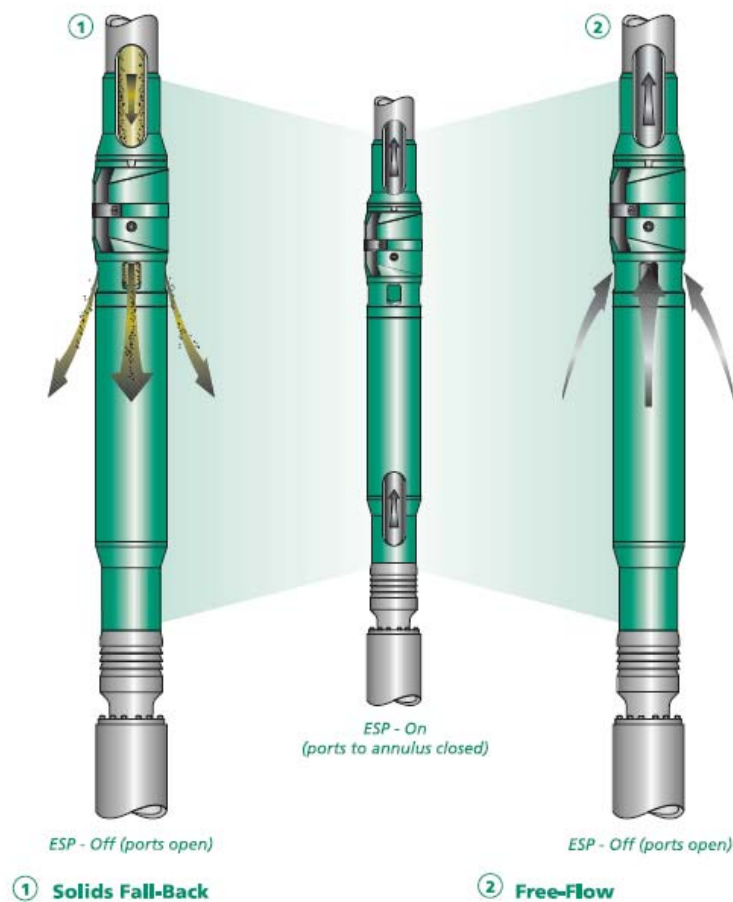


Figure 6.13, ADV operating schematic [22]

6.7. ESP secondary effect

Gyda is divided into 3 main units A-, B- and C-sand (chapter Gyda field), where the upper A-sand has the highest permeability.

When installing ESPs it is expected that the pumps will draw their near wellbore area pressure down with up to 200 bar. An effect of this will be that oil from the low permeability areas will migrate into the high permeability areas. Figure 6.14 shows how oil from the B-sand and lower A-sand migrates into the high permeability upper A-sand. There are large oil reserves in the low permeability zones that initially never would be produced, and this secondary effect can increase oil recovery significantly.

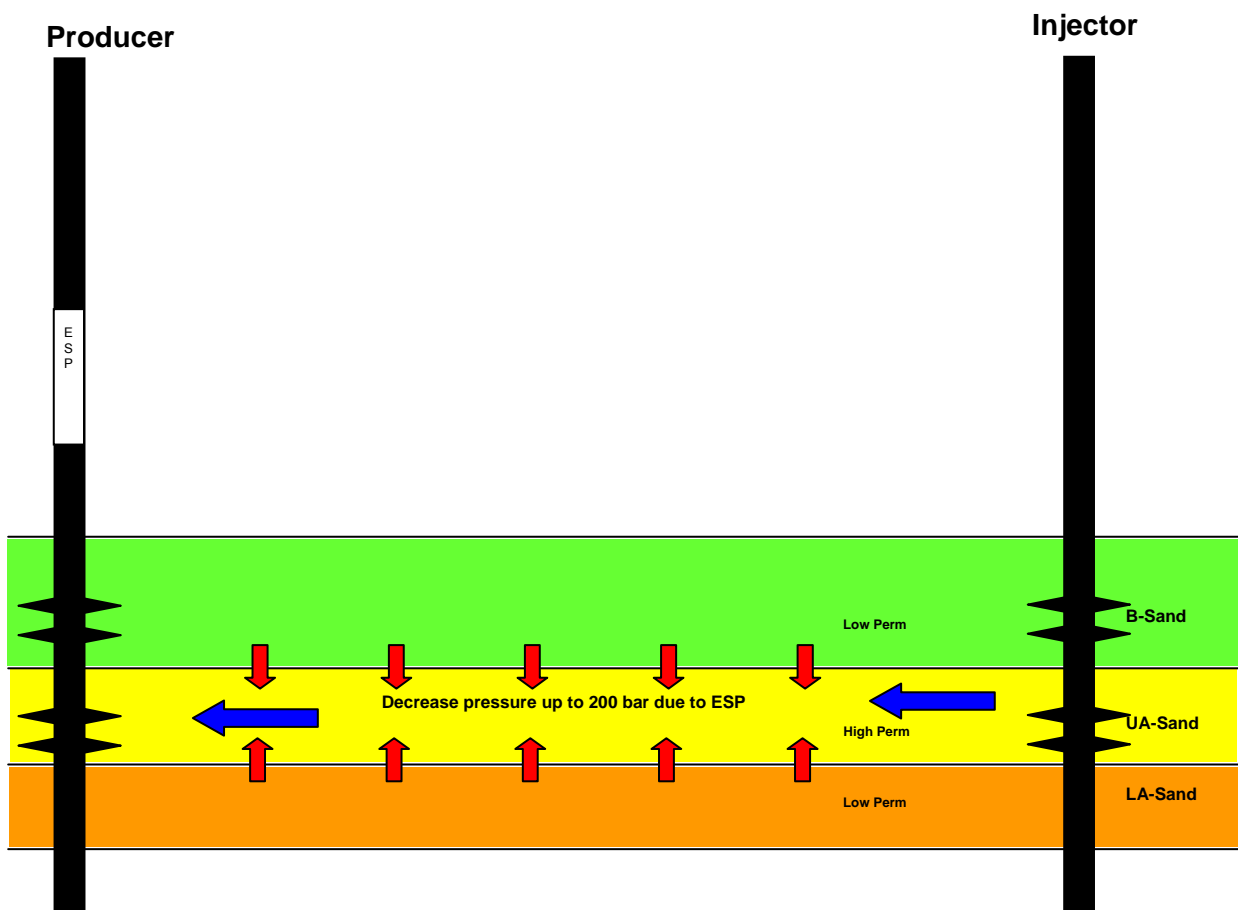


Figure 6.14, ESP secondary effect. Pressure drawdown makes oil migrate into the high perm. zone

This effect is not included in the production forecast later in this study, because it has not been accounted for in the initial reservoir model. However, it can be kept in mind that the result from the production forecast will be conservative and that there is a great possibility of a higher production because of this secondary effect.

7. Gas lift

Gas lift is the process of injecting gas in the annulus between tubing and casing where it will enter the tubing via a gas-lift valve located in a side pocket. The gas will then reduce the weight of the produced fluid column, which will lower the bottomhole pressure. Reservoir fluid will then experience lower resistance to flow, resulting in increased flow rates and increased production.

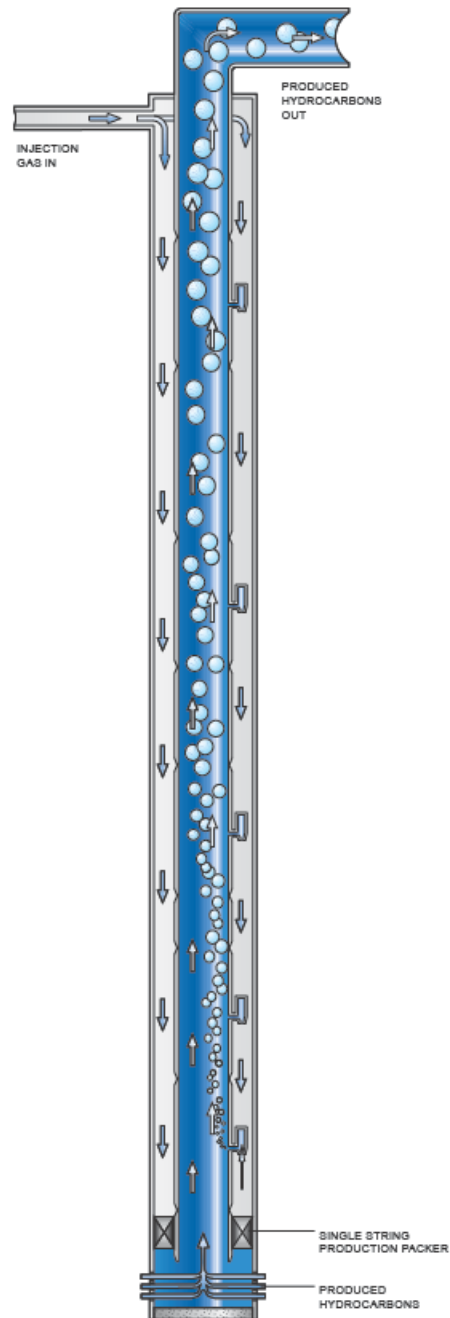


Figure 7.1, Gas lift. Gas is pumped down the annulus and into the tubing [18].

Gas lift is the artificial lift method that most closely resembles the natural flow process. The only major requirements are a supply of pressurized injection gas. Normally, the lift gas is supplied from other producing wells, separated from the oil, run through a gas compressor and pumped in the annulus at high pressure. The gas from the producing well is then recovered again, recompressed and re-injected. However, the gas compressing process is power consuming and expensive [16].

Figure 7.1 shows a typical continuous flow gas lift installation. Other methods are:

Intermittent gas lift:

If the gas is injected in intervals it is called intermittent gas lift. This can be used in low producing wells where one wants to enable some liquid to build up in the bottom of the well before one injects a slug of gas which carries the fluid to surface [18].

Dual gas lift:

Because of limited drilling slots on rigs, an alternative to drilling two separate wells to drain different reservoir sections is to have two independent tubing completions in the same well. If these require gas lift, the gas can be supplied from a common casing and injected into the different gas lift valves (GLV). Another way is to inject the gas in one string and produce from the other. This type of completion is called a dual gas lift.

Self lift:

One alternative to the process of injecting the gas from surface is to simply let it flow naturally from the gas reservoir located above the oil zone. This type of gas lift is called self lift, auto lift or natural lift. The well must penetrate both the gas cap and the oil zone to achieve this. A gas cap or reservoir capable of sustaining the well with sufficient rates for the lifetime of the well is needed for this completion. Self lift completions eliminate the need for surface gas compressors and other gas lift equipment. Such wells can be fitted with downhole flow-control valves and permanent monitoring equipment which qualifies the wells as intelligent wells [16].

7.1. The unloading process

After a well is completed or worked over, the fluid level in casing and tubing is usually at or near the surface. The gas lift pressure available to unload the well is generally not sufficient to unload fluid to the desired depth of gas injection. This is because the pressure caused by the static column of fluid in the well at the desired depth of injection is greater than the available gas pressure at injection depth. In this case a series of unloading valves is installed in the well. These valves are designed to use the available gas injection pressure to unload the well until the desired depth of injection is achieved. Figure 7.2 shows the unloading process in a continuous gas lift system.

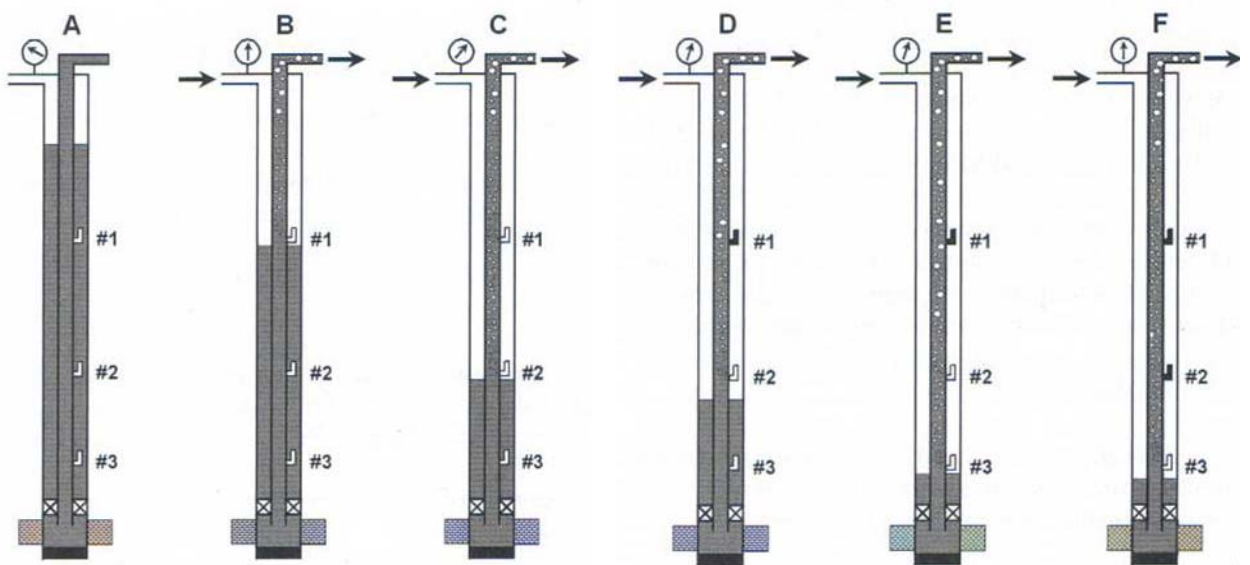


Figure 7.2, the unloading process.

The figure shows a well with 3 gas lift valves, the two uppermost are called unloading valves, while the lowest one is called operating valve. When gas reaches the first unloading valve, gas is injected into the tubing, as shown in part B of Fig 7.2. The liquid in the tubing gets aerated and the static tubing pressure at the valve depth decreases to a stabilized low value that corresponds to the gas liquid ratio (GLR). The lower valves are still open and the liquid level in the annulus continues to drop.

When the liquid level in the annulus reaches the next unloading valve, gas will be injected through the valve. This is the most critical moment in the unloading process, because both unloading valves inject gas at the same time as shown in Part C. The upper valve has to be closed in order to move the injection point down to the operating valve and ensure that gas is injected at a single point only. Proper design

and setting of the unloading valves ensure that the shallower valve closes just after the next lower valve starts injecting gas, as shown by part D.

As the middle valve continues injecting gas, the tubing pressure at that depth falls and the annulus fluid level continues to drop. If the unloading string is properly designed, the stable liquid level in the annulus will be just below the lowest valve, which is the operating valve. When gas reaches the operating valve, gas will be injected into the tubing. Then it is very important that the middle valve closes, as shown part F. By now the objective of the unloading process has been met and gas is injected through the operating valve only [2].

7.2. Gas lift performance curve

The gas lift performance curve is a plot of the well's liquid rate vs. the gas injection rate for a given surface gas injection pressure and shows the producing system's response to continuous flow gas lifting (Fig. 7.3). The figure indicates that at low injection rate, any increase in the gas volume increases the well's liquid output. As injection rates increase, the rate of liquid volume increase falls off and the maximum possible liquid rate is reached. After this maximum any additional gas injection decreases the liquid production. In this region of high gas injection rates, multiphase flow in the tubing is dominated by frictional effects. Consequently, bottom-hole pressure starts to increase and liquid inflow to the well diminishes.

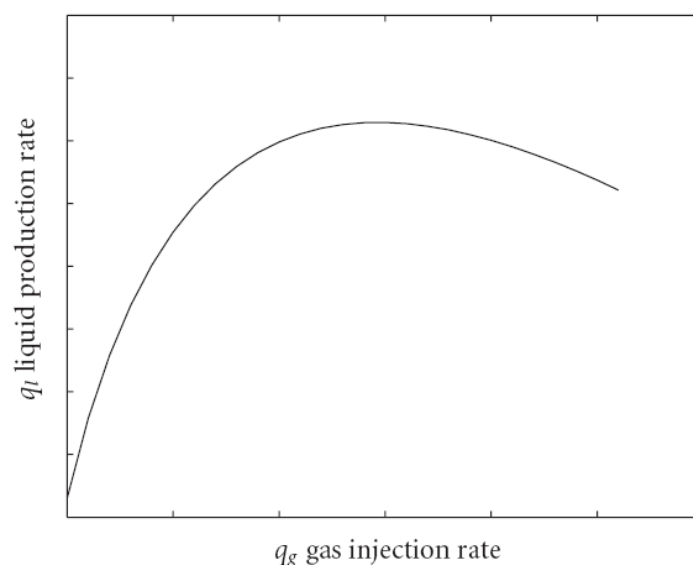


Figure 7.3, Gas lift performance curve. The figure shows the total production rate plotted against the rate of lift gas injected [14].

7.3. Gas lift valves

Unloading valves

The Injection Pressure Operated (IPO) valve is the most commonly used type of unloading gas lift valve, and is currently used on Gyda. Other types worth mentioning are Production Pressure Operated (PPO) valves, balanced bellows valves, balanced flexible sleeve valves, and Pilot valves.

A standard IPO valve contains a nitrogen pre-charge chamber and a flexible bellows assembly, which provide the closing force of the valve. The axial position of the stem determines if the valve is open or closed for gas injection. When injection gas pressure exceeds the closing force the bellows compresses, thus lifting the valve stem off its seat, allowing gas to be injected through the valve. The schematic of a conventional IPO unloading valve is shown in Fig. 7.4. The reverse flow check valve consists of a spring loaded dart and a seat. When the check valve is closed tubing pressure from below push the dart against the seat. Despite the check valve, tubing pressure can act on the valve stem due to pressure trapped between the port and check valve and unavoidable imperfection in the check valve seal.

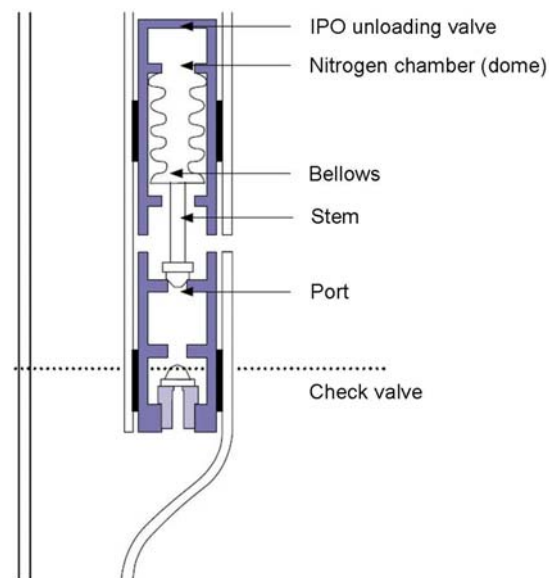


Figure 7.4, conventional unloading valve [24].

By writing the force balance for the valve stem, the conditions for opening and closing can be found. In the closed position nitrogen dome pressure P_d acts on the area of the bellows A_d and provides enough force to keep the stem against the port. All other forces try to open the valve, the largest force comes from the injection pressure P_i , which acts on the doughnut shaped area of the bellows A_d minus the area of the port A_p . A much smaller force comes from the production pressure P_p

that acts on the port area A_p of the stem tip. The valve opens when the sum of the opening forces exceeds the closing force:

$$P_i (A_d - A_p) + P_p A_p > P_d A_d \quad (\text{Eq. 7.1})$$

Solving this equation for injection pressure P_i when forces are in equilibrium:

$$P_i = P_d A_d / (A_d - A_p) - P_p A_p / (A_d - A_p) \quad (\text{Eq. 7.2})$$

To simplify, introducing the term $R = A_p / A_d$, gives the equation for the injection pressure necessary at valve depth to open the valve:

$$P_i = P_d / (1 - R) - P_p R / (1 - R) \quad (\text{Eq. 7.3})$$

As seen from the equation (7.3), to open the valve from the closed position depends not only on injection pressure, but also on production pressure. If production pressure is constant, the valve will open when injection pressure exceeds the value calculated by this equation. When the valve starts to open injection pressure will act on the whole area of the bellows and completely lift the stem off the seat. When the valve is fully open a new force balance can be written. Closing force is as before from the dome pressure P_d , acting on the bellows area A_d . The opening force is provided by only injection pressure P_i acting on the bellows area A_d . The closing equation is therefore:

$$P_i A_d = P_d A_d \quad (\text{Eq. 7.4})$$

$$P_i = P_d \quad (\text{Eq. 7.5})$$

The valve will close when injection pressure becomes lower than the dome pressure. A graphical presentation of the operating principle is shown in Fig. 7.5. When production pressure is higher than injection pressure, the valve is closed by the check valve, that is shown by the area above the line $P_p = P_i$. At injection pressures lower than the dome pressure, the valve will be closed, as shown by the shaded area. Opening of the valve occurs along the bold line where equation (7.3) is in equilibrium. Closing occurs where dome pressure equals injection pressure, as shown by the vertical line and equation (7.5). In the triangular area between the opening line and the closing line, the state of the valve depends on its previous state. This design allows for flexibility should production conditions change, such as water-

cut increase. The disadvantage of this type of valve is that the maximum depth of injection is reduced for each unloading valve used, because casing pressure has to be reduced in order to close an unloading valve [2].

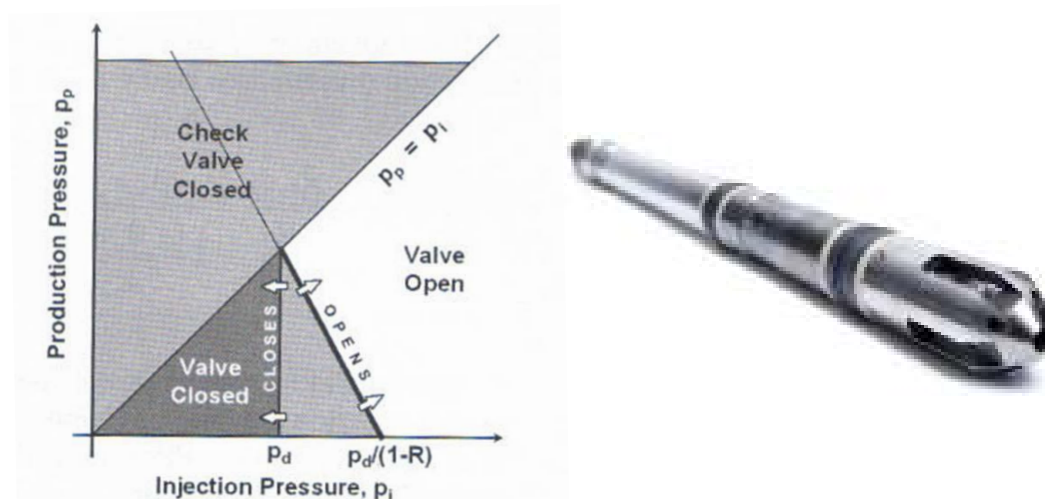


Figure 7.5, IPO gas lift valve operating principle [2]

Operating valve

The lowest valve is often referred to as the operating valve or orifice valve. For a continuous gas lift system it is recommended to use a "Nozzle-Venturi valve" which will provide a more constant gas rate than the old "square-edged orifice".

In a conventional square edge orifice, the gas rate through the valve increases as differential pressure over the valve increases gradually until critical flow is achieved at a critical pressure ratio of about 0,55. At critical flow, supersonic velocity is reached in the orifice, and a further increase in differential pressure will not cause increased gas rate. A typical continuous gas lift installation operates in the subcritical range; this implies that that gas injection rate will change due to inevitable pressure fluctuations at valve depth. When tubing pressure at valve depth increases, the injected gas rate will decrease and vice versa, since the valve is in the sub critical range. This behaviour is opposite to the basic principle of steady continuous gas lifting, which is that there should be more gas injected when it is needed.

Therefore square edge orifice valves are usually not recommended due to instability problems and occurrence of heading in tubing and casing. The orifice size or cross sectional area of the throat will have to be sized according to the gas rate to be

injected to achieve critical flow. A common mistake in gas lift design is to install a too large orifice size which would cause a lower percentage of critical flow. To prevent the problems associated with sub critical flow and instability, replacing the square edge orifice with a converging-diverging venturi nozzle as shown in Fig 7.6, will ensure that critical flow is achieved at a significantly lower differential pressure ratio. A venturi valve will achieve critical flow at as little as roughly 0,9 in differential pressure ratio as shown in Fig 7.7 . This means that with a venturi valve the gas injection rate will stay stable and independent of tubing pressure fluctuations, and prevent heading and instability. The disadvantage of this valve is that it is less flexible for future changes, since the injection rate through it is almost fixed, and that could possibly lead to a lower production rate if a higher production rate is achievable at another rate.

For preventing backflow into the tubing/casing annulus, they are equipped with standard reverse flow check valves.

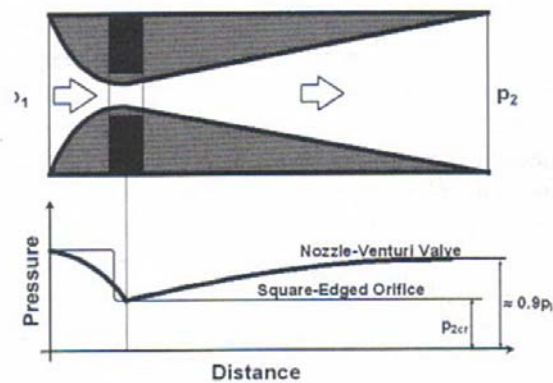


Figure 7.6, cross section of square edge orifice and venturi valve [2].

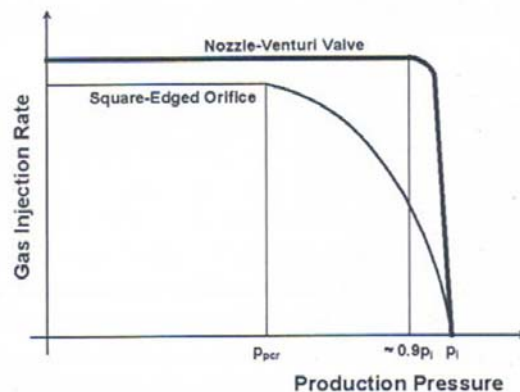


Fig 7.7, Gas passage characteristics comparison [2].

7.4. Gas lift completion procedure

The tubing is fitted with a sidepocket mandrel, where the sidepocket can have a gas-lift valve, a chemical-injection valve or similar. The gas-lift valve can either be preinstalled or it can be placed in the sidepocket by means of wireline. If it is not preinstalled the sidepocket will contain a dummy valve which isolates the tubing from the annulus. Setting and pulling a gas-lift valve is normally done by slickline. But if the well has a deviation of over 65 degrees, an electrical wireline in combination with a well tractor is used. In both cases, a kickover-tool (KOT) is run in the well.

The KOT is lowered into the hole and a location finger will locate an orientation groove in the sidepocket mandrel. It is important to be careful in the transition between pup joint and sidepocket as the location finger can get stuck and one can risk triggering the KOT prematurely. Pulling on the wireline with a predetermined force will orient the KOT in the right direction. Pulling further will shear a pin in the tool allowing the arm with the valve to kick over. It can then be lowered into the empty sidepocket if the well is vertical or pushed by a stoker tool if it is deviated. One should then pressure up the tubing or bleed down the annulus to make sure that the valve is properly latched into the sidepocket. Hopefully, the pressure difference will be sufficient to push the valve in place.

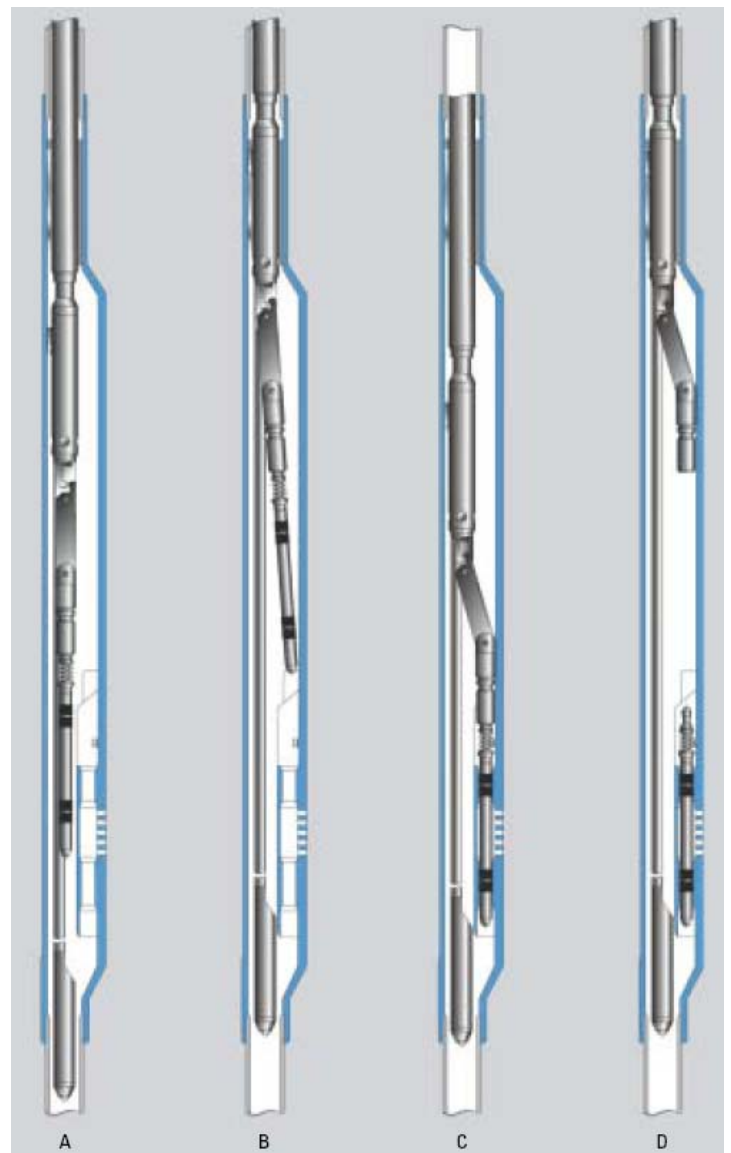


Fig 7.8, Valve installation with KOT. [24]

When the valve is latched into the sidepocket one can pull on the wireline with a predetermined force or activate the stroker and another pin will shear, freeing the running tool from the gas-lift valve. Further pulling on wireline or activation of stroker will shear another pin in the KOT. The tool string can then be pulled out of the well. Figure 7.8 shows the running process. The sequence of pulling a valve is identical, with a pulling tool replacing the running tool [24].

8. PROSPER

PROSPER is the industry standard single well performance design and optimization software, it can model most types of well completions and artificial lifting methods. PROSPER is used by major operators worldwide. The software allow building of well models with the ability to address all variables such as well configuration, fluid characteristics (PVT), multiphase VLP correlations and various IPR models. Tuning of the models is possible by matching real field production data, the benefit of matching is the ability to model different scenarios with increased accuracy.

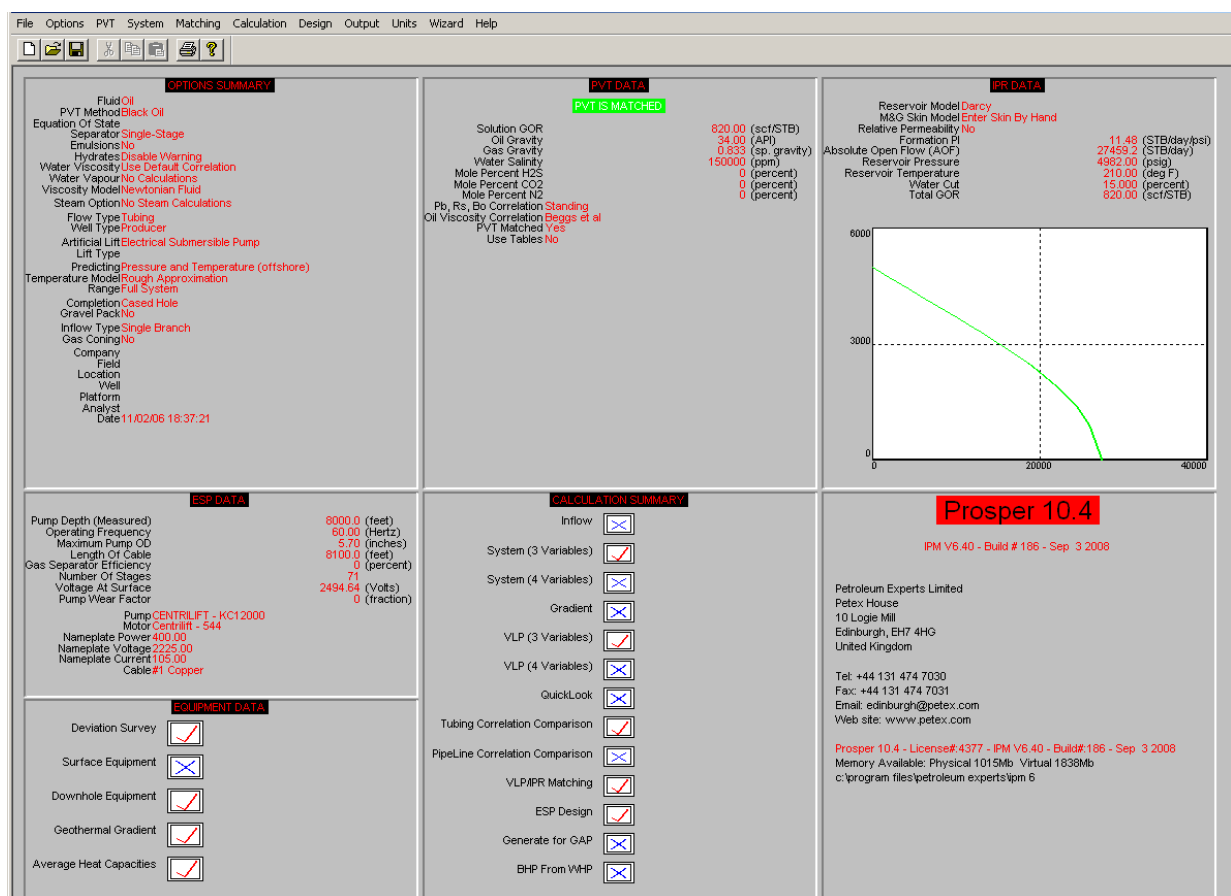


Figure 8.1, PROSPER front display.

Calculation of VLP using multiphase flow correlations with evaluation of VLP variables is the major application of the PROSPER software. Sensitivity analysis on future changes of parameters that affect VLP and IPR are easily assessed.

The artificial lifting methods available are:

- Electric Submersible Pump - ESP
- Gas Lift
- Hydraulic Pumps - HSP
- Progressive Cavity Pumps - PCP
- Jet Pumps
- Sucker Rod Pumps
- Multiphase Pumps
- Injection of diluents
- Gas lift with coiled tubing

A full range of well types can be modelled in PROSPER including gas, oil, water, condensate and steam. Different configurations such as angled, multi-layer and multi-laterals can also be modelled. A full range of IPR models can be used in Prosper including: PI entry, Vogel, Composite, Fetkovich, Jones, horizontal well model plus several others. Various completion configurations such as gravel pack, open, cased and perforated hole are also available. [21]

8.1. Basic theory of PROSPER

To predict pressure and temperature changes from the reservoir, along the wellbore and flow line tubular it is necessary to accurately predict fluid properties as a function of pressure and temperature.

The Black Oil PVT model is used for the vast majority of applications.

Different applications can be chosen for The Black Oil model in PROSPER. It can be tuned to a retrograde condensate model, dry and wet gas model, or an oil and water model. The oil and water model which is used for this study, takes the surface production of oil and associated gas together with the water cut to determine the well mass flow rate. PVT correlations are used to find the amount of gas at each pressure and temperature. B_o , B_g and B_w are evaluated at each calculation step to find the phase densities.

When both basic fluid data and some PVT laboratory measurements are available, the program can modify the Black Oil model correlations to best-fit the measured data using a non-linear regression technique. When detailed PVT laboratory data is provided, it can be entered in table format.

The second option is the Compositional model. This is used when a full Equation of State (EOS) description of the fluid is available and all the PVT can be obtained from a Peng-Robinson or a Soave Redlich Kwong description of the fluid phase behavior. The EOS method relies on empirical correlations for predicting density, viscosity etc. and should only be used for specific specialized applications.

VLP correlations describe various methods of calculating pressure losses in inclined pipes. While the basic form of the pressure loss equation is the same for all correlations, the treatment of multiphase friction and gas/liquid slip (holdup) varies considerably. The various VLP correlations were designed around specific sets of lab data. They can therefore be expected to perform best for field conditions that approximate the experimental conditions.

There is no universal rule for selecting the best correlation for a given well. The correlation must be selected on the basis of flow regimes and closeness of fit to measured pressure data. In making a selection the purpose of analysis should be considered. A slug flow correlation that closely matches current production may not be applicable if, for example, the GOR is expected to increase greatly in the future.

The IPR describes pressure drawdown as a function of production rate. The drawdown is a complex function of pressure drawdown, fluid PVT properties, formation permeability (absolute and relative), effective overburden etc. For practical

engineering purpose, a number of IPR models have been developed and implemented within PROSPER. For this study the PI Entry model (described in section 3.2.) is used [6].

8.2. Building a base model for A-19 and A-26

The first step when modelling a new well in PROSPER is to fill out a system summary like figure 8.2 shows. The Black Oil model, with the oil and water option describing the fluid, is used for both A-19 and A-26. It is also here the choice of artificial lift method is made, which allows us to fill in information and design a system at a later stage.

The screenshot shows the 'System Summary' dialog box for well GYDA-A26. The dialog is organized into several sections with dropdown menus and text boxes for configuration.

Section	Parameter	Value
Fluid Description	Fluid	Oil and Water
	Method	Black Oil
	Separator	Single-Stage Separator
	Emulsions	No
	Hydrates	Disable Warning
	Water Viscosity	Use Default Correlation
	Viscosity Model	Newtonian Fluid
Well	Flow Type	Tubing Flow
	Well Type	Producer
Artificial Lift	Method	None
Well Completion	Type	Cased Hole
	Gravel Pack	No
Reservoir	Inflow Type	Single Branch
	Gas Coning	No
User information	Company	Talisman
	Field	GYDA
	Location	Norway
	Well	G-A26
	Platform	D
	Analyst	Knut Stanghelle
Date	14 March 2009	
Comments (Ctrl-Enter for new line)		

Figure 8.2, System summary.

8.2.1. PVT

The next step is to fill in the PVT data. First the basic data for the Black Oil model for the well is entered (table 8.1). Second, PVT test data is entered and matched to the Black Oil correlations.

The correlations are mathematical best fits to sets of lab measurements. They represent the PVT behaviour of average hydrocarbons. Each individual fluid sample will behave similarly on average, but not exactly as predicted by the correlation. By comparing the values predicted by the correlation and measure lab data, adjustment factors for the correlation can be found that minimise the overall difference.

PROSPER uses a non-linear regression to do this by applying a multiplier (Parameter 1) and a shift (Parameter 2) to each correlation. Figure 8.3 shows how the software matches the data. Parameter 1 should be close to one and Parameter 2 close to zero. Standard deviation represents the overall closeness to fit and should be as small as possible.

PVT - Correlation Parameters (GYDA-A26 uten løft.Out) (Oil - Black Oil matched)						
<input type="button" value="Done"/> <input type="button" value="Cancel"/> <input type="button" value="Main"/> <input type="button" value="Export"/> <input type="button" value="Report"/> <input type="button" value="Reset All"/> <input type="button" value="Help"/>						
Bubble Point						
	Glaso	Standing	Lasater	Vazquez-Beggs	Petrosky et al	Al-Marhoun
Parameter 1	1.82837	1.08221	1.57053	0.88077	1.20522	1
Parameter 2	-2364.89	-158.978	-1060.61	-56.2116	-769.125	0
Std deviation	8.6317e-5		0.00017263			
	<input type="button" value="Reset"/>					
Solution GOR						
	Glaso	Standing	Lasater	Vazquez-Beggs	Petrosky et al	Al-Marhoun
Parameter 1	1.03211	1.00287	0.88954	1.21268	2.55142	1
Parameter 2	37.2735	0.86859	7.57112	3.61969	-666.997	0
Std deviation	108.737	48.175	84.5332	44.1198	2.40315	
	<input type="button" value="Reset"/>					
Oil FVF						
	Glaso	Standing	Lasater	Vazquez-Beggs	Petrosky et al	Al-Marhoun
Parameter 1	1.06121	0.9991	0.98196	1.18951	1.02518	1
Parameter 2	-0.045057	0.0070866	0.029804	-0.22872	-0.027162	0
Parameter 3	1	1	1	1	1	1
Parameter 4	1.05759	0.87506	0.76234	0.74306	0.85595	0
Std deviation	0.046364	0.045775	0.035161	0.038242	0.020337	
	<input type="button" value="Reset"/>					
Oil Viscosity						
	Beal et al	Beggs et al	Petrosky et al	Eqboqah et al		
Parameter 1	0.45985	0.29297	0.84374	1		
Parameter 2	0.13052	0.11987	-0.031811	0		
Std deviation	0.060047	0.030112	0.007242			
	<input type="button" value="Reset"/>	<input type="button" value="Reset"/>	<input type="button" value="Reset"/>	<input type="button" value="Reset"/>		

Figure 8.3, PVT correlations.

Table 8.1, General PVT input for A-19 and A-26

Input parameters	A-19 and A-26
Solution GOR, Sm ³ /Sm ³	159,4
Oil Gravity, kg/m ³	804,2
Gas Gravity, kg/m ³	1,07864
Water salinity, ppm	172995
Mole percent H ₂ S	0
Mole percent CO ₂	1,77
Mole percent N ₂	0,868

8.2.2. IPR

When the PVT data has been properly matched, one can start making the IPR curve. As mentioned in the well performance chapter there are a lot of models for making the IPR. The most used model for Gyda wells are the simple “PI entry”. This model is based on equation 3.4 which generates a straight line above the bubble point. The Vogel empirical solution (Eq. 3.5) is used below bubble point. The Productivity index entered is used to calculate the IPR. The IPR rates are always given as liquid rates. Hence the PI refers to liquid rate.

The data in table 8.2 and 8.3, which is entered into the IPR section, is based on an Eclipse reservoir simulation made by the TENAS reservoir department. The reservoir simulation covers a “base case”, where no artificial lift method is installed, and an “ESP case”. There has not been made a prediction for a “gas lift case” yet, but it is assumed that a gas lift installation would lower the static BHP with 20 bar compared to the “base case”. “Base case” water cut is also assumed for the gas lift.

The water cut is lower for the “ESP case”. ESPs will drastically draw down the pressure in near wellbore area. This makes the oil expand, thus less water is produced.

The GOR is approximately the same for both the simulated scenarios, so the same GOR is assumed also for gas lift. Because A-26 is currently dead, there is no “base case” simulation for production and hence no prediction of GOR or water cut.

However, since it is assumed that the GOR is independent of lift method, the same GOR as for ESP production is assumed. The “base case” water cut is based on the latest well test.

All the base simulations (PROSPER) in this study are based on the predicted reservoir conditions for May 2010 which is the planned finish of artificial lift installation in A-19 and A-26.

Table 8.2, IPR input for A-19

IPR data for A-19, predictions for May 2010	
Reservoir pressure, barg	400
Reservoir temperature, °C	155
Water cut, %	53, 44 for ESP
Total GOR, Sm ³ /Sm ³	140
PI, Sm ³ /d/bar	6

Table 8.3, IPR input for A-26

IPR data for A-26, predictions for May 2010	
Reservoir pressure, barg	400
Reservoir temperature, °C	155
Water cut, %	86, 81 for ESP
Total GOR, Sm ³ /Sm ³	160
PI, Sm ³ /d/bar	9

8.2.3. Equipment

For PROSPER to be able to calculate the pressure and temperature profile along the well, completion, survey and temperature data is needed.

For A-19 and A-26 the following survey data is entered:

DEVIATION SURVEY (GYDA A19 uten løft.Out)

Done Cancel Main Help Import Plot Filter
Insert Delete Copy Cut Paste All

Input Data

	Measured Depth (m)	True Vertical Depth (m)	Cumulative Displacement (m)	Angle (degrees)
1	0	0	0	0
2	121.5	121.5	0	0
3	480	479.47	19.4862	3.11584
4	990	966.24	171.654	17.3596
5	1490	1416.03	390.032	25.8971
6	1990	1859.65	620.686	27.4715
7	2490	2305.17	847.649	26.9958
8	2990	2749.45	1077.03	27.3071
9	3490	3197.89	1298.17	26.2491
10	3990	3656.67	1496.96	23.428
11	4431	4059.76	1675.85	23.9308
12				
13				
14				
15				
16				
17				
18				

MD <-> TVD

Calculate

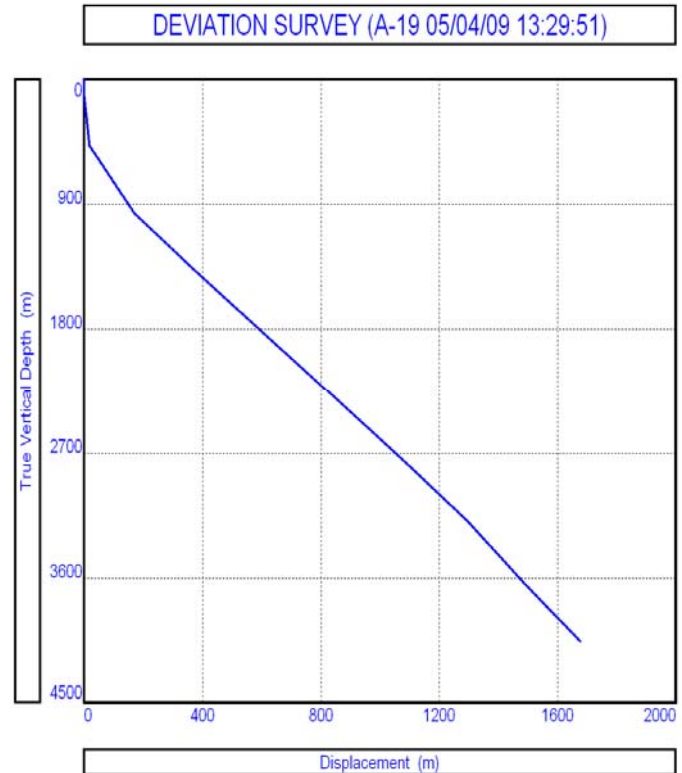


Figure 8.4, survey data for A-19. The well path is plotted to the right.

DEVIATION SURVEY (GYDA-A26 uten løft.Out)

Done Cancel Main Help Import Plot Filter
Insert Delete Copy Cut Paste All

Input Data

	Measured Depth (m)	True Vertical Depth (m)	Cumulative Displacement (m)	Angle (degrees)
1	0	0	0	0
2	121.5	121.5	0	0
3	390	389.9	7.3278	1.56389
4	510	509.8	12.2261	2.3394
5	660	659.2	25.6282	5.12608
6	810	808.4	41.0997	5.92021
7	990	987.2	61.8497	6.61963
8	1230	1225.7	88.6409	6.40928
9	1350	1345.5	95.5654	3.30802
10	1500	1495.5	95.5654	0
11	1650	1644.9	108.969	5.12672
12	1740	1733.3	125.864	10.82
13	2000	1984.2	194.049	15.2036
14	2500	2465.4	329.867	15.7616
15	3000	2946.2	467.094	15.9295
16	3525	3449.8	615.46	16.4155
17	4025	3930.8	751.984	15.8458
18	4172	4076.1	774.275	8.72192

MD <> TVD

Calculate

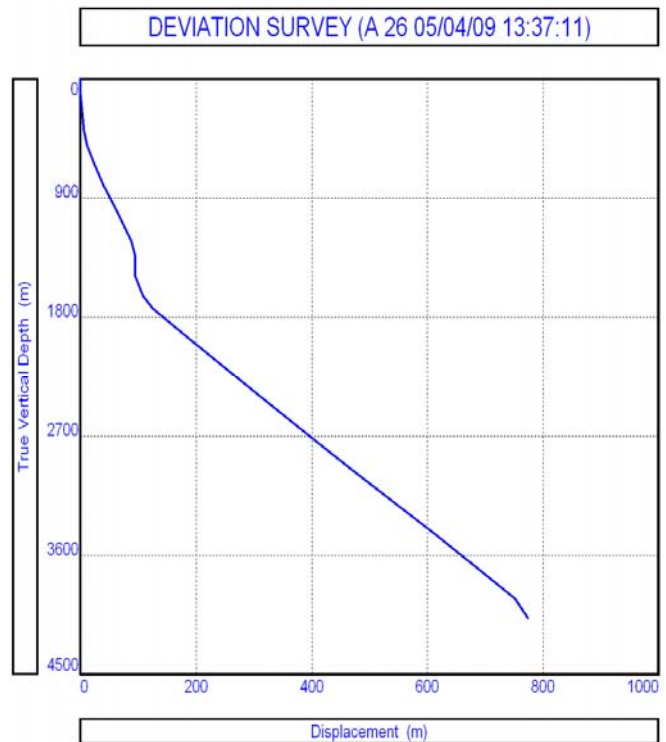


Figure 8.5, survey data for A-26. The well path is plotted to the right.

For implementation of gas lift or ESP in the two wells a full workover is necessary. ESPs are a part of the tubing, and the wells does not contain side pockets so that gas lift valves can be installed by wireline. However, the geometry of the production tubing would look very much the same as for the old wells. Therefore the current well completion is used for the PROSPER simulations. Inner and outer diameter of casings, tubings and liners are put into the model. Inner diameter of restrictions like the downhole safety valve is also accounted for. A tubing and casing inside roughness of 0,0006 inch is used. Figure 8.6 and 8.7 shows the current completion schematics of the two wells.

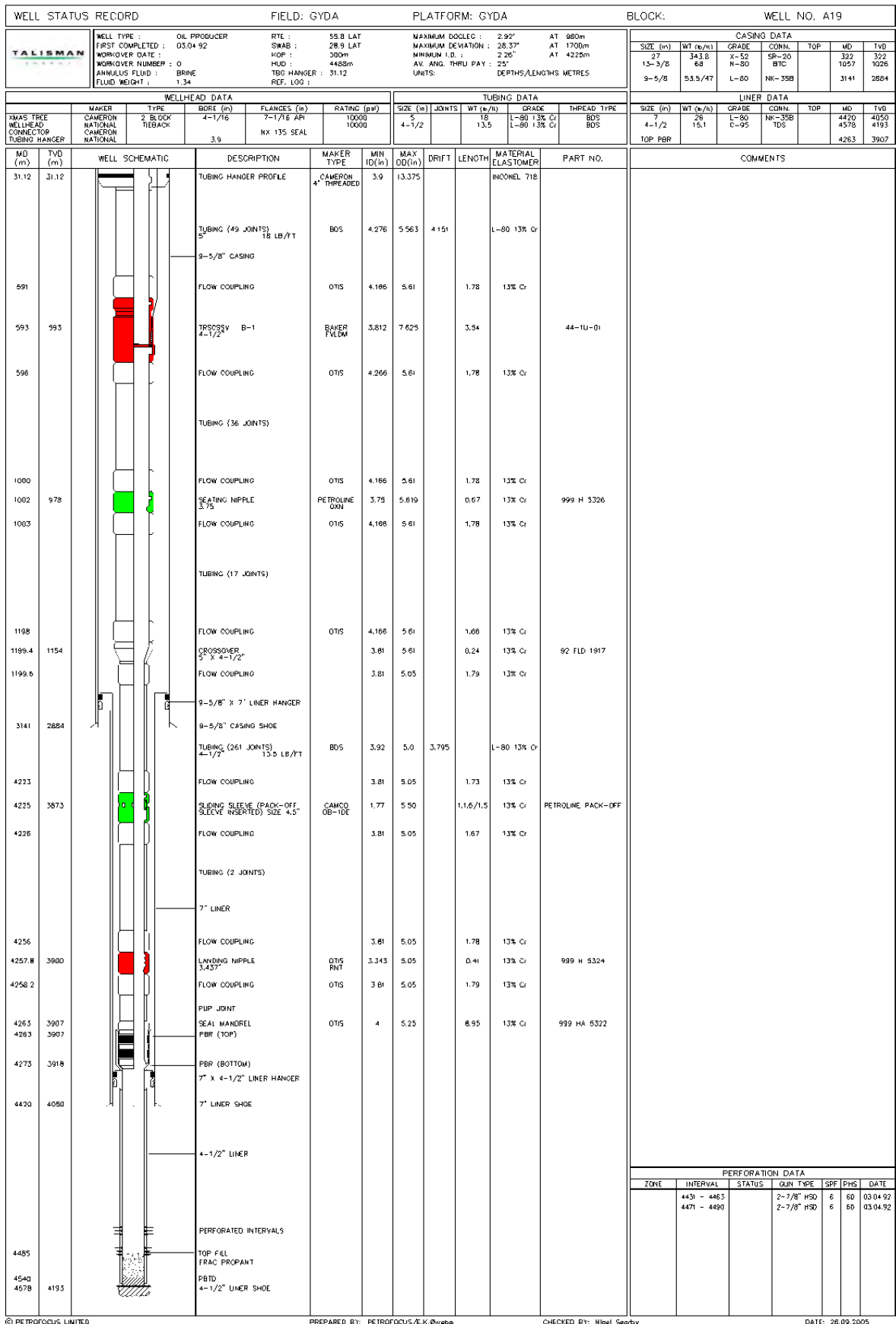


Figure 8.6, Completion schematic of A-19

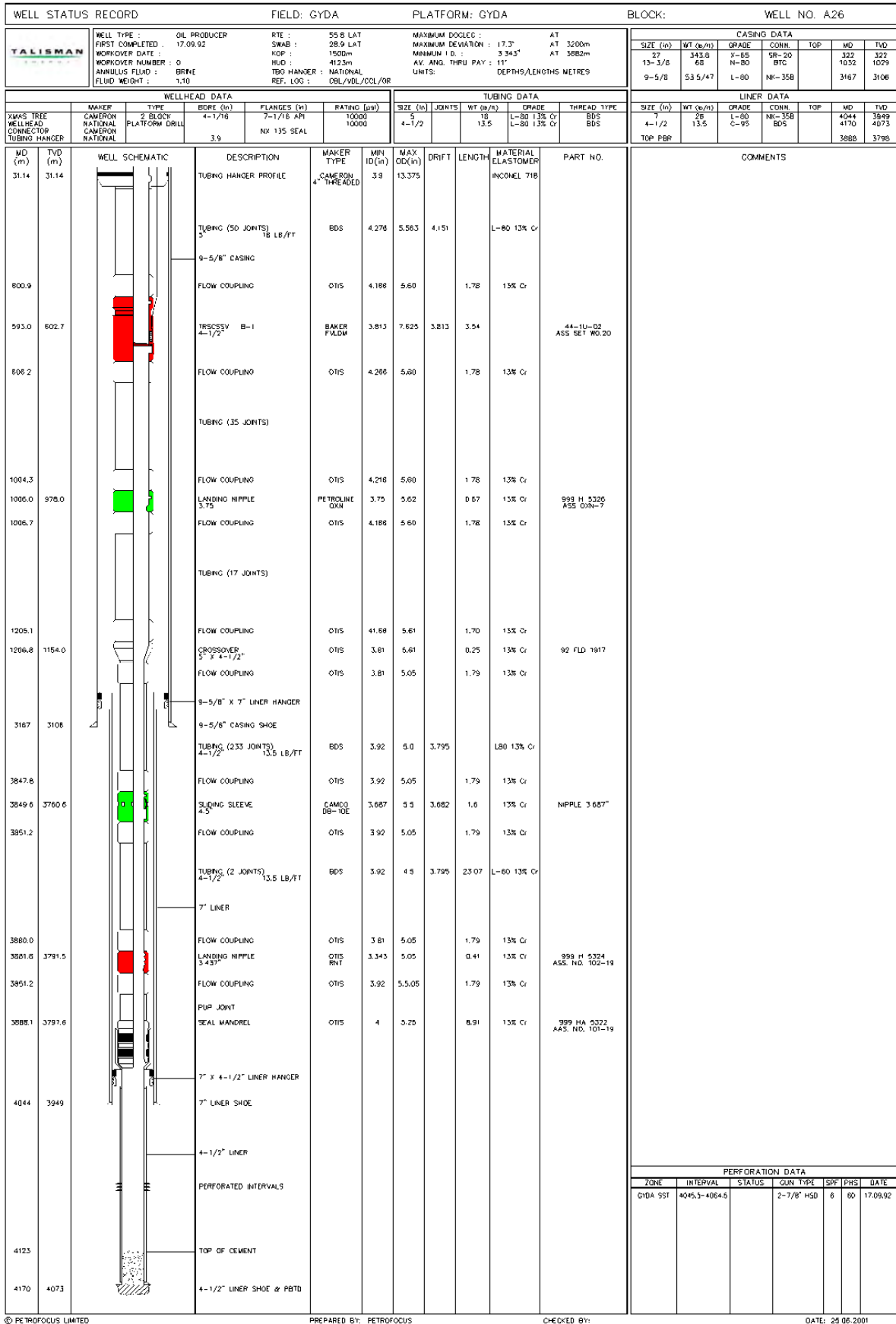


Figure 8.7, Completion schematic of A-26

For both wells the temperature profile in table 8.4 is used. Default values for heat capacities are entered.

Table 8.4, Temperature profile

Position	Temperature
Wellhead	10 °C
Seabed	6 °C
Top perforation	155 °C

8.2.4. Results

Given these input parameters PROSPER gives a production profile, with no artificial lift, for A-19 and A-26 in May 2010. A-19 has an oil production of 2381 bbl/d and A-26 produces 234 bbl/d of oil. The reason why we see a production in A-26 could be that there is enough pressure support from injectors and in 2010 A-26 actually can produce. However, the well must be considered as dead because it doesn't take more than a small change, which is well within the margins of error, in water cut or reservoir pressure for there to be no production point again (figure 8.10). Figures 8.8 and 8.9 show the production point in May 2010, which is the intersection between the VLP and IPR curve.

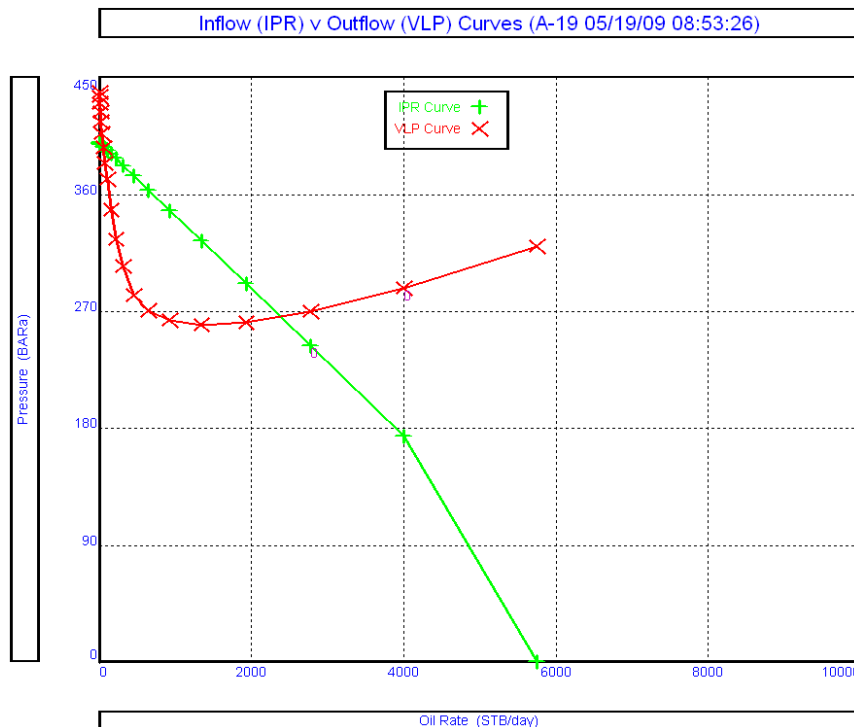


Figure 8.8, production point of A-19 in May 2010

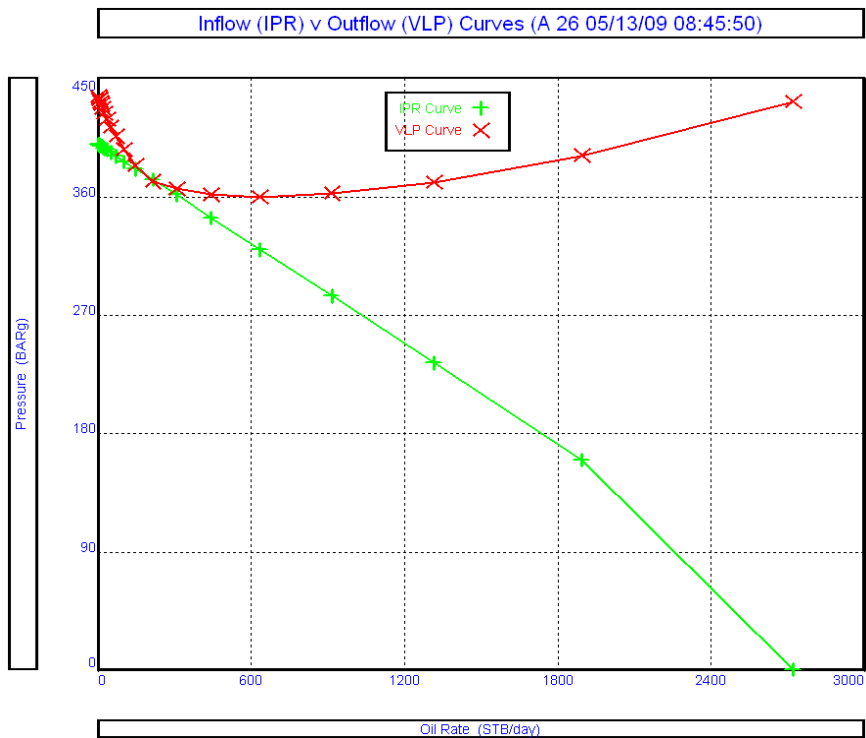


Figure 8.9, production point of A-26 in May 2010

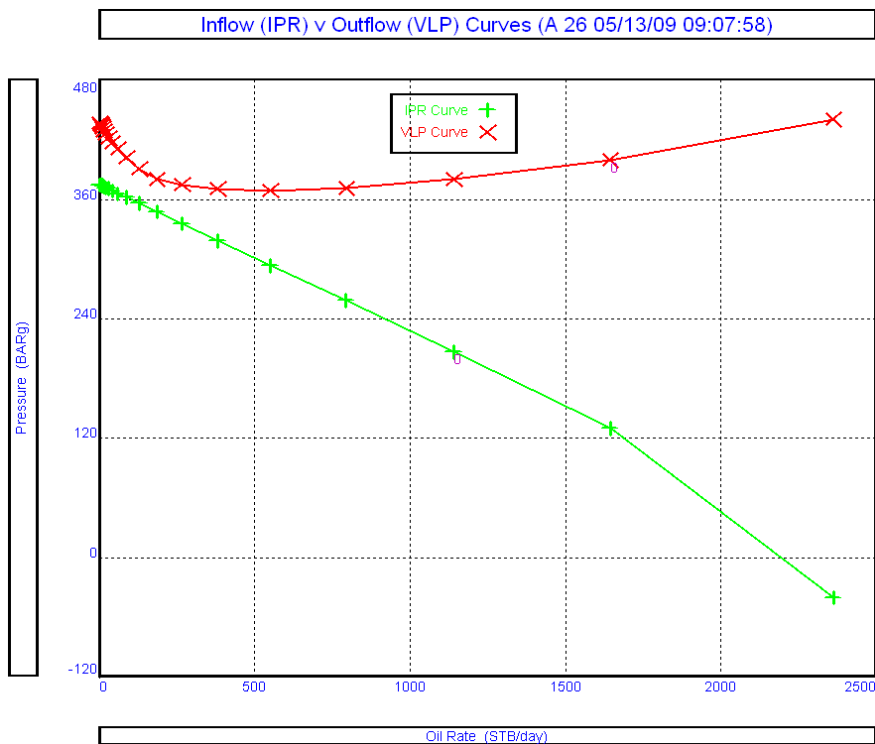


Figure 8.10, A-26 with no intersection between IPR and VLP (situation today)

9. Gas lift design

When performing a gas lift design, the best compromise between a number of objectives are sought:

- Find optimum production and lift gas injection rates.
- Inject gas as deep as possible.
- Determine depth and number of unloading valves. Check if design has sufficient flexibility to handle current and future well conditions (increased WC, declining reservoir pressure and PI etc)
- Produce at stable conditions without "heading" and avoiding pressure surges that could result in multipoint injection and cause pressure fluctuations large enough to be disruptive to surface facilities.
- Optimize in terms of revenue by accounting for cost of produced water disposal and lift gas compression.

The biggest obstacle for performing proper gas lift on Gyda is the capacity of the compressor. It currently gives 56 600 Sm³/day with an injection pressure of 165 bar. There is much more gas available, but for a full scale gas lift campaign a bigger compressor has to be purchased.

For this study, full capacity of 56 600 Sm³/day is assigned to each well. This is assumed to be a realistic scenario for a full scale gas lift campaign, with a proper compressor.

Studies done by TENAS has shown that the older Gyda casings, like the ones in A-19 and A-26, which was drilled in the early nineties, can not handle the pressure from gas lift injection lower than 2600 m TVD. This implies that maximum injection depths in these wells will be at 2830 and 2650 m MD.

When designing a gas lift system with more than one well, one should optimize the allocation of available gas, so that the total production is maximized. The developers of PROSPER has made a software for this (GAP), but this is not the scope of this study and has not been done.

9.1. Modelling A-19 and A-26 with gas lift

When modelling a gas lift well a number of parameters have to be entered into the system. Figure 9.1 shows the gas lift design menu. The gas available for lifting has the following characteristics:

Table 9.1, Lift gas data

Gas lift gas gravity, sp. gravity	0,784
Mole percent H2S, %	0
Mole percent CO2, %	2,76
Mole percent N2, %	0,98

GasLift Design - NEW WELL (GYDA-A26 gas lift.Out) (Matched PVT)

Continue Done Cancel Report Export IPR Help

Design Rate Method: Calculated From Max Production

Maximum Liquid Rate: 18000 STB/day

Input Parameters	Value	Unit
Maximum Gas Available	56.6	1000Sm ³ /d
Maximum Gas During Unloading	56.6	1000Sm ³ /d
Flowing Top Node Pressure	15	BARg
Unloading Top Node Pressure	15	BARg
Operating Injection Pressure	165	BARg
Kick Off Injection Pressure	165	BARg
Desired dP Across Valve	10	bar
Maximum Depth Of Injection	2650	m
Water Cut	86	percent
Minimum Spacing	60	m
Static Gradient Of Load Fluid	0.1	bar/m
Minimum Transfer dP	10	percent
Maximum Port Size	20	64ths inch
Safety For Closure Of Last Unloading Valve	0	bar
Total GOR	160	Sm ³ /Sm ³

Valve Type: Casing Sensitive
Min CHP Decrease/Valve: 3.4473 bar

Valve Settings: Pvc = Gas Pressure

Injection Point: Injection Point is ORIFICE

Dome Pressure Correction Above 1200psig: Yes

Check Rate Conformance With IPR: Yes

Vertical Lift Correlation: Petroleum Experts 2

Surface Pipe Correlation: Petroleum Experts 4

Use IPR For Unloading: Yes

Orifice Sizing On: Calculated dP At Orifice

Thornhill-Craver DeRating: DeRating Percentage For Valves: 100 percent; DeRating Percentage For Orifice: 100 percent

Current Valve Information: Manufacturer: Camco; Type: BK; Specification: Normal

Current Valve Type Tree:
 GasLift Valve Database
 - Valve1
 - McMurry-Macco
 - Camco
 - RP-6
 - RCB
 - R-20
 - PK-1
 - BKT-1
 - BKT
 - BKLK-2
 - BK-1
 - BK
 - Normal
 - Carbide
 - Baker

Port Size	R Value
20	0.255
16	0.165
12	0.094
8	0.042

Figure 9.1, gas lift design menu.

The operating injection pressure is set to 165 bar. Desired dP across valves, 10 bar, is entered to ensure well and gas injection system stability. Minimum spacing between valves is set to 60 m. Sea water is assumed as the load fluid before gas lift start, which result in a static gradient of 0,1 bar/m. Also maximum injection depth for each well is set.

The most used valve type by TENAS is the casing sensitive, which is also chosen here. Valve settings is chosen to “Pvc = Gas Pressure”. Then PROSPER sets valve dome pressure to balance casing pressure at depth. Unloading valves will close when the casing pressure drops below this value.

For this study a “Camco BK Normal” valve is chosen from the PROSPER database. The software calculates which port sizes that will generate optimal production. A valve from another manufacturer would maybe require different port sizes, but PROSPER still calculates the same optimal production. Therefore the choice of type is not that important as long as it is casing sensitive.

Now PROSPER is able to calculate a gas lift performance curve. Figure 9.2 and 9.3 show the curves for A-19 and A-26 with the May 2010 conditions (table 8.2 and 8.3).

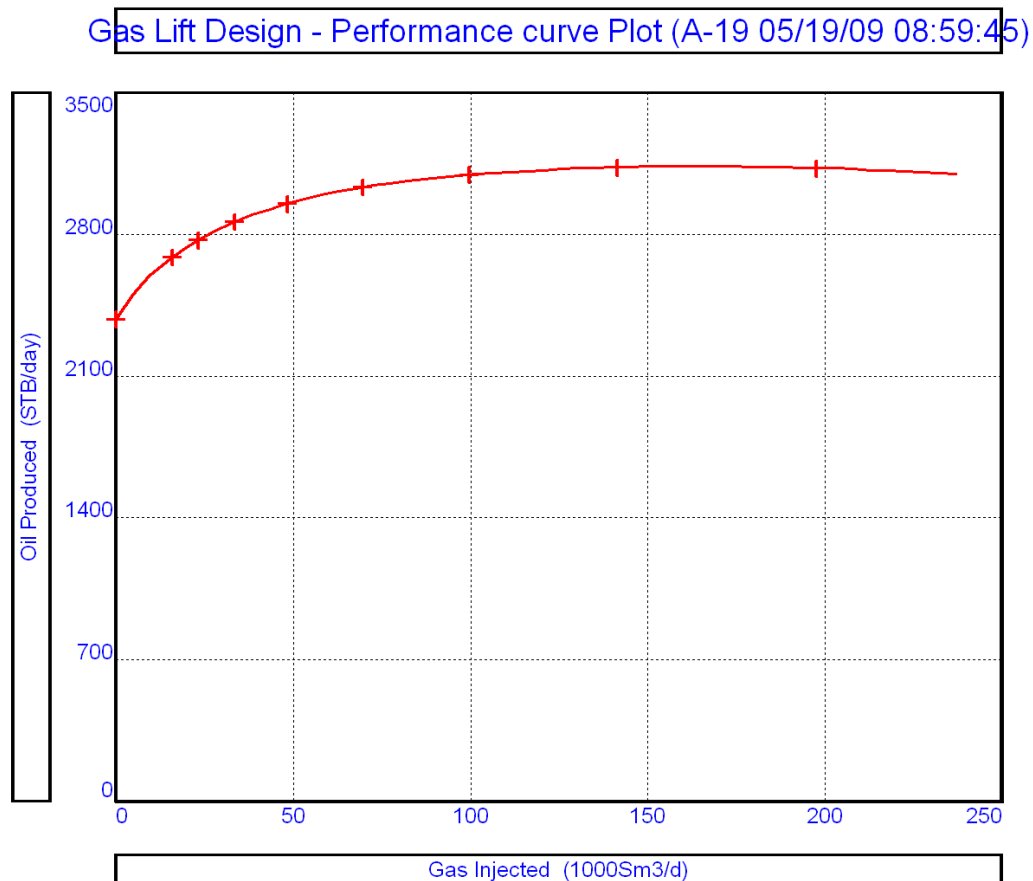


Figure 9.2, Gas lift performance curve for A-19

Gas Lift Design - Performance curve Plot (A 26 05/19/09 10:14:46)

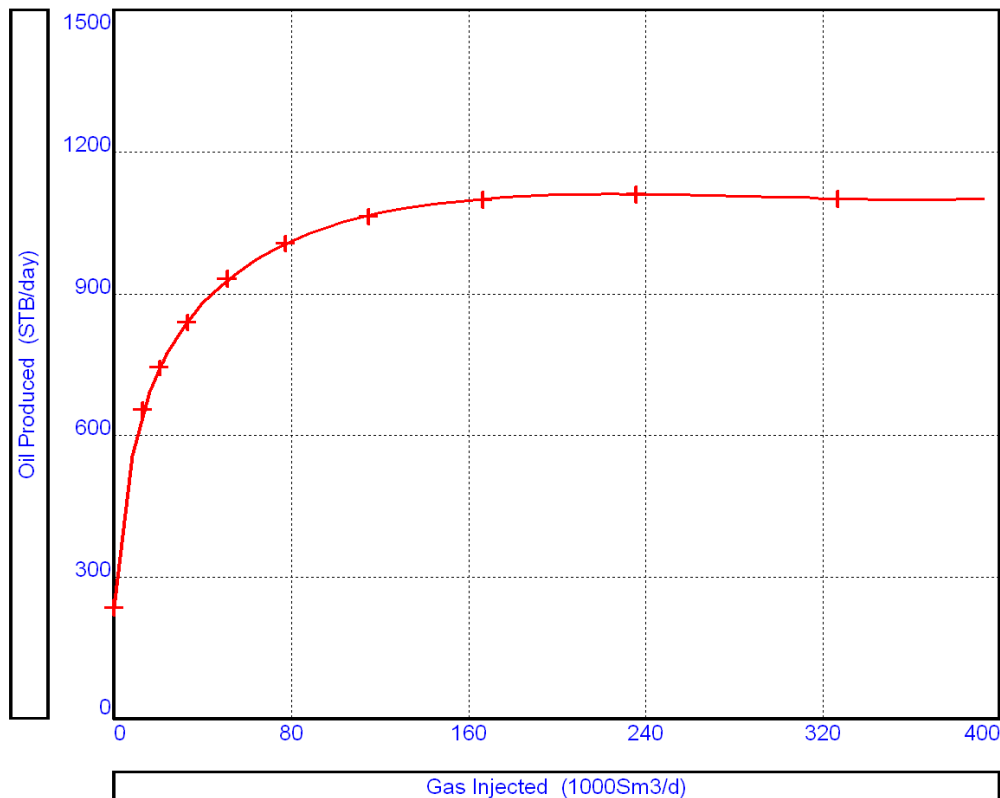


Figure 9.3, Gas lift performance curve for A-26

The performance curves give us a plot of oil produced versus the gas injected. The injection gas rate that gives the highest production rate can be found, although that might not be the optimum point of injection in terms of revenue. That point is where the incremental additional cost of compressing gas equals the incremental revenue of the additional oil produced. The economic optimum gas injection rate is often found to the left of the maximum production rate in such a curve. When looking at the curves it is clear that none of the wells will reach maximum production with an injection rate of 56 600 Sm³/day. A-26 is producing in a steeper part of its curve, but an increased injection in this well might not increase the total production. A-19 produces larger oil volumes, so even if we inject more gas into A-26, and get a larger percentual increase of out of this well, A-19 will give more oil with the same gas injected. This shows the importance of a full system analysis.

Looking at the curve from A-19 one can see that it starts from approximately 2380 bbl/day. This coincides with the result from the base model where A-19 produced 2381 bbl/day with natural flow. The same goes for A-26.

9.2. Positioning of valves

Valve spacing is not affected by the choice of unloading method (casing or tubing sensitive), but of whether the well IPR is used for calculating the unloading rate or not. When designing the valve system PROSPER can be set to check whether the solution rate is achievable with respect to the IPR. If necessary the design rate is reduced and the spacing calculation is repeated. Figures 9.4 and 9.5 shows the result of valve spacing design for A-19 and A-26.

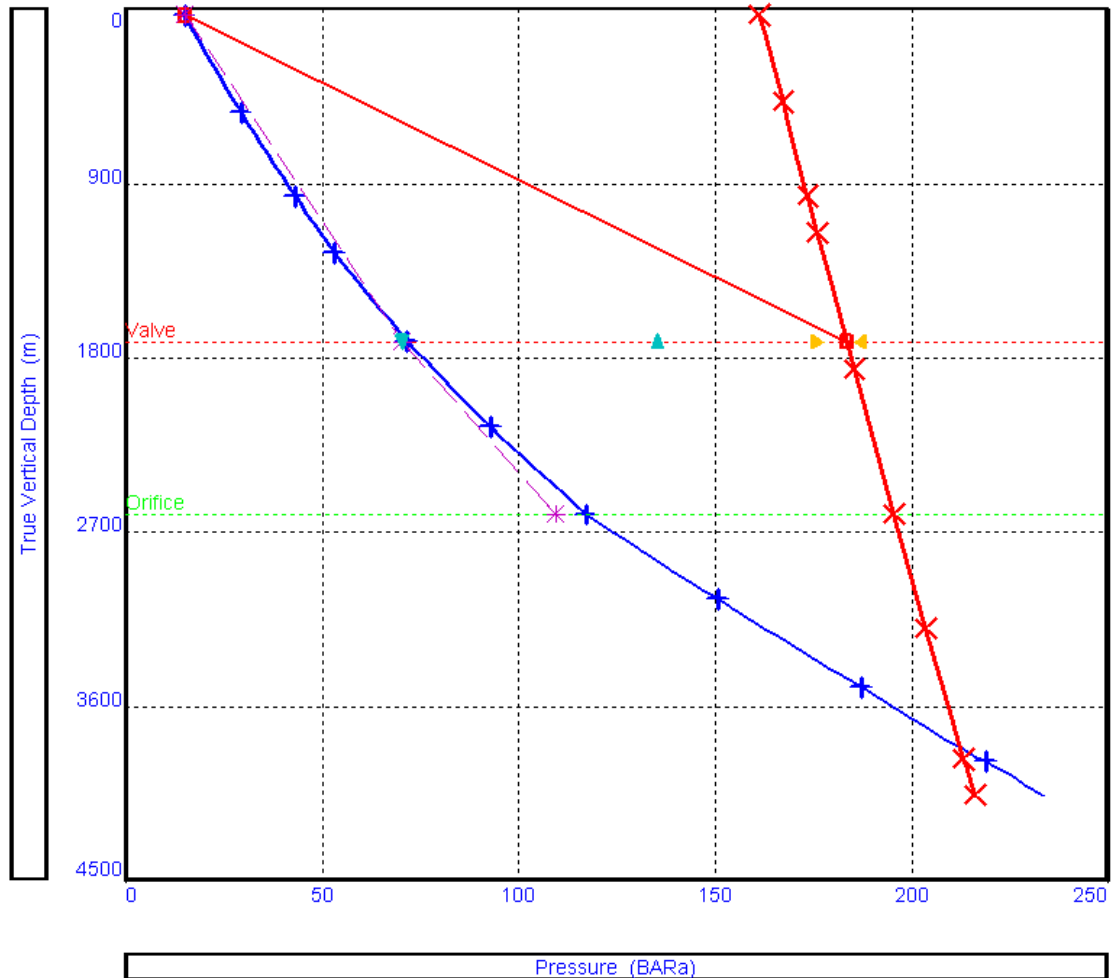


Figure 9.4, valve spacing for A-19

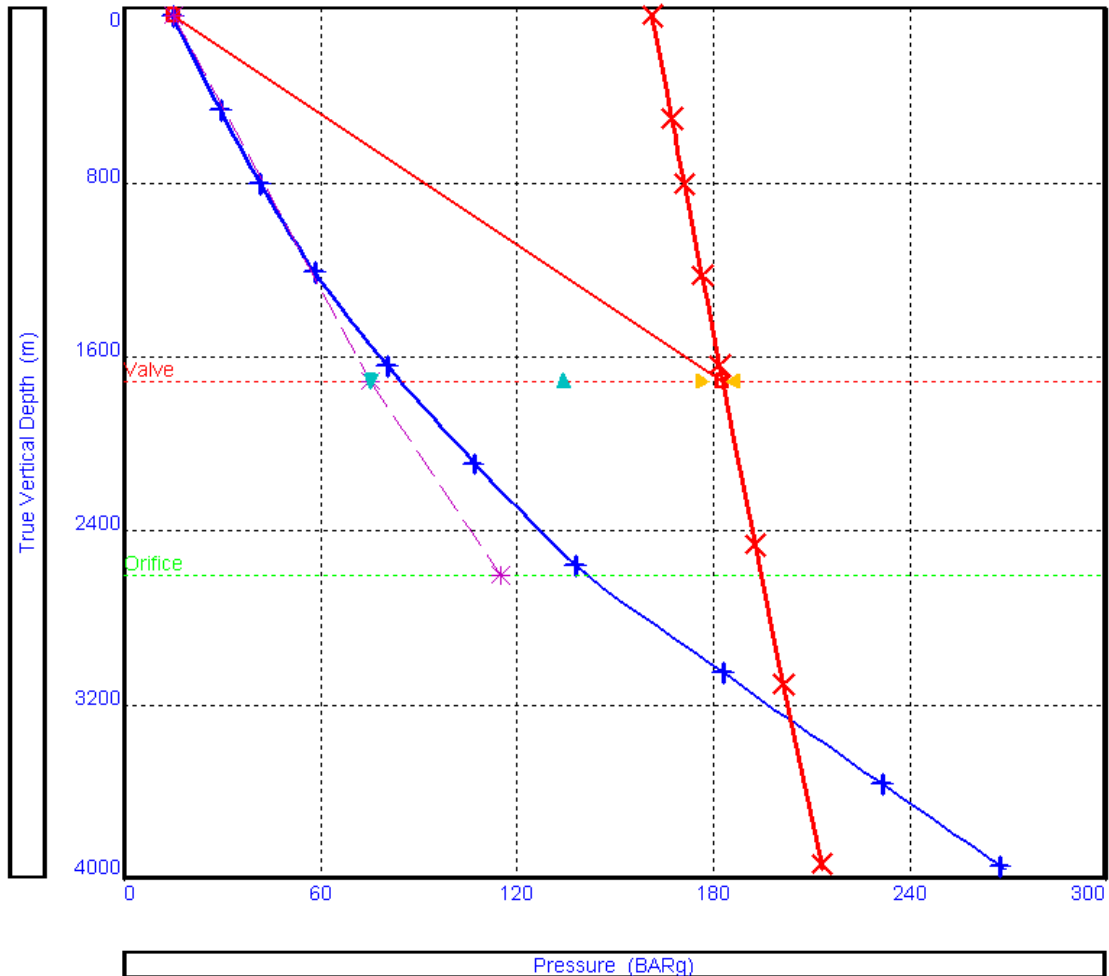


Figure 9.5, valve spacing for A-26

The valve spacing calculations is done in the following way:

For the tubing, with the designed injected gas rate, a pressure traverse is calculated from the surface and downwards using the gas lifted flowing gradient (blue line). A similar plot is made for the casing pressure (right red line).

The injection depth (orifice valve) is the depth at which the flowing tubing pressure equals the casing pressure gradient less the designed pressure loss across the orifice. However, injection depth is often limited by well design, for example by a production packer or weak casings like on Gyda.

The shallowest unloading valve is placed at the depth that balances the tubing load fluid pressure (left red line) with the casing pressure at that depth. Further unloading valves are placed by traversing down like this between the casing and gas lifted tubing pressure gradient lines.

Valves are placed ever deeper until the inter valve spacing equals a pre-set minimum, or the maximum injection depth has been reached.

Once the first design is complete, the software can re-calculate the flowing tubing gradient using the current operating valve depth. This was not necessary for A-19 and A-26 because both wells were able to inject at the pre set maximum injection depth.

9.3. Results

The result from the gas lift design is given in table 9.2:

Table 9.2, Results from gas lift design

Result / Well	A-19	A-26
Depth unloading valve, m MD	1828	1714
Unloading valve port size, 64ths inch	12	14
Depth operating valve, m MD	2830	2650
Operating valve port size, 64ths inch	14	14
Oil rate with gas lift, bbl/day	2988	948
Oil rate without gas lift, bbl/day	2381	234

The results show that both wells get a significant increase in production from gas injection. Both wells only needed one unloading valve. This is a combination of the operating valve setting depth, gas lift injection pressure and load fluid density. For example if the wells did not have a depth constrain and was displaced to a 800 kg/m³ fluid instead of seawater when starting the injection, the operating valve could be set deeper and we would see an increased production. This will be discussed in the next section.

9.4. Sensitivities of injection depth

To see the effect of injection depth a sensitivity analysis was run on this. PROSPER allows the injection depth to be a variable, and calculates production for each depth entered. Table 9.3 shows at which depths the analysis was run and the corresponding results.

Table 9.3, injection depth analysis on A-19 and A-26

A-19		A-26	
100 m MD	2392 bbl/day	100 m MD	309 bbl/day
500 m MD	2435 bbl/day	500 m MD	492 bbl/day
1200 m MD	2597 bbl/day	1200 m MD	721 bbl/day
2000 m MD	2810 bbl/day	2000 m MD	876 bbl/day
2830 m MD	2988 bbl/day	2650 m MD	948 bbl/day
3000 m MD	3021 bbl/day	3000 m MD	979 bbl/day
4000 m MD	3178 bbl/day	3850 m MD	1033 bbl/day

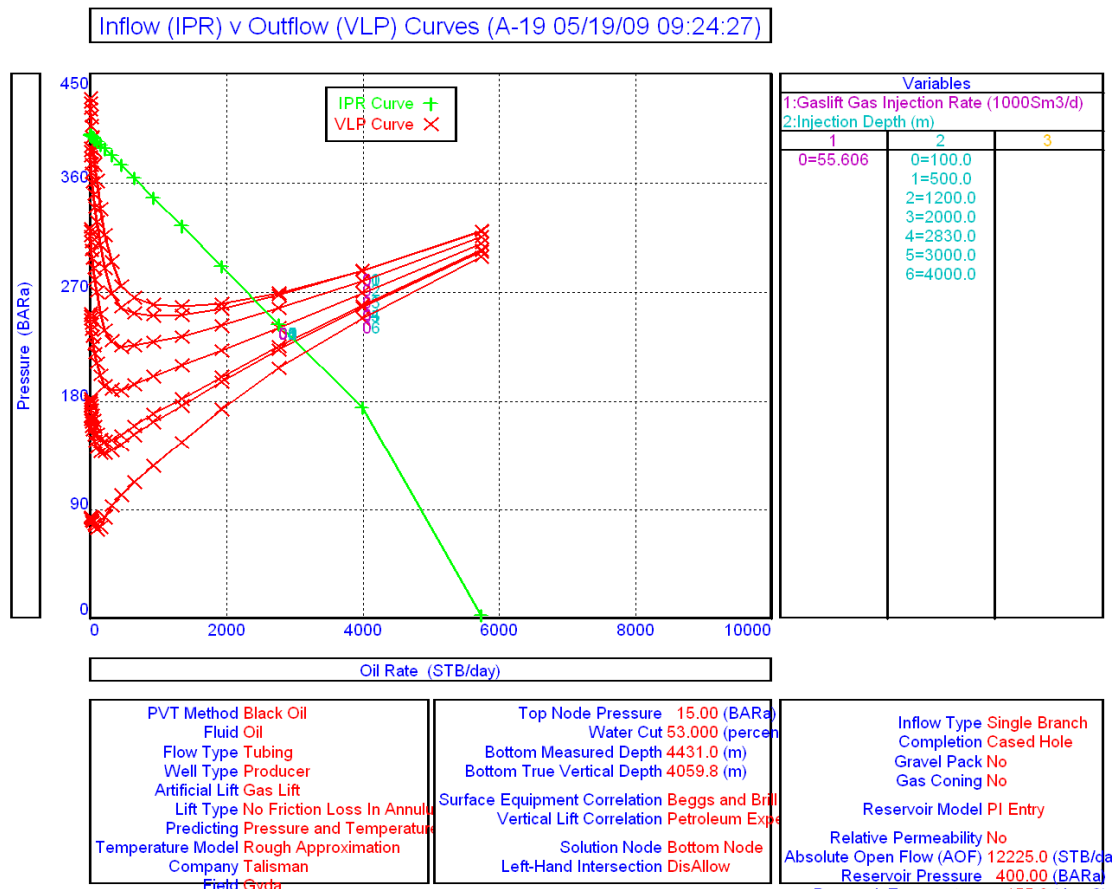


Figure 9.6, injection depth analysis on A-19. The figure shows how the VLP curve is moved as a function of injection depth.

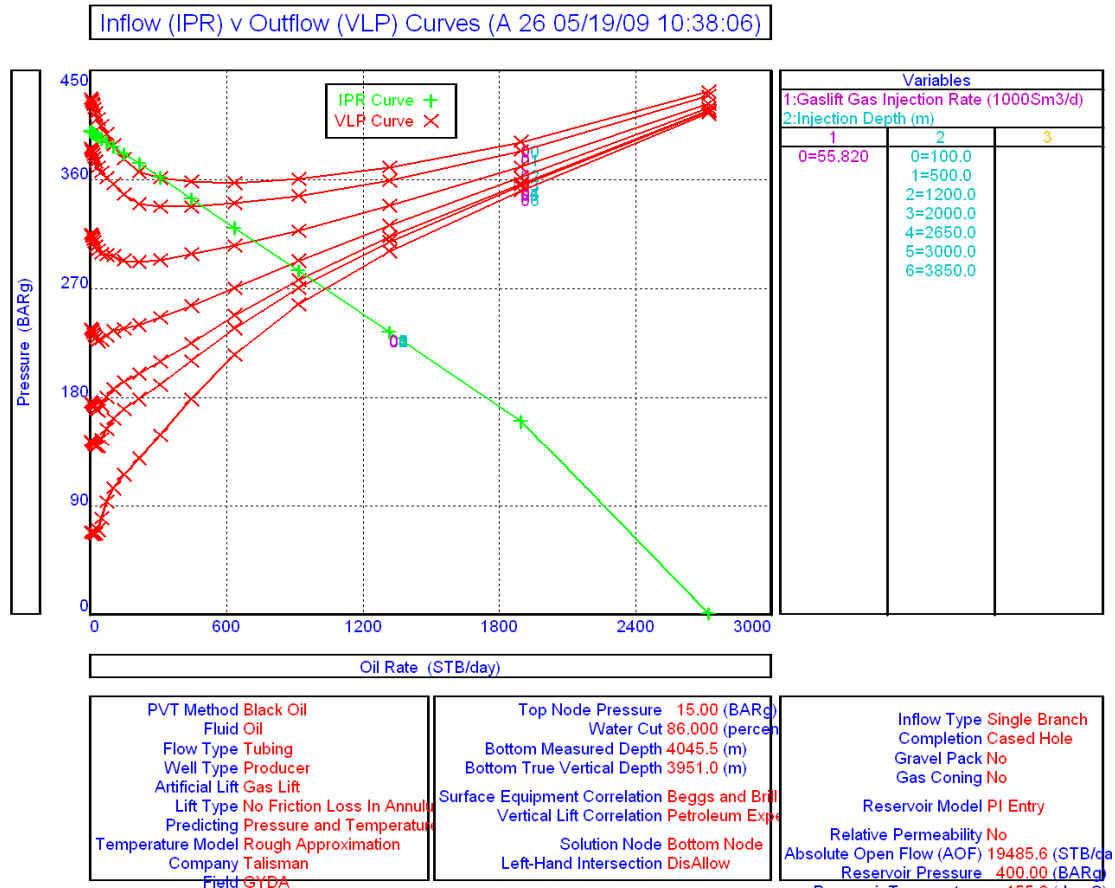


Figure 9.7, injection depth analysis on A-26. The figure shows how the VLP curve is moved as a function of injection depth.

The results show that a deeper setting depth of the operating valve gives an increased production. However, the results also show that the effect of moving the valve to the bottom of the 9 5/8" casing, at approximately 3000 m MD in both wells, has a minimal effect (See completion drawings). There is a bigger effect of moving the valves down to the bottom of the tubing inside the 7" liner (4000 m and 3850 m MD), which gives 190 and 85 bbl/day more. This has not been done on Gyda but has been tried with success on another TENAS installation, Varg. This could be a possibility for newer Gyda wells with more solid casings than A-19 and A-26.

10. ESP design

Compared to the gas lift part of this study, an ESP system is not designed in PROSPER. A study and design done by Baker Hughes Centrilift has provided the system data given in table 10.1. Upper and lower systems are the same in both wells.

Table 10.1, ESP system data [19]

Equipment	A-19 and A-26
Pump	Centrilift 562 P110
Operating range	7000 – 13200 bbl/day (60Hz)
Motor	Centrilift 562 450 HP
Cable	Grade 1 copper
# Stages	84 for A-19, 60 for A-26

The 562 (Figure 10.1) series is designed for use in 7 inch wells where large production volumes are required and in 9 5/8 inch casings when space is limited. The outside diameter of the pump housing is 5,62 inches, but the pump is capable of operating in 7 inch wells when the casing weight is 26 lbs/ft or lower. All pump models in this series have a 1 3/16 inch shaft, which allows for a maximum horsepower rating of 1250 at 60 Hz. The 562 series comes standard with carbon steel metallurgy but certain configurations can be supplied in corrosion resistant alloys or with optional “Monel coating” when installed in corrosive environments.

As described in chapter 6.6. it is planned for a dual ESP and sealed shrouds solution. The units will be put inside the 9 5/8” casing as close to the 7” liner as possible. For this study they are set at a depth of 3050 m MD. The pump is planned to be operated in the range between 50 and 60 Hz .

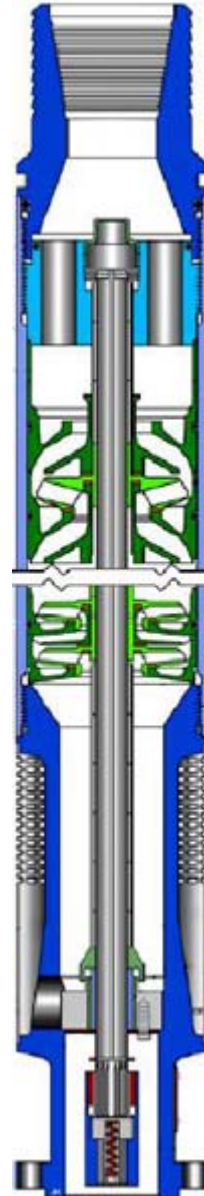


Figure 10.1, Centrilift 562 P110 [19]

10.1. Modelling A-19 and A-26 with ESP

Coefficients (appendix) for head and horsepower received by Centrilift is put into the PROSPER database. With these coefficients the software calculates pump curves so that one can simulate for any condition (Figure 10.2).

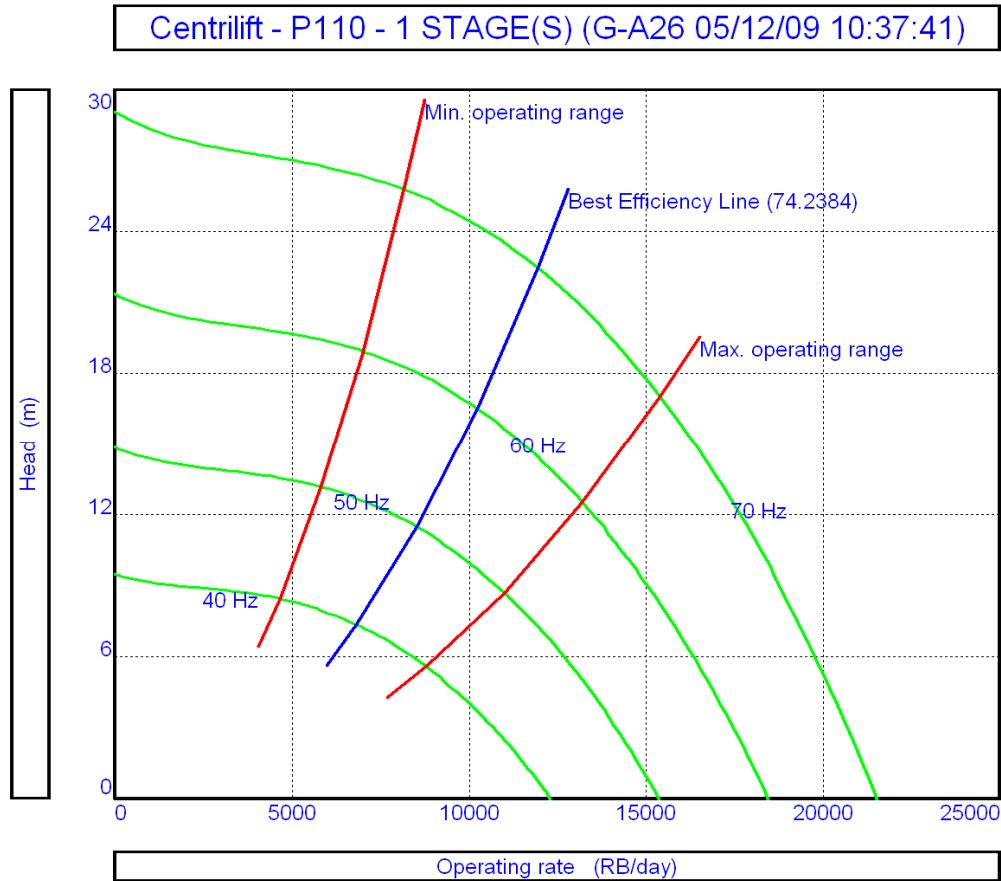


Figure 10.2, pump curves for the Centrilift 562 P110

From the figure we see that the minimum operating range, running at 60 Hz, is 7000 bbl/day and maximum is 13 200 bbl/day. The perfect operating point is at the best efficiency line. This is where the efficiency curve for the pump peaks (see section 6.1.).

There are two options when modelling an ESP well. One is to enter the design menu and let PROSPER design the ESP scenario, and choose a pump from the options that the software suggests. The second option is to enter the pump data directly when type of pump and motor is already decided, like in this case.

The data is put into the menu in figure 10.3. Pump, motor and cable are selected from the database.

ESP Input Data (GYDA A19 ESP.Out) (Matched PVT)

Done Cancel Report Export Help

Input Data

Pump Depth (Measured)	3050	m
Operating Frequency	60	Hertz
Maximum OD	6	inches
Length Of Cable	3050	m
Gas Separator Efficiency	0	percent
Number Of Stages	84	
Voltage At Surface	5500	Volts
Pump Wear Factor	0	fraction
Gas DeRating Model	<none>	

Current Pump

Centrilift P110 5.62 inches (1113-2098.8 m3/day)

Current Motor

Centrilift 562 450HP 2460V 105A

Current Cable

#1 Copper 0.85302 (Volts/1000m) 115 (amps) max

Figure 10.3, ESP input in PROSPER (A-19 as an example)

10.2. Results

Given the May 2010 conditions and ESP data PROSPER calculates production in the ESP wells:

Table 10.2, Results from ESP simulation

Result / Well	A-19	A-26
Oil rate with ESP, bbl/day	4619	1584
Total liquid rate ESP, bbl/day	8248	8405
Oil rate with gas lift, bbl/day	2988	948
Oil rate without artificial lift, bbl/day	2381	234

The wells show a significant increase in production compared both to the gas lift case and base case.

Both wells have a total liquid rate which lies well within the operating range of the pump, between the minimum and best efficiency line. This means that there is still a good capacity for handling more fluid.

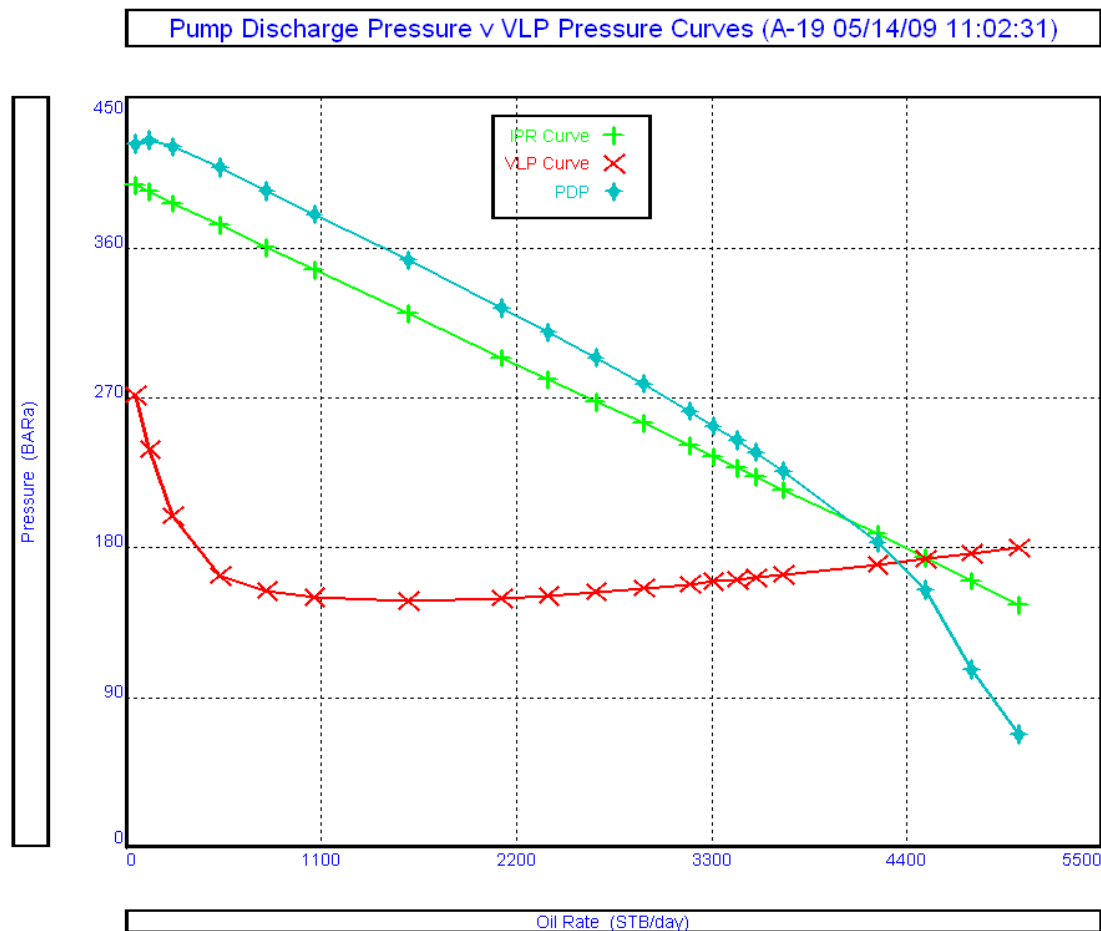


Figure 10.4, A-19 ESP system

For pumps in PROSPER e.g. ESPs, system analysis is conducted at the pump discharge (outlet of pump). Figure 10.4 has the following explanation:

The green curve is the IPR pressures referred to the bottom of the well.

The blue curve is the pump discharge pressure. This is the pump intake pressure corrected for dP added by pump.

The red curve is VLP from top of well to pump discharge (and not bottom of well).

The solution rate is obtained by the intersection of pump discharge pressure and the VLP.

11. Production forecast

Based on an Eclipse reservoir simulation a sensitivity analysis is made on water cut and reservoir pressure using PROSPER. PI and GOR are assumed constant. For other assumptions on water cut and GOR see section 8.2.2.

Exact reservoir pressure is difficult to estimate. The reservoir simulation gives flowing and static BHP, however this is only valid for the nearby wellbore area. The pressure that PROSPER need is the pressure far out in the reservoir pushing the fluid into the low pressure area near the wellbore created by the artificial lift. This pressure difference is what makes the drawdown.

The initial reservoir pressures in 2010 are based on well tests and reservoir simulation of the “base case” where there is no artificial lift. Both wells are set to 400 bar, which is a conservative estimate.

Field simulations show that the ESPs will draw down the average pressure of the field with 50 bar, and this is what the reservoir pressure prediction is based on, not the BHP. Table 11.2 shows how the reservoir pressure decrease. The reason why the reservoir pressure will not decrease to BHP is that there is pressure support from two injectors A-9 and A-28. This can also be seen from the constant reservoir pressure in the A-19 “base case”.

The gas lift is assumed to draw down the reservoir pressure 10 percent of what the ESPs does (see table 11.3).

The “secondary effect” of ESPs described in chapter 6.7 is not accounted for in the reservoir simulation this study is based on. Therefore the oil production forecast of the ESP wells will be conservative if this effect is valid.

11.1. Well A-19

Table 11.1, 11.2 and 11.3 show the result from the sensitivity analysis done from 2010, which is installation date, to 2019. Figure 11.1 shows the production forecast comparing the base case, gas lift and ESP

Table 11.1

A-19 "base case"										
Parameter/year	2010	2011	2012	2013	2014	2015	2016	2017	2018	2019
GOR	140	140	140	140	140	140	140	140	140	140
WC	53	55	60	65	67	70	71	72	74	75
Pres	400	400	400	400	400	400	400	400	400	400
Qo, bbl/d	2381	2200	1764	1342	1176	939	865	789	636	562

Table 11.2

A-19 "ESP case"										
Parameter/year	2010	2011	2012	2013	2014	2015	2016	2017	2018	2019
GOR	140	140	140	140	140	140	140	140	140	140
WC	44	48	55	60	63	67	71	73	76	78
Pres	400	375	360	355	355	355	355	355	355	355
Qo, bbl/d	4619	3929	3179	2717	2469	2140	1894	1732	1494	1260
Tot. liquid, bbl/d	8247	7555	7065	6791	6673	6483	6315	6187	5973	5729

Table 11.3

A-19 "gas lift case"										
Parameter/year	2010	2011	2012	2013	2014	2015	2016	2017	2018	2019
GOR	140	140	140	140	140	140	140	140	140	140
WC	53	55	60	65	67	70	71	72	74	75
Pres	400	398	395	395	395	395	395	395	395	395
Qo, bbl/d	2988	2807	2389	2022	1880	1672	1605	1537	1406	1341

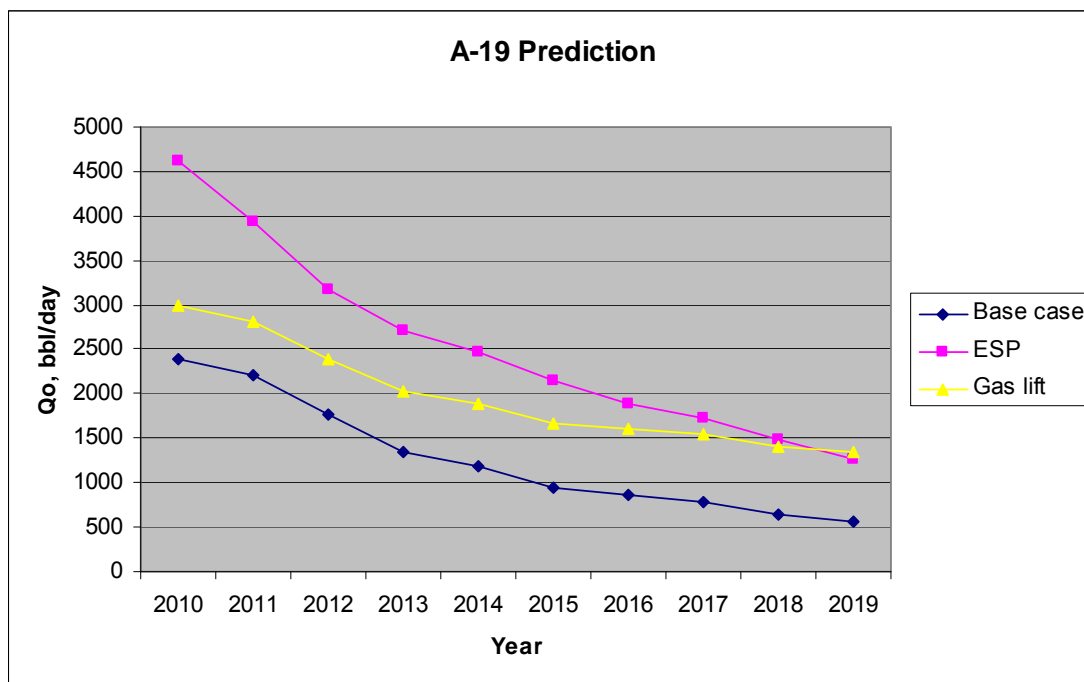


Figure 11.1, Production forecast for A-19. Production for the base case and the two artificial lift methods are plotted from start date to 2019.

The result of the production forecast show that the ESP solution gives a superior production rate compared to gas lift and the “base case”. From figure 11.1 it is observed that the gas lift production rate crosses the ESP production rate in 2019. This is a result of the initially higher water cut now being lower than in the ESP case. The gas lift scenario also does not see the same reservoir pressure loss as the pump.

The total liquid rate falls beneath 7000 bbl/day after 2012 in the “ESP case”. This is below the minimum operating range of the pumps running at 60 Hz. When this happens, the pumps have to be run at a lower frequency (Fig.10.2). When both the pumps fail, there should be a new analysis with the current conditions to see if another pump design would fit better. After running some years one would also learn more about the rates and how the reservoir responds to the pumps.

11.2. Well A-26

Table 11.4 and 11.5 show the result from the sensitivity analysis done from May 2010, which is installation date, to 2019. Figure 11.2 shows the production forecast.

There is no “base case” scenario because A-26 is considered as dead.

Table 11.4

A-26 "ESP case"										
Parameter/year	2010	2011	2012	2013	2014	2015	2016	2017	2018	2019
GOR	160	160	160	160	160	160	160	160	160	160
WC	81	84	85	87	88	90	91	92	93	93
Pres	400	375	360	355	355	355	355	355	355	355
Qo, bbl/d	1598	1130	939	741	663	516	448	382	320	320
Tot. liquid, bbl/d	8410	7063	6260	5700	5524	5162	4976	4773	4571	4571

Table 11.5

A-26 "gas lift case"										
Parameter/year	2010	2011	2012	2013	2014	2015	2016	2017	2018	2019
GOR	160	160	160	160	160	160	160	160	160	160
WC	86	88	89	90	91	91	92	92	93	93
Pres	400	398	395	395	395	395	395	395	395	395
Qo, bbl/d	948	787	703	631	561	561	493	493	426	426

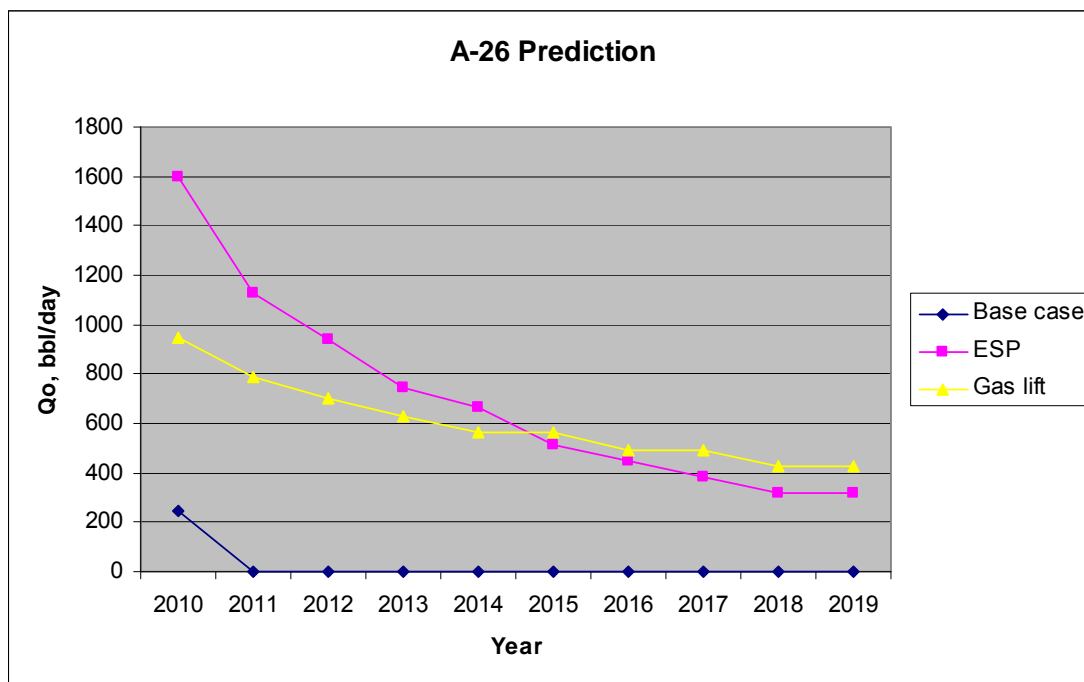


Figure 11.2, production forecast for A-26. Production for the base case and the two artificial lift methods are plotted from start date to 2019.

The results show that also in A-26 ESP give the largest production. However, gas lift shows a higher production rate already in 2015. Although the difference in production is not as impressive in A-19, one can still see from figure 11.2 that the area under the ESP curve is much larger than for the gas lift curve.

There is a small “base case” production included in 2010. The well dies with a small change in water cut and reservoir pressure.

The total liquid rate falls beneath 7 000 bbl/d after only two years. If the rate follows this prediction the pump has to be run at lower frequency or changed.

The reservoir pressure used is conservative, and a pressure of 450 bar instead of 400 bar is realistic. This would give a liquid rate of over 10 000 bbl/day. This shows that pumps is not necessarily oversized, but has to handle a wide range of scenarios and production rates.

The reliability of the production forecast is dependent of the reservoir pressure, and mostly the water cut. A small change in water cut gives a large change in oil production. The reservoir pressure is conservatively estimated, and the water cut trend is based on reliable reservoir simulations. In A-19 there has not been a major water break-through yet, and the timing of this breakthrough involves some uncertainty. However, the same reservoir data source is used for the different scenarios, so the comparison of the two artificial lift methods should be valid.

12. Economical evaluation

Before making a final decision a thorough economical analysis has to be done. As described in section 5.2.3, it is the profitability of a project that has to be the final decision criteria. TENAS is still in the evaluation phase, and a full economical analysis giving the NPV of the projects is not available yet. The NPV will give the value of a project through its entire lifetime taking capital costs, operating costs, depreciation and revenues into account.

However, the initial costs of the scenarios are analysed and can give a good indication of the project magnitude. Table 12.1 shows the capital cost e.g. the cost until end of installation of each project. This involves cost of procurement, construction, engineering, administration and operational cost during installation (rig rate etc.). The numbers do not include company costs such as company personnel, helicopter, catering etc.

Table 12.1, capital cost of projects.

Project	Total cost (1000 NOK)
ESP pilot, A-19 and A26	284 000
ESP full field project, 10 wells	1 420 000
Full field gas lift project	709 000

There has not been made any economical estimate on gas lift just for A-19 and A-26. The plan is either full field or nothing. The ESP full field project estimate is the pilot project times five. This is done so simple because it is too early to say what a full field project would imply. Ten wells producing with ESPs would need a new water handling facility etc. Thus a full field ESP project can be more expensive.

The relatively high expenses of full field gas lift project are caused by a new compressor having to be purchased, and a lot of the wells would need a full workover due to missing sidepockets.

The biggest cost for gas lift is at installation, while ESPs carries great operational expenses due to their limited lifetime. A workover for two wells with ESPs is estimated to 60 days. This means that an ESP solution has a great cost attached every two years. The operational costs are estimated to about 75% of the total costs of a pump change out. The loss of production during this time also needs to be accounted for.

The cumulative oil production can be multiplied with a factor of $(1 - 2/24)$, where 2 is the downtime and 24 is the expected lifetime in months. Compared, the cost of a gas lift valve change out by wireline is minor. This operation will only take a day or two.

13. Conclusions

Through consideration of the production profile, desired rate and advantages / disadvantages TENAS has decided for gas lift and ESP to be the most suitable artificial lift methods on Gyda.

Gas lifting is a simple, well tried method and has been proved efficient on Gyda before. Installation and change of gas lift valves is done by wireline, but since the A-19 and A-26 do not contain sidepockets, a full workover is required at first time installation.

There is a positive effect of setting the valves deeper. When the compressor outlet pressure is limited, the fluid density in the well is important. The valves can be set deeper with a less dense fluid, and this can also make the difference in number of unloading valves needed.

A new compressor has to be purchased to reach the injection rates used in this study. This will be one of the biggest costs of an artificial lift campaign based on gas lift.

Implementation of ESPs carries greater risk because of the complexity of the equipment and limited lifetime. When ESPs fail this require a full workover, which is costly mainly because of the required rig operation compared to a wireline operation. However, there are design choices and running procedures that will extend the lifetime. SAGD technology is used to cope with the high reservoir temperatures on Gyda. Monitoring production and the pump during operation is crucial to achieve extended lifetime. Sand production and scale is two of the biggest risks.

Expected lifetime of the dual ESP design on Gyda is 2 years.

Both gas lift and ESP give a large increase in production compared to the base case, but ESP is superior to gas lift in both A-19 and A-26. It is reason to believe that the same difference would be seen in a full field artificial lift campaign. In this study the so called "ESP secondary effect" is not accounted for, this can increase production as well as the recovery factor for the field. So from a production point of view the ESPs is by far the best choice.

The difference in oil production between ESP and gas lift is largest in A-19. Both wells show basically the same total liquid production initially. However, as water cut increases and reservoir pressure decreases in both wells, A-26 can not follow A-19's production trend with ESPs. The reason seems to be the lower number of stages in

A-26, this shows that a re-evaluation of the design is needed when it is time for changing the pumps.

The water cut behaviour is the biggest factor for change in the oil production. To date A-19 has not seen any significant water breakthrough, but this is expected to happen soon. A water breakthrough is accounted for in the simulations done in this study. With lower water cut, A-19 will produce at a larger rate than predicted.

Since ESPs have never been run on Gyda before it is difficult to tell how the reservoir will react. Reservoir pressure and water cut is difficult to predict and the pumps must be able to handle a wide range of fluid ranges and properties. Baker Hughes Centrilift's design seems to be valid for the conditions predicted for May 2010, where production lies to the left of the best efficiency point (Figure 10.2). At this point they have extra capacity, and can also run at a lower rate.

According to the production forecast done in this study, there is a possibility for the pumps to fall beneath their production design limit in both A-26 and A-19 after some years. This again shows the importance of a re-evaluation of the design when a pump fail.

Comparing cost and production potential of the artificial lift methods, ESPs are the best choice. The pilot project with A-19 and A-26 would return invested capital in less than a year due to it's high production potential compared to the base case. But before a final decision is made an economical analysis of each project's lifetime should be carried out. The ESP projects will generate higher costs later in life than the gas lift project. A NPV evaluation will account for all costs and depreciation of each project.

References

1. Michael Golan and Cutis H. Whitson, Well Performance, Prentice-Hall Inc., 1985.
2. Gabor Takacs, Gas Lift Manual, PennWell Corporation, 2005.
3. Dake, L., Fundamentals of Reservoir Engineering, Elsevier Science B.V., 2002.
4. Clegg, J.D., editor. Production Operations Handbook. SPE, USA. 2007.
5. Rune W. Time, Two phase Flow in Pipelines, Course compendium, University of Stavanger, 2007.
6. PROSPER v.10 User Manual, Petroleum Experts. 2008.
7. Clegg, J.D., Bucaram, S.M., Hein Jr., N.W., Recommendations and Comparisons for selecting Artificial-Lift Methods, SPE 00024834, 1993.
8. Lloyd R. Heinze, Herald W. Winkler, James F. Lea, Decision Tree for Selection of Artificial Lift Method, SPE 29510, 1996.
9. Gaviara, F., Santos, R., Rivas, O., Luy, Y., Pushing the Boundaries of Artificial Lift Applications: SAGD ESP installations in Canada, SPE 110103, 2007.
10. Vogel, J.V., Inflow Performance Relationships for Solution-Gas Drive Wells, SPE 1476-PA, 1968.
11. Kilvington, L.J., Thomson, J.Y., Brown, J.K., Electric-Submersible-Pumping Success in the Beatrice Field, North Sea, SPE 16638-PA, 1989.
12. Meihack, S., Performance of Jet Pump in the Gyda field, Internal document of Talisman Energy Norge AS, Stavanger, 1997.
13. Zerrouki, T., Paul, H., Monkman, J., Yme: Expected ESP Run Life, Internal document of Talisman Energy Norge AS, Stavanger, 2006.
14. Saepudin, D., Soewono, E., Sidarto, K.A., Gunawan, A.Y., Siregar, S., Pudjo, S., An Investigation on Gas Lift Performance Curve in an Oil-Producing Well, Hindawi Publishing Corporation, International Journal of Mathematics and Mathematical Sciences, Volume 2007, Article ID 81519.
15. Fleshman, R., Harryson, O.L., Artificial Lift for High-Volume production, Oilfield Review, spring 1999.
16. Jadid, M.B., Lyngholm, A., Opsal, M., Vasper, A., The Pressure's On: Innovations in Gas Lift, 2006, Volume 18.
17. Basic artificial lift, Canadian Oilwell Systems Company Ltd, available at: <http://www.coscoesp.com>

18. Baker Hughes Oil Tools, Gas Lift catalog, available at:
<http://www.bakerhughesdirect.com>
19. <http://www.bakerhughes.com>
20. <http://www.ptc-norway.com>
21. <http://www.petroleumexperts.com>
22. <http://www.pumptools.co.uk/>
23. <http://www.npd.no>
24. <http://www.slb.no>

Abbreviations (alphabetically)

ADV	Automatic Diverter Valve
BEP	Best Efficiency Point
BHP	Break Horsepower
EOR	Enhanced Oil Recovery
EOS	Equation of State
ESP	Electrical Submersible Pump
FBHP	Flowing Bottom Hole Pressure
GLR	Gas-to-Liquid Ratio
GLV	Gas Lift Valve
GOR	Gas oil Ratio
HP	Horse Power
IPO	Injection Pressure Operated
IPR	Inflow Performance Relationship
KOT	Kickover-tool
MD	Measured Depth
MTTF	Mean Time To failure
NPV	Net Present Value
OWC	Oil Water Contact
PI	Productivity Index
PPO	Pressure Operated Valves
RIH	Running In Hole
SAGD	Steam Assisted Gravity Drainage
SG	Specific Gravity
TENAS	Talisman Energy Norge AS
TVD	True Vertical Depth
VLP	Vertical Lift Performance
WC	Water Cut